Risk assessment tool for diabetic neuropathy

Jugal Manoj Dave

The thesis is submitted in partial fulfilment of the requirements of Faculty of Science and Technology, Bournemouth University for the degree of Doctor of Philosophy

In collaboration with Diabetes Centre, Poole Hospital NHS Foundation Trust

2019

Copyright Information

This copy of the thesis has been supplied on condition that anyone who consults it is understood to recognise that its copyright rests with its author and due acknowledgement must always be made of the use of any material contained in, or derived from, this thesis.

Declaration

I hereby declare that except where specific reference is made to the work of others, the contents of this thesis are original and have not been submitted in whole or in part for consideration for any other degree or qualification in this, or any other university. The work shown in this thesis is carried out by me the guidance of Prof. Venketesh N. Dubey and under Dr. David Coppini. This thesis contains nothing which is the outcome of work done in collaboration with others, except as specified in the text and Acknowledgements.

Jugal Manoj Dave

2019

Acknowledgements

I would like to express my thanks to Prof. Venketesh N. Dubey and Dr. David Coppini for their support, careful supervision, recommendations and strong guidance through my Doctoral research program. I am grateful to my supervisory team for their constructive criticism on this project. Also thanks to Naomi Bailey (Research Administrator) for administrating the process so efficiently.

Special thanks to Dr. John Beavis for guiding me in statistical part of the research. His insight and suggestions has motivated me in exploring my knowledge in the field of data analysis.

I would like to thanks Poole hospital NHS Foundation Trust for providing Neurothesiometer device which was used in this research to perform comparative study.

I would like to thanks my family for their love, patience and support during my study. Lastly, I would like to thank all my friends in United Kingdom and in India for their support and encouragement during my time as a PhD researcher at Bournemouth University.

Abstract

Peripheral neuropathy is one of the serious complications of diabetes. Symptoms such as tingling and loss of touch sensation are commonly associated with the early stages of neuropathy causing numbness in the feet. Early detection of this condition is necessary in order to prevent the progression of the disease. Out of many detection techniques vibration perception is becoming the gold standard for neuropathy assessment. Devices like tuning fork, Biothesiometer and Neurothesiometer use this technology but require an operator to record and manually interpret the results. The results are user-dependent and are not consistent. To overcome these limitations, a platform-based device "VibraScan" was developed that can be self-operated and results displayed on a user interface. The development of the device is based on studying the effect of the vibration on the human subject by identifying the receptors responsible for sensation. The requirement of generating vibration was achieved by selecting a specific actuator that creates vibration perpendicular to the contact surface. The battery operated VibraScan is wirelessly controlled by software to generate vibration for determining the vibration perception threshold (VPT). Care has been taken while developing the user interface for human safety with the vibration intensity. The device can be operated without any assistance and results are automatically interpreted in terms of severity level indicated similar to the traffic-light classification. In order to provide consistent results with the existing devices a study was undertaken between Neurothesiometer and VibraScan with 20 healthy subjects. The results were compared using Bland-Altman plot and a close agreement was found between the two measurements.

VibraScan accurately measures VPT based on the perceived vibration threshold, however, it does not predict any risk associated with neuropathy. In order to supplement this device with the progression of neuropathy a risk assessment tool was developed for automated prediction of neuropathy based on the clinical history of patients. The smart tool is based on the research related to the risk factors of diabetic neuropathy which was studied and analysed using summarised patient data. Box-Cox regression was used with the response variable (VPT) and a set of clinical variables as potential predictors. Significant predictors were: age, height, weight, urine albumin to creatinine ratio (ACR), HbA1c, cholesterol and duration of diabetes. Ordinary Least Squares Regression was then used with logarithmic (VPT) and the significant predictor set (Box-Cox transformed) to obtain additional fit estimates. With the aim to improving the precision of VPT prediction, a simulated patient data set (n = 4158) was also generated using the mean and the covariance of the original patient variables, but with reduced standard errors. For clinical or patient use, providing direct knowledge of VPT was considered less helpful than providing a simple risk category corresponding to a range of VPT values. To achieve this, the continuous scale VPT was recoded into three categories based on the following clinical thresholds in volts (V): low risk (0 to 20.99 V), medium risk (21 to 30.99 V) and high risk (≥ 31 V). Ordinal Logistic Regression was then used with this categorical outcome variable to confirm the original predictor set. Having established the effectiveness of this "classical" baseline, attention turned to Neural Network modelling. This showed that a carefully tuned Neural Network based Proportional Odds Model (NNPOM) could achieve a classification success >70%, somewhat higher than that obtained with the classical modelling. A version of this model was implemented in the VibraScan risk assessment tool. Integrating VibraScan and the risk assessment software has created a comprehensive diagnostic tool for diabetic neuropathy.

Publications

1. Dave, J.M., Dubey, V. N., Lowes, V., Beavis, J. and Coppini, D.V., 2018. A 'smarter' way of diagnosing the at risk foot: Development of a novel tool based on vibratory measurements in subjects with diabetes. *In: Diabetes UK Professional Conference, 14-18 March 2018, London.*

2. Dave, J.M., Dubey, V. N., Coppini, D.V. and Beavis, J., 2018. VibraScan: A smart device to replace Neurothesiometer for measuring diabetic vibration perception threshold *BioMedEng18*, (ISBN 978-1-9996465-0-9), Page no.200.

3. Dave, J.M., Dubey, V. N., Coppini, D.V. and Beavis, J., 2019. Predicting diabetic neuropathy risk level using artificial neural network based on clinical characteristics of subjects with diabetes. In: *Diabetes UK Professional Conference, 6-8 March 2019, ACC Liverpool*.

4. Dave, J.M., Dubey, V. N., Coppini, D.V. and Beavis, J., 2019. Comprehensive risk assessment of diabetic neuropathy using patient data *BioMedEng19.* (Submitted)

Poster presentations

1. Dave, J.M., Dubey, V. N., Coppini, D.V. 2018. An innovative device VibraScan for measuring vibration perception threshold. CoPMRE visiting Faculty day, Bournemouth University, UK.

2. Dave, J.M., Dubey, V. N., Coppini, D.V. 2017. A smarter approach to diabetic neuropathy. Visiting Faculty Day, Bournemouth university, UK.

Oral presentations

1. Dave, J.M., Dubey, V. N., Coppini, D.V. 2016. Medical Device development for Comprehensive Clinical Assessment of Peripheral Neuropathy. 8th Annual postgraduate Research Conference, Bournemouth Univeristy, UK.

2. Dave, J.M., Dubey, V. N., Coppini, D.V. 2016. Device for early detection and continuous assessment of diabetic peripheral neuropathy. Science and Technology Annul PGR Conference, Bournemouth University, UK.

Table of Contents

List of Figures

List of Tables

List of Abbreviation

DM - Diabetes Mellitus

WHO - World Health Organization

NHS - National Health Service

T1DM - Type 1 Diabetes Mellitus

T2DM - Type2 Diabetes Mellitus

VPT - Vibration Perception Threshold

ETD- Electronic Tuning Fork

DPN - Diabetic Peripheral Neuropathy

ASN- Acute Sensory Neuropathy

DR - Diabetic retinopathy

SINBAD - Site, Ischemia, Neuropathy, Bacteria infection and Depth

DNEP - Diabetic Nephropathy

DN - Diabetic Neuropathy

DSPN - Distal symmetric polyneuropathy

DAN - Diabetic Autonomic Neuropathy

CAN - Cardiac autonomic neuropathy

NCS - Nerve Conduction Studies

VST - Vibration Sensory Threshold

ESC - Electrochemical skin conduction

FSR - Force Sensitive Resistors

EMG - Electromyogram

GUI -Graphic User Interface

ERM- Eccentric rotating mass vibration motor

LRA - Linear Resonant Actuator

PWM - Pulse Width Modulation

AFH - Adaptive Frequency Hopping Feature

USB - Universal Serial Bus

C2HDLF - C2 High displacement and low frequency

CAD - Computer aided

LED - Light emitting diode

ANN - Artificial neural network

BMI - Body mass index

HDL - High density lipoprotein

LDL – Low density lipoprotein

ACR - Urine albumin to creatinine ratio

RBG - Random Blood Glucose

OLS - Ordinary least squares

OLR - Ordinal Logistic regression

MNSI - Michigan Neuropathy Screening Instrument

MNSD - Michigan Neuropathic Diabetic Scoring

DFA - Discriminant functional analysis

NNPOM - Neural Network based Proportional Odds Model

SPSS - Statistical Package for the Social Sciences

Chapter 1 Background literature on diabetic neuropathy

There are many chronic complications of the Diabetes Mellitus affecting eye, kidney and nerves. Microvascular complications with Diabetic retinopathy, nephropathy, and neuropathy are the commonest complications amongst them. Diabetic Neuropathy is one of the common long term diabetes complications which causes damage to about 50% of patients with diabetes (Mukesh et al. 2006). Early detection of neuropathy is necessary to avoid further complications that can lead to ulceration and foot amputation.

Long term poor control of diabetes can cause damage to the nerves that transmit the signal to and from spinal cord, skin, muscle and organs. Reduction of touch sensation on the skin causing numbness in feet and hands, reduced ability to feel pain and temperature changes, tingling or burning sensation, shooting pain or cramps and muscle weakness are the early symptoms of the disease (Jayaprakash et al. 2011). This symptom starts at the big toe and as the disease progresses it ascend proximally. If the disease is untreated and undiagnosed it may lead to long-term complications such as foot ulceration and non-traumatic lower limb amputation.

Despite much medical advancement, devices and methods available for diagnosis of diabetic neuropathy are very basic and the incidence of foot ulceration and lower extremity amputations are proportionately very high. There are many methods, treatments and medical devices available which are used to detect neuropathy, however, there is a need for an instrument which can accurately detect and assess the effects of neuropathy at an early stage. Thus, from early symptoms of the disease, it is possible to focus and develop residual measures which can arrest further progression and save from amputation.

This project focuses on developing a device for early detection of neuropathy and correlation to patient's clinical history. The device will focus on touch and vibration sensations on skin that can accurately provide data related to neuropathy. Based on the data generated from the device it would be possible to assess the level of neuropathy and how it progresses over time. This research will investigate on devices used to detect the neuropathy based on vibration, describing the way for conducting the test and will discuss the results of the test. After conducting a thorough literature survey and consulting with the clinicians we have put forward a plan for developing an intelligent, smart and user-friendly device.

1.1 Diabetes mellitus and its prevalence

Diabetes Mellitus (DM) is the chronic metabolic disorder which usually occurs due to hyperglycemia or the body cannot produce more insulin or the body is unable to use the produced insulin. Thus, looking at both the financial as well as effects on the patient's quality of life, control of the disease is important. Increasing sugar level or hyperglycemia is a common effect of uncontrolled diabetes. There are three major types of diabetes as type 1 diabetes, type 2 diabetes, and gestational Diabetes.

Type 1, Diabetes mellitus (T1DM) and Diabetic Neuropathy

Diabetes mellitus (T1DM) also called insulin-dependent diabetes as the body is unable to produce insulin. The pancreas is responsible for producing the hormone called insulin. When there is autoimmune destruction to the B-cells of the pancreas gland, the body is unable to produce insulin. Viral infection is one of the reasons to damage the pancreas, however, a common cause is body's own immune system. Worldwide the prevalence of Type1 DM is increasing. In 2014, Out of total 3.5 million diabetes patient in the UK, it has been estimated that including all adults and children 10% population is having type 1 diabetes and 90% people are having type 2 diabetes (DiabetesUK 2016). Type 1 DM causes major complications that affect eye, kidney, and nerve. T1DM affecting the nerves in such a way that the function of the nerves deteriorates commonly termed as diabetic neuropathy. There are various symptoms of diabetic neuropathy, and as the disease progresses there is a risk of foot ulceration.

Type 2, Diabetes Mellitus (T2DM) and Diabetic Neuropathy

Diabetes mellitus (T2DM) is also called non-insulin dependent diabetes. Previously it was known as adult onset diabetes however as a result of obesity in children, more teenagers are now suffering from type 2 diabetes. Type 2 DM is not as serious as type 1 diabetes as there is a lack of production of insulin in the body or body cells are restricted to it. People who are obese are at the high risk of developing type 2 diabetes as the body cells are resistance to it and results in increasing sugar level. Insulin resistance primarily starts in liver and muscle cells. However, the long-term effect of type 2 diabetes can affect small blood vessels. Diabetes is not curable however type 2 diabetes can be controlled by proper dietary therapy, exercise and nutrition management (Kumar et al. 1998). As mentioned in type 1 diabetes, type 2 diabetes can also cause complications which affect the nerve known as diabetic neuropathy. The number of type 2 diabetes patients is more than type 1 diabetes it is important to know the number of neuropathy cases under each category as well as the prevalence of severe neuropathies based on ulceration. A report published by Clinical Audit and Registries

Management Service Health and Social Care Information Centre is shown in Table 1.1 comparing type 1 and type 2 diabetes (Ince et al. 2008).

Table 1.1: The audit recorded for ulcer severity in 2014 and 2015 for England and Wales. Patient ulcer severity

Disease	Total number of diabetes N=5215		Type 1 diabetes N=610		Type 2 diabetes N=4089	
	Number	Percentage	Number	Percentage	Number	Percentage
Neuropathy	4309	82.6	534	87.5	3344	81.8
SINBAD score ≥ 3	2411	46.2	313	51.3	1842	45.0

SINBAD score refers to the Site, Ischemia, Neuropathy, Bacteria infection and Depth (SINBAD) which is useful in predicting ulcer outcome and comparison among them (Ince et al. 2008). Table 1.1 shows that ulcers occurrence due to the type 1 diabetes is higher than the ulcers occurrence due to type 2 diabetes; that is 51.3% compared to 45.0%. Looking at the above data, it can be concluded that rates of neuropathy due to type 1 is higher than type 2 diabetes.

Gestational Diabetes:

Gestational diabetes is the type of diabetes that occurs during pregnancy, as there is insulin resistance during pregnancy. This diabetes needs to be controlled once it is diagnosed. Usually, the disease is diagnosed at the later stage of the pregnancy. If the diabetes is not controlled then the high blood sugar levels in the mother can be circulated through the placenta to the baby which can hamper the growth and development of the baby. After pregnancy, this type of diabetes usually resolves itself. There is a 10% chance that the mother is at the risk of type 2 diabetes at the later stage of life. Type 2 diabetes usually occurs after few weeks or months or a year later. Due to gestational diabetes, there is a high risk to the unborn baby than that of the mother. Over gained weight before birth, breathing problem to the baby and diabetes at the later stage of life are the major risks to the baby. Due to an overly large baby, the mother has to go through the cesarean procedure and there could be risks of damaging heart, kidney, and eyes as well.

Effects of Diabetes:

DM has affected a large number of the population worldwide. According to World health organization, the number of people having diabetes have raised from 108 million to 422 million from 1980 to 2014 (WHO November 2016). In 2016, there were approximately 3.6

million people in the UK diagnosed of diabetes (Diabetes UK November 2016) and this figure predicted to exceed 5 million by 2025.

This growing rate of disease causes huge cost burden to the patient, NHS and the society as a whole. The Health and Social Care Information Centre recently published a report that the cost of primary treatment for diabetes is 2005-6 was £513.9 million and it has risen to £803.1 million in 2013-14 (NHS Digital, 2014). The total cost attributed to treating type 1 and type 2 diabetes in UK has been estimated to be 23.7 billion in 2010.

1.2 Complications of diabetes

Macrovascular complications of diabetes:

Macrovascular complications due to diabetes are the major cause of death which occurs two to four times more likely in the individuals with diabetes than without the disease (Kannel and McGee 1979; Morrish et al. 2001; Mulnier 2012; Vamos et al. 2012). Coronary artery disease, peripheral arterial disease, and stroke usually refer to Macrovascular complications of diabetes.

Microvascular complications of diabetes:

Because of Diabetes, there is a high risk of damaging eye, kidney, and nerves of the body which can lead to various types of Diabetic retinopathy (DR), Diabetic Nephropathy (DNEP) and Diabetic Neuropathy (DN).

1.2.1 Diabetic neuropathy

Diabetic neuropathy damages nerve which carries signal from brain, spinal cord, blood vessels, muscles, skin and organs. Controlling blood glucose level is the best way to prevent this nerve damage. There are about 3.6 million people diagnosed with diabetes in UK, out of which 50% of patients may get affected by neuropathies. Chronic painful neuropathy is the common type of neuropathy i.e. up to 26% of diabetic patients. It impairs quality of life, considerable mortality and increase morbidity (Alleman et al. 2015).

The exact cause varies based on the type of Neuropathy. Mostly it is believed that uncontrolled diabetes damages nerve that reduces the ability of transmitting signal causes diabetic neuropathy. It also affects the small blood vessels and restricts the supply of oxygen in blood. There are certain factors such as inflammation in the nerve due to autoimmune response, genetic factors and smoking. Smoking can also cause nerve damage as it narrows and hardens the arteries and reduces blood flow in limbs which will ultimately damages the

peripheral nerves. Usually the risk of developing diabetic neuropathy increases due to poor glycaemic control, diabetes history, overweight, and kidney disease because diabetes can damage the kidneys and due to toxins available in the blood can cause nerve damage. Diabetic neuropathy is classified into various types such as distal symmetric polyneuropathy, acute Sensory Neuropathy, diabetic amyotrophy, diabetic mononeuropathies and painful diabetic neuropathy. Diabetic neuropathy affects sensory, autonomous and motor neurons of nervous system.

(a) Distal symmetric polyneuropathy

DSPN occurs in both type 1 and type 2 diabetes mellitus. In this type of neuropathy, the patient may remain asymptomatic and could be unnoticeable for a longer period of time. On clinical examination, it is possible to diagnose neuropathy, usually symmetrical sensory loss in feet (Kasznicki 2014). The ankle reflexes are mostly small or absent. The abnormal muscles sensory function which causes imbalance also occurs in patients with DSPN (Van Deursen et al. 1998). 50% of patients with DSPN may suffer from these symptoms and pain. There is around 3% to 25% incidence of painful DSPN which mostly remains undiagnosed and untreated (Bril et al. 2011). In another study, it was found that painful DSPN occurs in 27% of diabetic patients (Harris et al. 1993). It was shown that the occurrence of painful DSPN mostly associated with the severity of DSPN rather than risk factors related to diabetes (Mondelli et al. 2012). The pain is usually symmetrical, distal and severe at night. The painful DSPN can be diagnosed through clinical ways or based on the pain as described by the patients. They mostly describe the pain as a deep ache, burning, sharp and prickling (Apfel et al. 2001). Diagnosis of DSPN should be performed using vibration perception (128-hertz tuning fork), 10 g monofilament test, ankle reflexes and pressure sensation (Boulton et al. 2005b).

(b) Acute Sensory Neuropathy

Acute sensory neuropathy (ANS) is the form of DSPN (Apfel et al. 2001). Most of the symptoms of ASN are similar to DSPN, however, there are major differences in onset, signs, and prognosis of the disease. In males, symptoms like weight loss, depression and erectile dysfunction are seen commonly. The pain is usually as deep and burning as described by the patients. ASN occurs usually in patients with poor blood glucose control. As per the report, achieving stable glycemic control can be helpful in resolving the symptoms in several months (Boulton et al. 2004).

(c) Diabetic amyotrophy (Radiculoplexus neuropathy)

Diabetic amyotrophy usually affects the nerves in the hips, thigh, buttocks or legs causing difficulty in standing, walking or climbing stairs. It is also known as proximal neuropathy or femoral neuropathy. It is commonly seen in patients with type 2 diabetes. It is characterised by progressive, acute, weakness and pain in the muscles of the proximal lower extremities (Pasnoor et al. 2013). It causes acute disability with varying degree of recovery (Nagsayi et al. 2010). The symptoms are usually at one side of the body such as causing severe pain in hip, thigh or buttock, causing weak and shrinking thigh muscles, abdominal swelling and weight loss. The diagnosis of diabetic amyotrophy is possible through neurological examination and getting a clinical history of the patients. There are several other neurological examinations available such as nerve conduction studies, nerve biopsy, electromyography, and imaging technique may be used to confirm the disease. For diagnosing this complication, nerve biopsy is considered only when the screening of diabetic amyotrophy remains unclear using other techniques. The pain due to neuropathy may be difficult to control. The severe pain may be resolved after several months of onset; however residual pain may last for years. It has been noted that doses of corticosteroids may be helpful to a few patients with diabetic amyotrophic to reduce severe pain (Pasnoor et al. 2013).

(d) Diabetic mononeuropathies

Mononeuropathies appears greater in patients with diabetes than in general subjects. Mononeuropathy or focal neuropathy damages nerve in the face or middle of the body. Neuropathies can be developed at the different areas of the body like an elbow (ulnar neuropathy), wrist (median neuropathy) and fibular head (peroneal neuropathy). It has been noted that if the neuropathies developed in upper extremities refers to mononeuropathies or multiple mononeuropathies rather than polyneuropathies (Dyck and Harper 1998). Mononeuropathy also occurred when a nerve is compressed. Carpel tunnel syndrome is the common type of neuropathy in the subject with diabetes which caused numbness in hand or fingers. Symptoms depend on the particular nerve which is involved. The patient may have pain in the lower back, front of the thigh, foot, abdomen or chest. These symptoms may resolve without any treatment within a week or months.

(e) Painful diabetic neuropathy

Painful diabetic neuropathy is the common phenotype of diabetic neuropathy. It is more significant in type 2 than type 1 diabetes (Hartemann et al. 2011). The pain is mostly bilateral which involves lower extremities especially foot and sometimes in upper extremities including palms and fingertips (Ziegler 2009). Pain is usually worse at night, during stress and fatigue (Davies et al. 2006). The pain described by patients are like hot, electric, jolts, sharp and pins and needle (Galer et al. 2000). Study shows that patients with painful diabetic neuropathy have a poorer quality of life than with patients with neuropathy without pain or with non-neuropathic pain (Davies et al. 2006). Due to the severe pain, it causes a significant increase in anxiety, depression and sleep impairment. It causes disability in walking in one-third of the patients and requires cane, walker or wheelchair due to neuropathy (Galer et al. 2000). Various methods such as nerve conduction studies, 10 g monofilament test, superficial pain sensation test, vibration tests, and electromyography are used for its diagnosis. The pain related portion of the Michigan Neuropathy screening instrument could be used to get the knowledge of painful symptoms.

(f) **Sensory Neuropathy:**

Sensory Neuropathy is considered as one of the most devastating nerve dysfunction. Sensory deficit and symptoms are appearing first at the distal portion of the extremities and progress proximally in the stocking-glove distribution (Bowker and Pfeifer 2008). As the loss of this fibre types recur there is an effect of diminishing light touch and proprioception later resulting in ataxic gait and unsteadiness along with weakness of intrinsic muscles affecting the feet (and hands) (Bowker and Pfeifer 2008). Ignoring these symptoms may lead to foot ulceration and lower limb amputation. As the disease progresses, chronically it will not directly cause ulceration and limb loss by itself, however, if the period of diagnosing the sensory neuropathy is shortened then it is possible to prevent these complications occurring in future. Various screening tools are used to check the loss of vibration perception and pressure perception which is the main area of interest for this research.

(g) Autonomic Neuropathy:

Diabetic autonomic neuropathy (DAN) is the most understood and least organized complications of diabetes (ERBAS 2001; Vinik et al. 2003). Autonomic neuropathy can

occur when nerves responsible for controlling involuntary functions are damaged. It affects the autonomic neurons of either or both the parasympathetic and sympathetic nervous system. Skin atrophic and sweating abnormalities of the feet at an early stage are the signs of autonomic neuropathy which is often connected to somatic polyneuropathy (Mayfield et al. 1998). A sensitive indicator of the skin may be called plantar callus (hyperkeratosis) (Murray et al. 1996; Pataky et al. 2002). Cracking of the skin, the formation of fissures and loss of sudomotor function are the indicators. One of the outcomes of autonomic neuropathy is auto sympathectomy which could lead to arteriovenous shunting, increase cutaneous blood flow, increased skin temperature and distension of the dorsal veins in the foot (Edmonds et al. 1982; Corbin et al. 1987).

(h) Motor Neuropathy:

Nerves which are responsible for controlling movements are affected due to motor neuropathy. This will lead to muscle weakness and wasting of nerves which receive the signals from the nerves being affected by an imbalance of flexor and extensor muscles causing foot deformities (clawing of the toes and prominence of the metatarsal heads). Abnormal plantar pressure occurs due to reduced subcutaneous tissue thickness at the metatarsal heads and anterior displacement of the sub-metatarsal fat pads (Pataky 2012).

Diagnosis:

For the diagnosis of diabetic neuropathy, test should include assessment of sensation of pinprick, examination of muscle power, vibration and touch sensation. Mostly for touch sensation monofilament test is recommended. Vibration test should be performed by 128 Hz tuning fork. Sensory test should be done on hands and feet bilaterally. Quantitative sensory test are not recommended for routine clinical practice (Shy and Frohman 2003). Nerve biopsy may be useful to find or explore the other causes of neuropathy. For assessment of polyneuropathy confocal corneal microscopy is recommended. The autonomic function tests which are available are based on blood pressure, heart rate response is commonly used in subjects with diabetes mellitus. As DN can be asymptomatic in nature therefore it has to be diagnosed very carefully.

According to San Antonio consensus statement held in 1988, for diagnosing diabetic neuropathy, consensus panel has recommended that at least one measure from each of the categories is needed like clinical symptoms, neurophysiology, clinical signs, autonomic function

test and quantitative sensory tests (Association and Neurology 1988). This may be needed for research protocol. However, in the clinical practice this is difficult to implement so two of five criteria have been recommended (Dyck 1988).

Complications of diabetic neuropathy

The complications in the individual subject may vary, as it depends on the root cause and which nerves been damaged. The early symptoms of diabetic neuropathy cause sensation loss result in numbness, burning sensation, tingling and pins and needles. In some cases, it may improve with time with proper treatment while in some cases it may cause permanent damage or get worse with time. If it is not detected at the early stage or the cause is not treated, it may cause serious complications like foot ulcers, further these ulcers may become infected and lead to gangrene if remain untreated. In the advanced stage, the affected foot may have to undergo amputation. The peripheral neuropathy may affect the autonomic functions of heart, due to which there could be a need for increased blood pressure.

(a) **Diabetic foot ulcers**

The neuropathic foot remains warm with palpating pulses, without sweating and skin remains dry. Due to dryness in skin, it is prone to fissures, fungal and bacterial infections. The broken skin takes longer time to heal or may not properly repair itself because of nerve damage. The numbness or the sensation loss feelings in the feet can get easy cuts by treading on something sharp, tight shoes, blisters and bruises can result in diabetes foot ulcers. The common risk factors of diabetic foot ulcers are neuropathy, hyperglycemia, poor blood circulation and walking without shoes.

The blood supply to the feet is restricted due to damage to the blood vessels or narrowed arteries. As the blood supply to the skin is less, it takes a longer time to heal and causes tissue damage leading to gangrene.

(b) **Gangrene**

Gangrene is developed by the poor blood circulation to a certain part of the body causing the tissue to die. There are two types of gangrene dry and wet gangrene. Dry gangrene is normally caused to the patients by having type 1 or type 2 diabetes. Due to hyperglycemia for a longer period of time, it damages blood vessels. The damaged blood vessels cannot carry oxygen and nutrition to the tissue and eventually the tissue will die causing dry gangrene.

The gangrene that is developed due to the infection causes wet gangrene. This type of gangrene is usually seen when foot ulcers or wound is badly infected. People with diabetes are less able to fight off the bacteria and other types of infections causing a risk of developing wet gangrene. Once the gangrene is developed it can be removed by surgical procedure or in severe cases toe or the foot needs to be amputated.

Advantages of early detection of diabetic neuropathy

It has shown that subjects with good glycaemic control can help in slow progressions of diabetic neuropathy in type 1 but less benefit in subject with type 2 diabetes. With the increasing number of type 1, type 2 diabetic patients, the incidence of diabetic neuropathy causes a huge impact on the quality of life of patients as well as their families. To deal with devastating complications such as foot ulceration, limb amputation due to diabetic neuropathy, early diagnosis and effective treatment is necessary. This is because once the peripheral nerves function deteriorates, it is difficult to regenerate. It may possible to slow down the progression through treatment but not reverse the damage. In case of severe neuropathy, there is a need for physical therapy to avoid muscle spasms and cramping. There can be a significant drop in the amputation rate by early detection and managing risk factors of diabetic neuropathy. Therefore, diagnosis is critical to minimise pain and loss.

For diagnosing neuropathy various tools and methods such as patient's questionnaires, an examination of nerve conduction velocities, tools based on vibration perception thresholds are available which will be discussed in the next chapter. By Studying the limitations and advantages of the existing technology based on vibration perception detection, the aim is to develop a smart and operator in dependent device for early detection of neuropathy which automatically defects the severity level based on the measured vibration perception thresholds.

1.3 Research questions

To start with the research, first the research questions were identified as listed below:

1. Considering the electromechanical device Neurothesiometer as the gold standard (Coppini et al. 2001), is it possible to develop an independent device which can generate the same nature of frequency and voltage with intelligent diagnosis features?

2. Is it possible to provide the vibration with the constant stimulus pressure?

3. Is it possible to predict the vibration perception threshold using the clinical history of the patients?

1.4 Aims and objectives of the project

- In order to detect diabetic neuropathy, develop a smart, operator independent and user-friendly device, which is capable of generating a vibration stimulus with a required frequency and varying amplitude.

- To be able to robustly detect diabetic neuropathy, develop a vibration generating device which can effectively increase the vibration intensity in order to detect the vibration perception threshold of the subject.

- To develop a more reliable device by maintaining a constant pressure while applying vibration stimuli to the patient.

- To develop the risk assessment tool that is capable of utilising the clinical characteristics of a patient to predict the risk level of Diabetic neuropathy.

1.5 Outline

The research outlined in section 1.3 and 1.4 are given in the following chapters.

- Chapter 2 discusses about the existing methods and devices available for early detection of diabetes and identified their limitations.

- Chapter 3 discusses about the designing the device. The device development is based on the requirements and limitations as discussed in the Chapter 2. This chapter involves design description of the device, its electronic circuit development, software programming and development of graphic user interface. It shows the way of conducting the test for diabetic neuropathy subjects.

- Chapter 4 discusses the experimental study performed using VibraScan and Neurothesiometer.

- Chapter 5 discusses the comparative study between VibraScan and Neurothesiometer using human subjects.

- Chapter 6 explain the development of risk assessment tool of VibraScan based on the clinical characteristics of the subject. This tool is developed based on the analysis of the clinical data. For data analysis various methods such as ordinary least squares, ordinal logistic regression, artificial neural network and neural network based proportional odds model were implemented. It shows the results obtained from all these methods for comparison purpose and uses of best suited model for the tool development.

- Chapter 7 concludes with the findings of this research and discusses the limitations along with future directions.

Chapter 2 Methods for diagnosing Diabetic neuropathy

This Chapter focuses on the study and understanding of the existing methods available for diagnosing diabetic neuropathy. There are various methods available for screening purpose, however, the aim is to analyse the limitation of methods and come up with an idea of developing an innovative and smart device that can overcome the gaps in the existing devices. All the existing methods which are used for diagnosing diabetic neuropathy have been discussed along with their limitations. Another focus is also to investigate the feasibility for the patients to use the technology independently of performing the screening test.

All these methods will be analysed and the best suitable method for developing the prototype will be selected based on the criteria that it is non-invasive, easy to use and accurate. Devices that use vibration perception are generally considered as the gold standard for neuropathy assessment as they can efficiently predict the onset and progression of the complication (Coppini et al. 2001). Therefore, devices based on vibration perception were studied along with their limitations which will be discussed in this chapter.

2.1 Methods used for diagnosing diabetic neuropathy

There are various methods such as different clinical scores and devices available commercially to help diagnose DPN which include nerve conduction studies, DPN check, sudorimetry, SUDOSCAN, Neuropad, cardiac autonimic Function test, skin biopsy, corneal microscopy and Semmes-Weinstein monofilament test.

(a) **Clinical scores**

Clinical scores such as neuropathy disability score (NDS), Neuropathy symptoms score and Michigan Neuropathy screening instrument (MNSI) are commonly available for diagnosing purpose.

Neuropathy disability score

Neuropathy disability score (NDS) is the scoring system for diabetic neuropathy. NDS examines muscle weakness, cranial nerves, sensations and reflexes (Dyck et al. 1980b). It used to access 35 items on both sides to examine the sign of neuropathy. Some of the items in NDS do not check the abnormality of neuropathy. At present, the updated/modified version of NDS is used in practice which considers ankle reflex, pinprick, vibration, heat and cold sensation at both the side of the big toe with the score of 10. During the examination, if the score is 6 or more then it is considered to be an abnormal reaction (Moreira et al. 2005).

Neuropathy symptoms score

Neuropathy symptoms score (NSS) consist of examination related to tingling or numbness, burning, fatigue, aching and cramping (Chawla et al. 2013). It consists of 17 items which are divided into symptoms of muscle weakness (8 items), autonomic symptoms (5 items) and sensory disturbances(4 items) (Dyck et al. 1980a). If the answer is negative/absent then score is zero, if the answer is positive then score is 1 which can maximum reach to 17. If the score is greater than or equal to 1, it is considered to be abnormal. The limitation of NSS is, it is not used to show the progression of diabetic neuropathy (Dyck et al. 1997).

Michigan Neuropathy screening instrument

Michigan Neuropathy screening instruments are used to find the degree of neuropathy. It includes two types of assessments. One with 15 self-administered questionnaires and foot examination which includes assessment of vibratory sensation and ankle reflexes. This questionnaire includes questions related to positive and negative sensory symptoms (such as numbness, tingling and burning), muscles cramps, weakness, foot ulcers, and amputation. The foot examination is mostly used with the maximum score of eight where both the foot are independently measured. If the MNSI score is greater than or equal to 2, it is considered as positive for diabetic neuropathy instrument (Feldman et al. 1994). It helps to classify the various form of diabetic neuropathy, to identify the other causes of neuropathy, and it also provides information which can be used to monitor the disease.

There are few limitations of clinical scores as they are not much reliable and reproducible. Hence, it can be used to assess pain severity but not the pain scores to evaluate the progression of diabetic neuropathy. Again these scores are user dependent and the devices or tools used to obtain the measurements.

(b) Nerve Conduction studies (NCS):

Nerve conduction studies are used for diagnosis of diabetic peripheral neuropathy; since the eighteenth century, the response of the peripheral nervous system to electrical stimulation had been recognized (Isaacson 2003). The NCS usually means stimulating the nerve and recording the responses elsewhere from the nerve. The modern clinical NCS usually stimulate the peripheral nerve and record the response from the skeletal muscle innervated by the nerve. Currently, most of the NCS are performed with the surface, stimulating and recording electrodes (Jones 2012). The

site of stimulation is very important as surface measurements may not precisely provide all the anatomical information and uncertainty of the selecting the proper sites of stimulation or recording may limit the value of the study. A large amount of current is required for stimulating the deeper nerve such as the lower trunk of brachial plexus. Due to this stimulation, there is a chance of stimulating nearby muscle which can introduce the recording of the response elsewhere on the limb. The degree of uncertainty increases when recording proximal muscles because of the surrounding muscles and is more challenging; therefore NCS of distal is easier as it is isolated from the limb and other muscles which can help the examiner to be more certain as what is being stimulated and what is being recorded.

The bipolar probe consists of anode and cathode and is generally used as a nerve stimulator. To stimulate proximal spinal nerve needle electrode is used. The cathode is placed in the direction where action recording is intended to place or oriented distally. For the impedance matching the targeted site should be properly cleaned. The stimulus is provided at a constant current in the range of mill amperes. The selected site for applying the stimulus, all the elements of the nerve should be completely depolarized and could be achieved by applying the successive stimulus and start increasing the current to that extent when current has increased but the size of the recorded potential remains the same. This stimulus is known as the supramaximal stimulus. The current should be increased gradually by a constant increment of 10 mA until the response is detected. The position of stimulating electrode is carefully placed in such a way that optimal point of the nerve stimulation is isolated. Supramaximal stimulus is achieved by increasing the current. Usually, the duration of current is 0.1 milliseconds but it could be increased to 1 millisecond if the supramaximal response is not achieved till 100mA of the current (Jones 2012).

Recording electrodes consist of active and reference electrodes which are placed at some distance from the active electrode. This distance is important to generate the recorded potential obtained due to the difference in charges (Kincaid et al. 1993). For recording muscle or nerve activity, metal or self-adhesive electrodes are used. Electrodes placed very close to each other will produce a small response and placed very far apart will produce unwanted environmental artifacts. These environmental electrical artifacts can be minimized by placing the surface ground electrodes between stimulus and at the recording sites gel is applied to the skin to minimize the

impedance mostly for the small amplitude responses (response is in the range of millivolts to microvolts depending on structured electrodes).

Although there is a wide application and use of NCS, NCS remains limited due to the time involved in performing the test, the cost involved, special arrangements and laboratories should be available and most importantly patient has to undergo difficulties of long wait and inconveniences due to NCS. Technically NCS is more helpful in detecting large fiber neuropathy but unhelpful in detecting small fiber neuropathy. Conduction block or demyelination that occurs proximally is quite difficult to detect (Jabre 1981; Weber 1998).

(c) DPN check
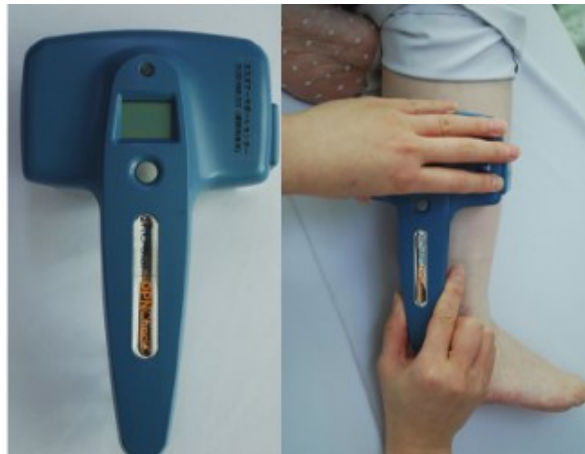
Figure 2.1: DPN check device (Hamasaki and Hamasaki 2017)

NC-stat DPN check is a point of care device, manufactured by NeuroMetrix Inc. is placed on the skin on the sural nerve to measures sural nerve conduction velocity (CV) and sensory nerve action potential (SNAP) as shown in Figure 2.1. The measurement is displayed in terms of numbers and based on the thresholds level of the measured value the abnormality or the severity can be pre-defined, lower the SNAP and CV more associated with diabetic neuropathy (Abraham and Abraham 1987). This can help patients to detect the presence of diabetic neuropathy. NC- Stat has shown the specificity of 82% and sensitivity of 92% compared to nerve conduction studies (Perkins et al. 2006).

The limitation of using DPN check is it is a bit difficult to locate the sural nerve for which trained operator is needed. There are small numbers of people in which sural nerve is not present and therefore NC-Stat DPN check is not possible to use for these patients.

(d) Neuropad

Neuropad usually measures the irregularities in the peripheral nerves. It consists of two tests per kit which can be used for each foot. For performing this experiment patient have to remove his/her shoes and socks and wait for a few minutes before starting the test (Malik 2008). The experiment has to perform under constant ambient temperature. The examiner places the Neuropad at the callus free area between the first and second metatarsals head to examine the colour change for 10 minutes (Ziegler et al. 2005; Papanas et al. 2013). It measures sweat production based on colour change. Cobalt 2 compound is used for the detection which changes the colour from blue to pink. The colour change occurs because of the chemical reaction between anhydrous cobalt 2 chloride present in the indicator and water from the sweat glands. If the sweat glands are functioning normally then water molecules are enough to change the colour within 10 minutes. It indicates that if the colour changes from blue (dry state) to pink (dermal foot perspiration), it indicates the normal function of sudomotor and if it remains blue or stays bit patchy at the time threshold or takes a longer period of time then considered as the reduced sudomotor function. The absolute time taken by the Neuropad to change the colour may suggest that this parameter can be used to determine the severity of diabetic neuropathy (Papanas et al. 2007). The advantage of using Neuropad is, it does not require subject cooperation as the test is based on the chemical reaction and may contribute to the early detection of diabetic neuropathy (Papanas et al. 2011). The limitations are that the time period is set to determine the severity level i.e. 10 minutes; however it has not achieved high applicability. Because of this reason, various different threshold level was set like 15 or 20 minutes, however, these thresholds have not shown many significant changes (Papanas et al. 2011).

(e) Sudorimetry

Sweat glands dysfunction is also one of the early symptoms of the DPN. Autonomic nerve dysfunction is an important aspect which is always undiagnosed or overlooked (Papanas and Ziegler 2011). Sweat glands are affected at the early stage of the diabetes mellitus which are innervated by small myelinated cholinergic sympathetic fibres. Due to sweat glands dysfunction, the skin will remain dry that is more prone to a bacterial and fungal infection which can cause foot ulceration. To prevent this complication diagnosing sweat glands dysfunction could be a useful screening tool for

DPN (Sumner et al. 2003; Yajnik et al. 2012). Stewart et al (1992) found that autonomic nerves controlling heart rate are less likely to damage than that of the sympathetic sudomotor fibers which proved that sudorimetry is the useful tool for diagnosing DPN at the early stage. There are various methods used for the detection of sweat glands dysfunction such as qualitative sudomotor action reflex, silastic imprint method, electrochemical sweat conduction, and thermoregulatory sweat test. Small-fiber polyneuropathy can be detected with a sensitivity of 80% by qualitative sudomotor action reflex test (QSART) (Thaisetthawatkul et al. 2013). The sweat production is measured by infusing acetylcholine into the skin to stimulate the postganglionic nerve. The limitations of this test are, it is time-consuming and requires expensive equipment (Illigens and Gibbons 2009). Electrochemical sweat conductance (ESC) test is performed by a chemical reaction between electrodes and chloride of the sweat glands after applying low-level voltage stimulation. Studies showed that Lower ESC refers to increasing vibration perception threshold (VPT) after testing on 265 diabetic patients. Thus the study concludes that lower ESC refers to sweat gland dysfunction and can be the sign of the early stage of DPN (Yajnik et al. 2012). In a thermoregulatory sweat test, the sweat production is evaluated by increasing the temperature of the skin and after that, the dye is used to measure the sweat production. This test is non-quantitative and can be used either to test local area or for whole body sweat production (Illigens and Gibbons 2009). In Silastic imprint method the sweat is produced using acetylcholine and silastic material are placed on the skin to quantify the test (Stewart et al. 1994). The drawback of the test is, silastic material is prone to dirt and hair.

(f) SUDOSCAN

SUDOSCAN is the device which is non-invasive, easy to use sudomotor test for assessment of sweat gland function (Mayaudon et al. 2010). It consists of two sets of stainless steel electrodes for both hands and feet which are connected to the computer for recording and maintaining data of the subjects under test. These electrodes are alternately used as cathode or anode where the DC voltage of less than 4V is applied to the anode. The examination is based on electrochemical reaction occur between the stainless steel plate electrodes and the chloride ions present in the sweat glands when hand and feet are placed (EH Schwarz et al. 2011). Low voltage of less than 4V is applied to the electrodes to attract the chloride ions from the sweat

glands. Due to the reverse iontophoresis process the voltage is developed at the cathode and current between anode and cathode is based on the chloride ion concentration. Iontophoresis is the process where electric current is applied through electrodes to deliver a chemical substance to the skin based on electromotive forces (Zaid et al. 2018). This will measure the conductance of palms and soles from the derivative current of the applied voltage (Ayoub et al. 2010). The electrochemical skin conduction (ESC) is measured as the ratio between the generated current and DC low voltage applied to the electrode is expressed in micro siemens. ESC is helpful in determining sudomotor dysfunction in the subjects with diabetes. The severity of ESC is divided into four different categories based on the threshold value of ESC i.e. no dysfunction if >60 μS, moderate dysfunction if between 60 and 40 μS while severe dysfunction when <40 μS (Casellini et al. 2013).

This tool is used for the measurement of small fibre neuropathy and peripheral autonomic dysfunction. Still, more studies are required which can clearly show that SUDOSCAN outcomes are predictive for diabetic neuropathy development and foot ulceration (Selvarajah et al. 2015).

(g) Cardiac autonomic reflex tests

Cardiac autonomic neuropathy (CAN) is one of the chronic and serious complications of diabetic neuropathy which occur in patients with long term type 2 diabetes mellitus. The report shows that it is found in one-quarter of type 1 and in one-third of type 2 diabetic subjects which might predict the change of development of stroke. CAN patients may suffer from complications like tachycardia, exercise intolerance, postural hypotension, enhanced and myocardial infarction (Vinik et al. 2013). This type of cardiac dysfunction may affect the quality of life of diabetic patients and major risk of life-threatening outcomes.

There are various methods available for diagnosing CAN such as evaluating symptoms and signs through clinical practice, cardiac autonomic reflex tests (CARTs) depending on heart rate and blood pressure and using blood pressure monitor (Spallone et al. 2011). CARTs examine the cardiac autonomic function by time domain HR response to breathing, Valsalva maneuver change, and the response of the heart rate and blood pressure changes. In autonomic testing, indirect autonomic measures are considered as the gold standard. The non-invasive, easy and safe technique of measuring heart rate variations during deep breathing, heart rate measured during lying and standing

and Valsalva maneuver refers to parasympathetic function (Vinik et al. 2013). Orthostatic hypotension, sustained isometric muscular strain and blood pressure response to a Valsalva maneuver refers to sympathetic function (Vinik et al. 2013). CARTs are considered to be sensitive, specific, reproducible, safe and standardized. It has been suggested that CAN assessment should be performed with more than one heart rate tests. These tests are relevant for diagnosis of CAN which is the complication of diabetic neuropathy.

(h) Skin Biopsy

Skin biopsy can be performed at the required site of the body using disposable punch with the diameter of around 3mm under local anesthesia using lidocaine. This techniques has not reported any side effect and can be performed without the need of suture. Healing process mainly complete within a week where scar may not last for more than 3 months. This is used to examine innervation of epidermis, dermis, and sweat glands . To investigate the only innervation of epidermis, an even less invasive technique names "blistter technique" can be used (Lauria and Lombardi 2007) . Skin biopsy is usually considered to be safe, cheap and painless technique used for the evaluation of the small fiber neuropathy (include the symptoms of burning, deep and aching pains in the feet). Using bright field microscopy to measure the density of the fibers. It can also be repeated within nerve fiber territory to determine the effect of the treatment in which steroids and immunoglobulin also used to determine the progression of diabetic neuropathy. According to one of the study, the positive predictive value is estimated as 93% in the detection of small fibre neuropathy, with the specificity of 97% and sensitivity from 69% to 82% (Lauria et al. 2005). Skin biopsy is used to investigate the various function of the small fiber which is helpful in clinical practice. This technique is useful in pain neuropathy to detect the abnormality i.e. unmyelinated axon that carries pain sensation of the target nerve. Skin biopsy is also used for detection of demyelinating neuropathies (Pan et al. 2003). The limitations of skin biopsy are, it is an invasive technique, It has to be performed in a limited number of specialised clinics and where the diagnosis of the abnormalities has to be preceded in the established laboratory (Lauria and Lombardi 2007).

(i) Corneal confocal microscopy

It has been reported that the evaluation of corneal nerve structure performed using corneal confocal microscopy (CCM) has been considered as a reliable measure of

diabetic neuropathy. CCM of human eye is one of the new screening modality which is used for early demonstration of nerve fibre damage. In this technique, CMM makes use of a light beam to pass through the aperture which is focused by the objective lens into the layer of cornea. Elimination of all the light is done by beam splitter and a photodetection device. Using this technique, three methodologies such as tandem scanning CCM, split scanning CCM and laser scanning CCM has been developed (Papanas and Ziegler 2013). Split scanning CCM and laser scanning CCM are used to examine corneal nerve damage in patients with diabetes with or without diabetic neuropathy (Papanas and Ziegler 2013). It is considered to be an effective non-invasive, repeatable measurement technique for the detection of diabetic neuropathy. Considering the fact that corneal nerve fibre damage is more common and severe in subjects within DSPN, it is recommended to use CMM for its diagnosis. It was noted that in the recently diagnosed diabetic patients also, CMM is sensitive enough to determine corneal nerve fiber perturbations (Ziegler et al. 2014b). This technique is used for the early diagnosis of high-risk foot and nerve damage with moderate sensitivity and specificity (Papanas and Ziegler 2015). Finally, CMM is the non-invasive, fast, reproducible, measures small fiber nerves and quantitative technique. However, many more critical questions need to be addressed like whether CMM parameter is capable enough to predict patients oriented results such as the pain and disability. Hence, this technique can be useful in diabetic neuropathy assessment with the further implementation of more image processing/analysis techniques for improving its performance.

(j) Semmes-Weinstein Monofilament examination – pressure perception examination

Physicians use many quantitative methods for the detection of diabetic sensory peripheral neuropathy. This method is mostly used for the detection of the protective loss or for the pressure perception examination. The threshold of 5.07/10 gram monofilament was established in 1985 (Birke and Sims 1986). The different size of the monofilament 4.17, 5.07 and 6.28 were tested on 72 patient with leprosy and 28 patients with diabetes mellitus. The test has concluded that 5.07 monofilament is the threshold for detecting DPN as no patient with foot ulceration was able to sense the 5.07 monofilament. Another study was performed where 199 patients were tested and it was concluded that 5.07 is best for predicting foot ulceration in diabetes mellitus patients (Olmos et al. 1995). The main advantages of using Monofilament

examination are it is non-invasive, low cost, rapid, routinely self-assessment and easy to use the method. Different sites on the plantar surface of the foot have been chosen for the monofilament examination. However, it is not fixed which sites and how many times each site needs to be examined. Usually, three or five sites are used for the monofilament examination. International Working Group on Diabetic Foot has recommended using three sites that are planter surface of the distal hallux, first and fifth metatarsals head for the examination (Karl Guttormsen 2017). The cost of disposable monofilament is about $0.50 (Feng et al. 2009) and the sensitivity of the monofilament test is >87% and specificity is ranging from 68% to 100% (Boulton et al. 2005a; Dros et al. 2009). Various methods used such as pinprick and a light touch, however, one of the most important limitations of these modalities is the application of stimulus which is inconsistent while the application of monofilament stimulus provides constant pressure (Smieja et al. 1999; Schaper et al. 2016). This test is widely used as a screening tool for DPN (Mayfield and Sugarman 2000) but not for the definite diagnosis of sensory neuropathy. The Procedure for using Monofilament test is as described below:

Figure 2.2: Vibration sites for application of monofilament test (Schaper et al. 2016)

- The patient should feel relax and ready for the 10g Semmes-Weinstein Monofilament examination. The test should be performed in a quiet environment.
- Apply the 10g Monofilament on the hands so that the patient is aware of the type of applied pressure.
- Apply the monofilament on any of the test sites as shown in Figure 2.2.
- Monofilament should be applied perpendicular to the sites for 1 second until it bends.
- The total duration of applying the monofilament and removal should be around 2 seconds.
- Apply the pressure in all the three sites of both the foot and the patient is asked to respond whether they feel the pressure or not and where they feel the pressure.
- The test needs to be repeated for 3 times at each site. Note the answers responded by the patient.

- Pressure perception/protective sensation is present if the patient's two out of three answers are correct and there is a loss of protective sensation if two out of three answers are incorrect for that particular site (Schaper et al. 2016).

(k) Ankle jerk

The Ankle jerk is also known as an ankle/Achilles reflex test. This test is performed using a standard reflex /neurological hammer. The shape of the hammer is a triangle and flat part of the hammer is used to find the reaction of the reflex on the Achilles tendon. The clinician/practitioner holds the standard hammer using the handle with their thumb and forefinger where the flat part is towards the subject's Achilles tendon area. Other than standard hammer there is an availability of advanced reflex hammer similar to pendulum hammer.

Figure 2.3: Ankle jerk test (Tanenberg and D. Donofrio 2008)

This test is simple and a part of lower limb examination. It can be used for diagnosing complications like peripheral neuropathy, hypothyroidism or Charcot Marie tooth disease by measuring the grade of Achilles tendon. In this test, the patient should be laying on the examination table with their Achilles tendon is exposed from superior calf to plantar aspect of the foot (Ziff and Stark 2017) shown in Figure 2.3. When the examiner strikes the Achilles tendon directly with the standard reflex hammer, it is considered as positive if the calf muscle contracts and foot plantar flexes. The degree of the positive results is graded based on the scale from 0 to 4+, where 0 is the no response, 1+ is considered to diminish, 2+ is considered average, 3+ is above average and 4+ is considered as hyperactive with clonus (Ziff and Stark 2017).

This test is used only for finding the Achilles reflex with rare complications of performing this test. There may be a possibility of post-test pain or soreness if performed poorly by the practitioner.

2.2 Devices based on vibration perception thresholds

Vibration perception threshold (VPT) is also one of the widely used concepts for the diagnosis of sensory neuropathy. It is defined as the lowest voltage at which vibration is detected up to 50% of the time tested (Michelle Branigan 2014). VPT is considered as quick and low risk for the detection of long-term complications of neuropathy based on the type of the instruments used as per the expert opinion (Garrow and Boulton 2006). Clinical tools such as 128-hertz tuning fork, a semi-quantitative electromechanical instrument as Biothesiometer and Neurothesiometer are commonly used for measuring VPT.

(a) Tuning Fork

There are mainly three types of tuning fork used for the assessment of VPT such as non-graduated tuning fork, graduated tuning fork and an electronic tuning fork. A simple non-graduated 128 Hertz tuning fork is just used to measure the absence and presence of vibration perception in the patient, because of this limitation it is psychophysical in nature and due to lack of standardization it cannot be used for clinical findings. There was a need for a more advanced instrument that can predict the amplitude at which vibration is perceptible led to the development of graduated tuning fork. The graduated tuning fork uses the vibration extinction threshold with the scale from 0 to 8. When the score is (less than 4/8) then it is the alarm for high-risk complications of neuropathy (Garrow and Boulton 2006). There are several advantages of using a tuning fork it is easy to use, quick and portable where the patient does have to undergo for the long and complex procedure. The procedure for the test is fairly simple as shown in Figure 2.4.

Figure 2.4: Procedure to conduct a tuning fork test (Schaper et al. 2016)

The sensory exam should be carried out in a quiet and relaxed setting. First, vibrate the tuning fork and apply the tuning fork on the patient's wrists (or elbow or clavicle) so that he or she knows what to expect.

- Tuning fork is applied on a bony part of the first toe on the dorsal side of the distal phalanx. The patient must not be able to see whether or where the examiner applies the tuning fork

- Apply the tuning fork perpendicularly with constant pressure.

- Repeat the procedure for two times and at least one 'mock' where tuning fork is not vibrating.

- If the patients is giving correct answers i.e. vibration is provided and subject could be able to sense at least two out of three applications then considered as normal and if two out of three answers are incorrect then the patient is under the risk of ulceration.

- If the patient is unable to sense the vibrations on the big toe, the test is repeated more proximally (malleolus, tibial tuberositas).

- Encourage the patient during testing by giving positive feedback (Schaper et al. 2016).

(b) Electronic tuning fork

As discussed, 128 Hz tuning fork have used for the detection and progression of diabetic neuropathy. Although tuning fork is the sensitive tool, however there is a lack standardisation and qualification of neuropathy findings (O'Brien and Karem 2014b). For improving the standardisation of the testing there is an introduction of a novel 128 Hz electronic tuning fork (ETF) (O'Brien and Karem 2014b). The ETF produces the vibration and the decay rate is the same as the standard tuning fork. In order to perform the timed vibration test more accurately the integrated timer is introduced electronically that facilitate reproducible timed vibration test (O'Brien and Karem 2014a). The time vibration test have shown improved method for detecting diabetic neuropathy (Botez et al. 2009).

The method of using ETF is simple and straight forward. When the device is activated, it starts the vibration and integrated timer. When it is applied on the hallux, subject will be asked to verbally indicate 'yes' or 'no' after they perceive the vibration. If they indicate 'no' it needs to indicate as 0 sec elapsed time. If they say 'yes' then they need to ask when vibration has subsided after their perception of vibration by saying 'now' and at that moment vibration needs to be stop to record the elapsed time.

The limitation of ETF is there is no variation in applied vibration stimulation in terms of vibration amplitude with constant frequency. So if the vibration amplitude can vary then it may possible to measure precise vibration perception threshold of diabetic patients.

(c) **Biothesiometer and Neurothesiometer**

Biothesiometer and Neurothesiometer are quick, portable and inexpensive instruments (Garrow and Boulton 2006). They are semiquantitative electromagnetic in nature. It is easy to categories the high risk and low risk of ulceration based on VPT scores. If VPT is more than 25 score, the patient is at high risk of ulceration and patients having less than 15 scores, the patient is at low risk of ulceration (Van Deursen et al. 2001).

Biothesiometer is the electromechanical device which is used to produce vibration through vibration probe. It is basically used to determine vibration perception threshold. Biothesiometer (BioMedical, Newbury, Ohio, USA) is widely used by clinicians (Figure 2.5), however, as Biothesiometer is operated on main electric supply has raised the concern for safety in United Kingdom that led to the development of battery-operated Neurothesiometer (Arnold Hoi-well, London, UK)(Watts et al. 1986) as shown in Figure 2.6.

Figure 2.5: Biothesiometer (BioMedical, Newbury, Ohio, USA)

Figure 2.6: Neurothesiometer (Neurothesiometer 2016)

With the advancement of technology, the Analog Biothesiometer is replaced by Digital Biothesiometer. The Biothesiometer is the electronic tuning fork where the amplitude is completely adjustable in a particular range and based on this amplitude it is possible to record the human sensation of vibration which operates on electricity.

(d) Procedure to use Biothesiometer / Neurothesiometer

Figure 2.7: Testing using Biothesiometer (Singh et al. 2012)

Biothesiometer is very simple, convenient and easy to use. Normally pulp of the big toe,1st,3rd and 5th metatarsals are chosen as the vibration sites as shown in Figure 2.7 (Singh et al. 2012). Vibration probe is placed perpendicular on the selected sites and allowed to vibrate at different intensities. The manual potentiometer is used to adjust the vibration intensity. The range of the dial is from 0 to 50 Volts in order to provide the vibration at different intensities. The operator has to hold the vibration probe on the site to be examined. The Vibration intensity is increased until the patient feels the vibration. The patient is asked to respond 'Yes' whenever vibration is felt. It records the exact voltage at which the patient feels the vibration. The degree of loss of sensation depends on the recorded voltage. Higher the recorded voltage, the patient has more susceptibility to the loss of sensation and greater risk of foot ulceration. According to this study (Singh et al. 2012), if the VPT score less than 15V then subject is having a low risk of DPN, between16 to 24V the risk is moderate and greater than 24V is the high risk for DPN.

To diagnose the sensation loss, the Biothesiometer uses the vibration to stimulate the human receptors so, frequency and amplitude of the vibration have to be taken into consideration. When measuring this, there are mainly four type receptors Meissner receptor, Pacinian corpuscles, Merkel disks and Ruffini endings situated at the dermis and epidermis layer of the skin Figure 2.8. In order to diagnose the sensation of the receptors, there are guidelines for receptor nature, its activation and measurements parameter.
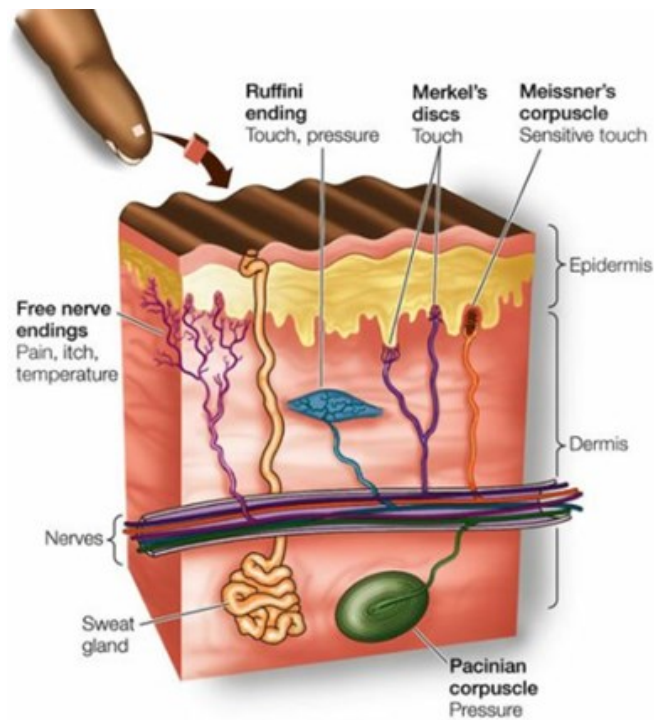
Figure 2.8 : Epidermis of the skin (Rochester 2007)

Meissner receptor

This receptor is responsible for high sensing pressure and primarily related to touch and faster movements. In order to activate the Meissner receptor, the activation frequency should be (Rochester 2007) in the range of the 40 to 100 cycles per seconds (Goldberg and Lindblom 1979).

Pacinian corpuscles

Pacinian corpuscle is concentrated at fingertips, palms, soles, toes, muscle, around the blood vessels, joint ligaments, nerve trunks and bony periosteum (Bolanowski and Zwislocki 1984; Temlett 2009). Displacement of subcutaneous tissue and periosteum which contains Pacinian corpuscle gets activated by the vibration from the energized tuning fork. If horizontal displacement or the stretch is applied then it may be less effective to activate Pacinian corpuscle (Mountcastle et al. 1967). It can be activated at frequencies as low as 0.4 Hz.

Merkel disks are sensitive to pressure and slower movements: Although not targeted, these are insensitive to changes in frequency and consequently, yields a curve that is essentially flat (Verrillo and Bolanowski 2003).

Ruffini ending are sensitive to pressure and slower movements and can be accessed by using an extremely small contractor surface driven at high intensities.

The utility of Biothesiometer and Neurothesiometer based on above perception signifies that receptors are responding to the frequency of vibrations. Biothesiometer utilizes 100 hertz which is the frequency between Pacinian corpuscles (around 250) and Meissner corpuscles (around 40) (Duke et al. 2007). However, other studies have found that vibration threshold at lower frequencies (for Biothesiometer at 50 or 60 Hz) there is an effect of temperature difference within the normal skin temperature (Halonen 1986). Looking at the Biothesiometer and Neurothesiometer vibration frequency, different manufacturer have utilized different frequencies that are either 50 - 60 Hertz or 100 hertz which ultimately comes under the frequency range to target Meissner and Pacinian corpuscles. Young et al (1993) have done the comparative study between Biothesiometer and Neurothesiometer. They concluded that Neurothesiometer instrument is developed to replace the Biothesiometer to measure the vibration perception threshold for the screening of diabetic neuropathy. In this study 85 diabetic patients having an average duration of diabetes for 12 years and mean age of 61 are selected for measuring VPT using both Biothesiometer and Neurothesiometer. There was a close correlation between two devices (r = 0.93 p < 0.0001) when both VPTs are compared. Biothesiometer VPT was 29.9 ± 15.2V and Neurothesiometer VPT was 26.2 ± 13.4 V. Biothesiometer operated from the mains power vibrates at 50 Hz of frequency and Neurothesiometer which is battery operated vibrates at 56 Hz. The patient coefficient of variance for Biothesiometer and Neurothesiometer was 8.6% and 8.1% respectively. Although Neurothesiometer is more expensive than Biothesiometer but it is self-contained, battery operated and well suited for screening for DPN.

Limitations of Biothesiometer/Neurothesiometer:

1. The VPT normally increases with age so that above the age of 70- a normal VPT score is already close to the maximum output of the Biothesiometer (Bloom et al. 1984).

2. Many subjects with neuropathy appear to have scored at the limit of the Biothesiometer amplitude scale – close to or at 50 V indicative of a ceiling effect (Van Deursen et al. 2001).

3. It is noted that the Biothesiometer probe does not vibrate in a single plane. There was a large difference between two Biothesiometer in relation to the applied voltage and the actual stimulator movement (Goldberg and Lindblom 1979).

4. Biothesiometer has not been taken into routine practice perhaps because of the confounding effect of limb temperature, psychological factors, the amount of pressure

applied by the vibratory probe and choice of the limb as well as tactile surface of the skin (Pourhamidi et al. 2014)

5. Biothesiometer is not sensitive enough to detect the small fiber neuropathy but might be useful for the early detection of the neuropathy when used in the combination with the measure of small nerve fibres function such as skin biopsies (Pourhamidi et al. 2014).

6. Biothesiometer has the disadvantage of being larger and requiring attachment to an electrical point to drive an accelerometer to activate the probe although may apply vertical pressure more accurately and objectively. However, this limitation has been overcome by developing battery operated Neurothesiometer (Ohnishi et al. 1994).

7. As the vibration probe is handled by the operator, the pressure of the applied stimuli may vary while testing vibration perception threshold.

8. Neurothesiometer and Biothesiometer utilize fixed frequency to vibrate the probe, it cannot be changed once it is manufactured (Table 2.1).

Table 2.1: List of companies' manufacturer of Biomethiosmeter/Neurothesiometer with frequency specifications

Serial Number	Company	Device	Fixed Frequency(Hertz)
1	Diabetic foot care India Private limited (Biothesiometer 2017b)	Digital Biothesiometer	120
2	Beijing beauty equipment company (Biothesiometer 2017a).	Biothesiometer	50
3	Algeo Ltd (UK) (Neurothesiometer 2017)	Neurothesiometer	50
4	Trimbio (Neurothesiometer 2016)	Neurothesiometer	50

Going through the above limitations of the devices used for the detection of DPN using vibration perception method there are several parameters which are really important to consider for developing a smart device. The limitations are vibration frequency dependent, vibration sites, the pressure of the probe on the skin and temperature are the other factors to consider. If all these parameters are considered properly then it will be easy to accurately detect neuropathy at an early stage based on receptor activation Figure 2.9 shows factors associated with accurate determination of DPN.
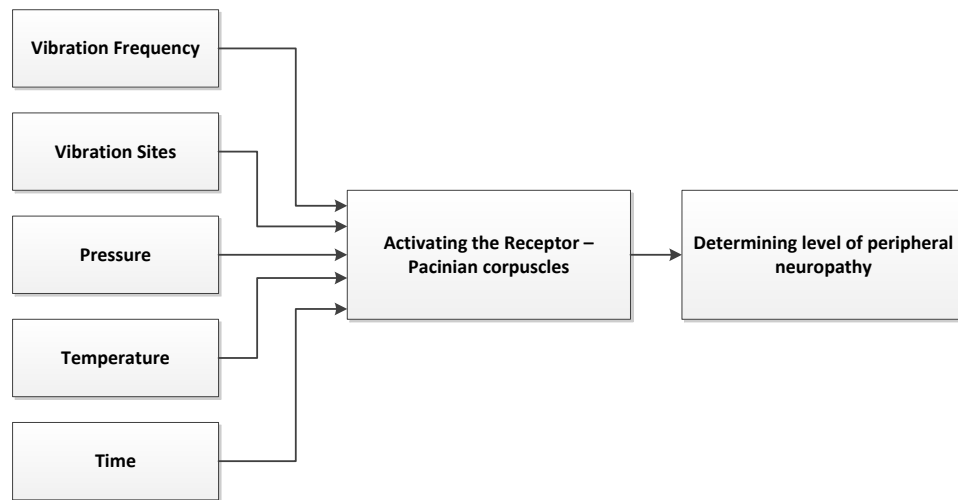
Figure 2.9: Activation of receptors to determine peripheral neuropathy

As per the gathered information from the literature search, all the necessary parameters such as pressure, vibration sites, vibration amplitude, and temperature were considered as shown in Table 2.2.

Table 2.2: Key design parameters identified through Literature survey

Author	Description
Pressure	
Lowenthal et al (1987)	By increasing the weight from 200 g to 400 g, that is increasing the pressure of the applied stimulus is increased, there is a considered reduction in the vibration sensory threshold (VST) however, this was not seen when weight is > 400. In peripheral neuropathy, VST decreases as the pressure of applied stimulus increases (Lowenthal et al. 1987).
Vibration sites	
Williams et al (1988)	Vibration perception threshold was measured at both big toes and both medial malleoli for screening of diabetic neuropathy using Biothesiometer (Williams et al. 1988).
Van Deursen et al (2001)	The Plantar surface of the feet was chosen because this area is routinely used in screening to characterize the risk of ulceration in diabetic neuropathy (Van Deursen et al. 2001).
Loseth et al (2007)	Great toe was chosen to be examined using 256 Hz and128 Hz tuning fork (Løseth et al. 2007).
Singh et al (2012)	Various points on the foot like the pulp of the big toe, first, third and fifth metatarsal head were used for examination using Biothesiometer (Singh et al. 2012).

Author	Description
Vibration amplitude	
Van Deursen et al (2001)	The vibration of 1000 micrometer applied to the foot is quite severe and can travel through the limb so that it will be perceived at the ankle, the knee or even more proximally, despite the fact that they took measures to avoid this as much as possible (Van Deursen et al. 2001).
Temperature	
Verrillo et al (2003)	The Pacinian channel at suprathreshold levels of vibratory stimulation is affected by the temperature at the surface of the skin as is the Ruffini channel. As temperature increases, the perceived intensity of vibration increases in an orderly manner. Temperature has an effect on the Pacinian channel above 100 Hz. The subjective magnitude of vibration is not appreciably influenced by skin temperature at frequencies that optimally activate the Meissner and Merkel channel (Verrillo and Bolanowski 2003)
O' Brien et al (2014)	An ambient temperature of 70F to 72 F(21 to 22-degree Celsius) was set constant during the VPT test using 128-hertz electronic tuning fork in the treatment room (O'Brien and Karem 2014a).
	If the examiner detected vibration for less than 20 sec in total hallux score (10 sec per hallux), the patient was considered to have normal sensation. A score greater than 40 Sec (20 sec per hallux) indicated neuropathy (O'Brien and Karem 2014a).

In conclusion, most of the methods and test available for diagnosing diabetic neuropathy were studied in details. Devices such as tuning fork, Biothesiometer/Neurothesiometer are available to measure vibration perception threshold, however, these techniques are operator dependent and pressure measurement is not taken into consideration. To overcome limitations the aim of developing a standalone, portable, operator-independent device where the result can be automatically interpreted is taken into account for developing a device. The technique of diagnosing DN through vibration perception is considered for the development of the smart device.

Chapter 3 Development of Device

This chapter focuses on the development of the neuropathy assessment device. As discussed in Chapter 2, various methods available for detection of diabetic neuropathy were carefully studied, the techniques based on the vibration perception threshold were considered for the development of the device. Device development involves various steps like requirement gathering phase (focuses on parameters like pressure, vibration sites, vibration characteristics, and vibration direction), design drawing, hardware designing, electronic circuit and software development which will be discussed in detail. As the device is based on the vibration sensation, various available vibrator motors/actuators such as Eccentric Rotating Mass Vibration (ERM), linear resonance actuators and C2 HDLF tactor were experimented to identify their vibration characteristics (like amplitude, frequency and vibration direction). The analysis on selecting these motors were performed and to come out with specific. C2 HDLF tactor which is capable of generating required nature of vibration. **Pulse width modulation technique** was used for controlling the motors in terms of amplitude and frequency. For real-time monitoring of the pressure, Force sensitive resistors were used and its placement was critically analysed. The initial design was developed for one foot for the evaluation phase. The evaluation phase involved hardware design, electronic circuit and software development for the initial version of device.

Based on the evaluation results the design was upgraded for both feet. In the latest version of design, to avoid the vibration leakage, the **vibration isolation technique** was implemented using springs with its technical analysis. The step by step development of the device is explained in the chapter. Graphic user interface was made user-friendly, easy to understand with real time pressure monitoring option. The technique of conducting the test is also updated which reduces the overall time of conducting the test. The whole setup is wirelessly controlled using Bluetooth module which will be described in the electronic circuit section. Later on, the plan to perform comparative study with Neurothesiometer device for standardisation has been presented with experiments on the human subjects.

3.1 Requirements for Device development

The following parameters were considered for the device development:
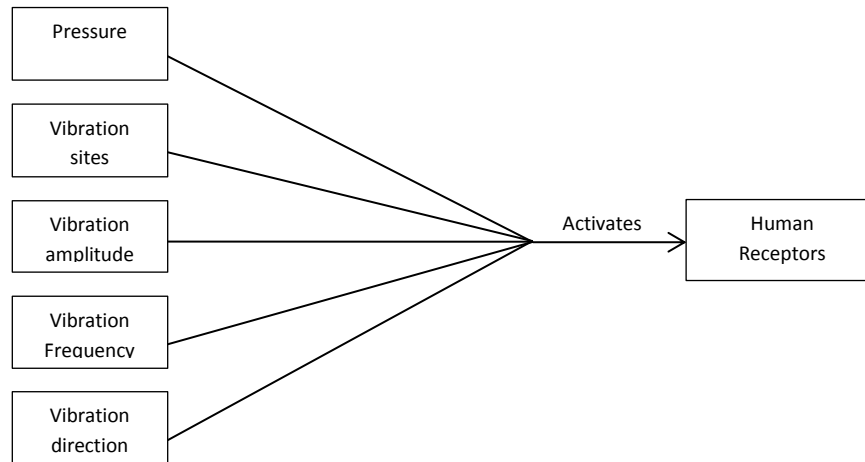
Figure 3.1 : Requirements for activating human touch receptors

(1) *Pressure* is considered while applying vibration to the human subject. Neurothesiometer is used for detection of neuropathy where the vibration stimulus is provided by holding the vibration probe against the body contact surface. During the contact, there is a possibility of applying vibration with varying pressure. Applying vibration with inconsistent pressure may affect the activation of the receptors. According to a study when the weight is increased from 200 grams to 400 grams the vibration perception threshold increases and that when the Neurothesiometer vibration probe at rest position it exerts the pressure of 320 grams (Lowenthal et al. 1987). In order to apply uniform and consistent pressure, innovative design has to be developed. In this project a weighing scale like platform is proposed where vibration motor can be fixed on the plate and subject is allowed to comfortably place their feet on the plate to receive vibration. The plate for placing the feet is kept inclined and Force sensitive resistors are used to monitor the pressure. They are used for the continuous monitoring of the pressure applied on the plantar surface of the foot. Pressure will be monitored during entire test so that it provides consistent result.

(2) It is important to identify the correct *vibration sites* to apply the vibration, as this is the key point for the early detection of diabetic neuropathy. There is a loss of touch and vibration sensation at the early stage of the disease. Therefore those sites can be selected which are primarily affected and are more likely to experience the early consequences of the complication. Usually, for monofilament test as discussed in Chapter 2, according to International Working Group on the Diabetic Foot (2015) for

conducting the monofilament test, *Big toe, third and fifth metatarsals* are selected as vibration sites (Foot 2015). Vibration perception threshold examination using Biothesiometer were carried out on the *big toe, first, third and fifth* metatarsal as the vibration sites (Singh et al. 2012). An advice for conducting the tuning fork test by International Working Group on the Diabetic Foot (2015), *big toe* is selected as the vibration site (Foot 2015). Based on these studies, *Big toe* is considered to be the most appropriate site for applying the vibration in the proposed study.

(3) Vibration characteristic is defined by two parameters, Frequency and Amplitude. The *vibration amplitude* is the peak point referred to as the maximum excursion of the wave from the zero or equilibrium point. And peak to peak amplitude refers to the distance from positive peak to negative peak in the vibration wave. Vibration amplitude is measured in three different units such as displacement (mm/microns), velocity (mm/s), and acceleration (mm/s^2). The displacement is also related to voltage. Vibration amplitude is important to precisely identify the vibration perception threshold of the skin since the subject will feel the effect of the vibration. As the amplitude increases, the effect of sensing the vibration will become more prominent. To correlate this information with sensation, the specification of biothesiometer and neurothesiometer are studied. In biothesiometer (Beijing Beauty Equipment Company) the peak amplitude range of vibration probe is between 0μm - 25μm, maximum peak amplitude range of vibration probe is 25μm, the error range of ± 10mm (Biothesiometer 2017a). For Neurothesiometer (by Algeos), the range may be switched to Normal = 0 to 50 volts/0-250 microns and Expanded = 0 to 25 volts/0-62.5 microns (Neurothesiometer 2017). This shows that the maximum displacement of the vibration goes up to 250 microns which means the vibration amplitude by our proposed method should be equal to or more than the required range. This point is to be considered and range of the vibration for the proposed design is to be from 0 to 350 microns (maximum peak amplitude) at 100 Hz.

(4) *Vibration frequency* plays a vital role in activating the receptors. As discussed in Chapter 2, there are four types of receptors and have different ranges of the frequency. Meissner receptors respond at around 40 hertz and Pacinian receptors respond at around 250 hertz. To activate these groups of receptors biothesiometer and neurothesiometer vibrates at a specific frequency. According to the specifications of these existing devices, as discussed in Chapter 2, both 50 Hz and 120 Hz vibration

frequencies are provided to the vibration probe and the frequency is generally fixed, the user cannot change it. In the proposed design a wide range of frequencies is possible to vibrate and can be fixed as well. So the range of the frequencies available in the proposed design is from 50 Hertz to 120 hertz.

(5) Other than vibration frequency and amplitude, activation of the receptor also depends on the *vibration or displacement direction*. Vibration could be on the horizontal or in the perpendicular direction of the skin. If horizontal displacement or stretch is applied then it may be less effective to activate Pacinian corpuscle (Mountcastle et al. 1967). So vibrator motor in the proposed design is selected that vibrates in perpendicular to the skin to activate the receptors.

Considering all these parameters, development of platform based device was considered; here the method of conducting the test will be different from the Neurothesiometer/ biothesiometer. The detailed design of the device is discussed below.

3.2 Designing the device

For providing the vibration stimulus at the big toe, a platform based device was considered. So the question here is whether a subject should stand on the plate and start the test or should sit on chair while placing the feet on inclined plate. While standing on the platform, there could not be the possibility of changing the pressure and depending on the weight of the person the pressure may vary while conducting the vibration perception test. However, this is not a comfortable position, the idea of conducting the test by placing the feet on the platform after sitting on the chair seems more comfortable. In this way, the pressure exerting on the vibration motors can be monitored using sensors while vibration is applied.

The design of the device is first modelled using computer aided software called Solidworks. At first it was designed for one foot (left). The intension was to create a portable and easy to use device. Keeping that in mind the design consists of three main parts. One is the base plate, test plate and the holder plate. It is designed such that there is a possibility of changing the inclination angle of the plates.
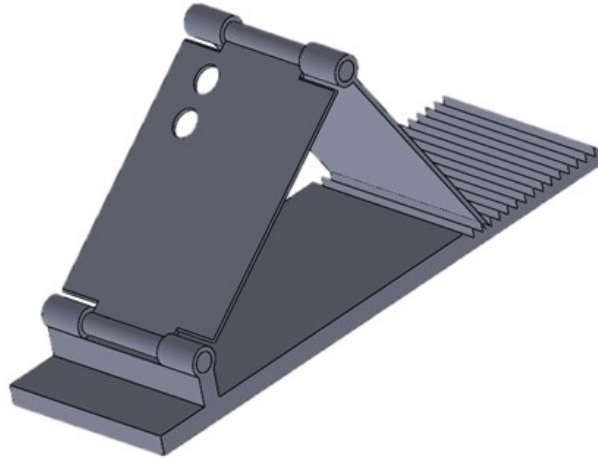
Figure 3.2 : Solid works design model of the device

The design is shown in the Figure 3.2, the inclination angle can be adjusted according to the ankle joint of the subject.

Design Description:
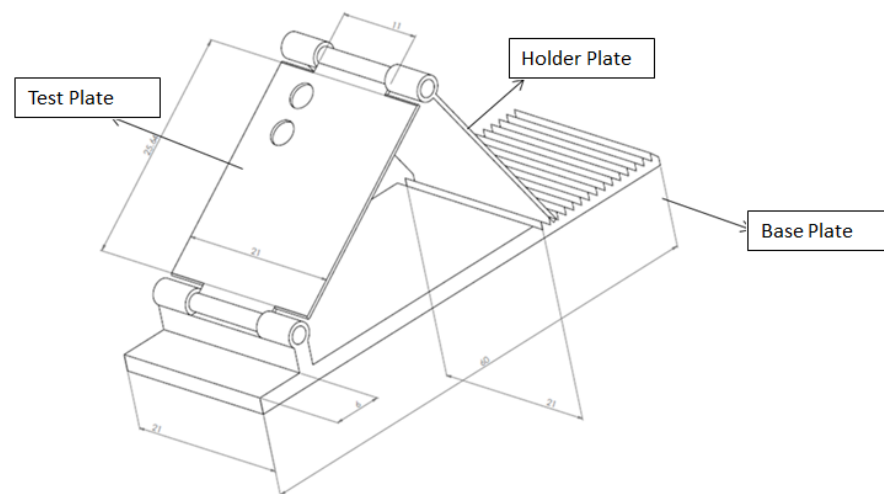
Figure 3.3 : Schematic diagram of the model

The design with three plates is shown in Figure 3.3. The base plate is 60 cm long and used to support the whole assembly. The base plate consists of 16 V-girders to provide the inclination and also gives the support to other two plates. The holder plate is 25.6 cm long, 21 cm wide and 0.5 cm thick used to change the inclination whose one part is on the V-girders to fix the inclination angle and another part is connected to the test plate with a hinge joint. The test plate is also 25.6 cm long, 21 cm wide and 0.5 cm thick which is connected to the second plate and connected to the base via a hinge joint. This test plate will be used by the subject to comfortably place their foot on it.

To make it light and portable, the whole design is made up of the high-quality acrylic plastic sheet due to its durability, easy to use, transparency and chemical resistance. It comes in different colors, thickness, and grades. For the current purpose, the clear acrylic sheet has been used with thickness of 0.5 cm. The overall weight of the device is not more than 3 kilograms. The hardware device has two holes to mount the vibrations motor shown in Figure 3.4.

Area to mount the vibration motors

Figure 3.4 : Placement of the vibration motors

Four hinge joints are used, two between the holder and test plate and another two between the test and base plate. These joints are used for changing the inclination angle of the test plate for testing in a comfortable position.

3.2.1 Vibration stimulation techniques

In order to generate the vibration stimulation, there is a need for an external source to generate the vibration. One of the technologies which are widely accepted for detection of neuropathy is vibration through the electromagnetic coil. It has been implemented on devices like Neurothesiometer and Biothesiometer which are operated by alternating signal to generate the vibration. When current flows through the coil, the magnetic force is exerted by the coil which varies with applied voltage. For varying the voltage, potentiometer is used. For this project, different types of vibration motors were studied and experimented to understand the effect of vibration on the surface of the skin. Using tuning fork and neurothesiometer vibration probe, it was noticed that the vibration should be provided in the perpendicular direction to the skin surface to provide the effective stimulation. The technology used in Biothesiometer/ Neurothesiometer have several limitations:

1. The vibration frequency in these devices is fixed.
2. Electronic circuits were used.

3. The vibration parameter such as amplitude is manually controlled using potentiometer.

Criteria for vibration motor selection:

1. The vibration should be provided in the perpendicular direction to the skin to provide the required stimulation.

2. The physical characteristic of the vibration such as frequency, vibration amplitude range should be adjustable i.e. the system should be capable enough to generate the vibration in the required range.

   - Frequency range – should cover at least 100 hertz as that of the Neurothesiometer.

   - Vibration amplitude should at least cover the Neurothesiometer range that is from 0 to 250μm (Neurothesiometer 2017).

3. The surface area of the motor contactor should be large enough to provide the required vibration.

With the available information on vibration generation the challenge was to find a suitable vibration motor that could fit these requirements. The aim was to find a vibration motor which is capable enough to generate the vibration with required parameters (frequency and amplitude). Based on these criteria, various vibration motors such as eccentric mass vibration motor, linear resonance actuator and tactor (linear actuator) were examined.

3.2.2 Eccentric mass vibration motor
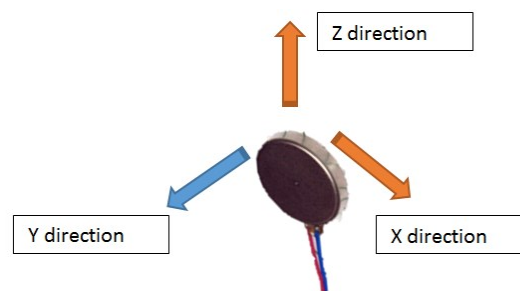
Figure 3.5 : Eccentric rotating mass vibration motor

There are wide applications of this type of motors. Eccentric rotating mass (ERM) vibrator motors were mostly used in pagers and mobile phones or by cell phone industries, however, it is still being widely used in smartphones. Model 312-101 is a coin ERM DC motor and it is also known as shaft less or pancake motor. The benefits of using coin ERM motor, are it is easy to use and cheap. According to the specifications of the motor, it is having 12 millimeters of body

diameter, vibration speed is 12500 rpm that is 208 Hz of frequency and vibration direction is in X and Z directions but not in Y – direction which is required for this application as shown in Figure 3.5.
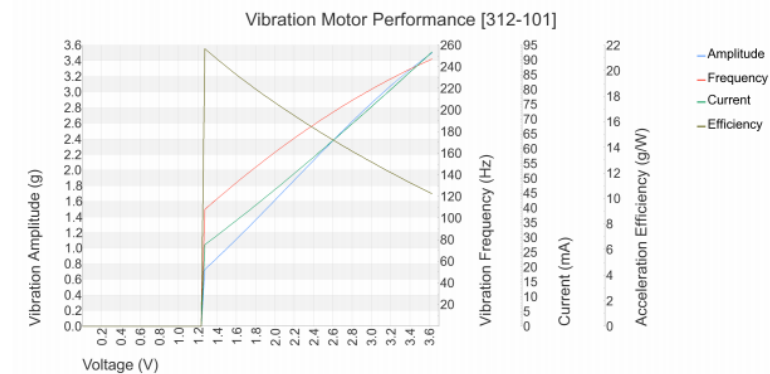
Figure 3.6 : Performance characteristic of the ERM motor (ERM 2017)

The performance graph of this motor is shown in Figure 3.6. When a voltage is increased from the 0 to 3.6 volts the frequency is increased from 60 to 260 Hz. With fixed frequency, the motor is unable to vary the amplitude. For example, it is possible to generate 120 Hz of frequency by applying a fixed 1.4 Volts. As per the requirement of the device, the frequency should remain constant with varying voltage (see Appendix D).

Limitations of this motor:

1. Frequency increases with increasing the voltage.
2. The vibration is in both directions that is X and Z direction as shown in Figure 3.5, so when experimented with this motor by mounting on the inclined plate, the whole plate was vibrating making it unsuitable to stimulate the required area of big toe.

3.2.3 Linear Resonant Actuator

This is also a coin type of the motor but it is different from ERM motors in terms of its working principle, and longevity. Although it has the long lasting life, driving the motor is bit complex. LRA motor drive is similar to the loudspeaker which means it requires an analog signal of the particular frequency to drive it. From the name itself, it is clear that resonance frequency is required to turn it ON. As per the available specifications, it has 10 millimeters of body diameter; 175 Hz of frequency and vibrates in Y directions as shown in Figure 3.7.
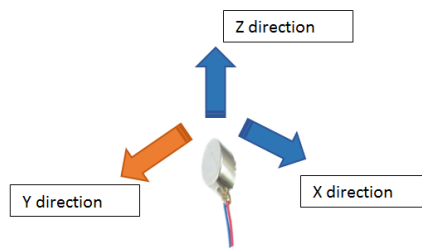
Figure 3.7 : Linear resonant Actuator with its vibrating direction
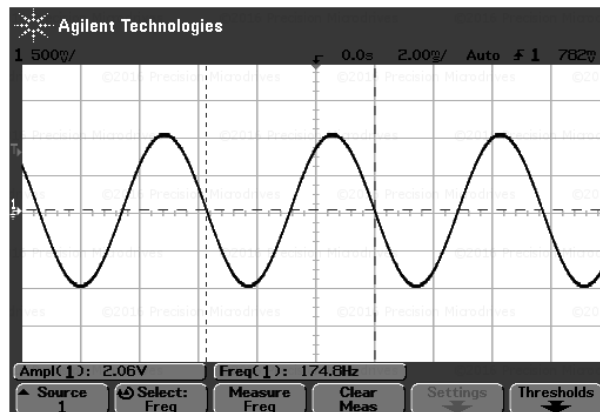
Figure 3.8 : Input signal to drive Linear Resonant Actuator

For the above model, 175 Hz of the alternating signal is required as shown in Figure 3.8 to vibrate it. In LRA motor is it possible to fix the frequency and change the amplitude from 0 to 2 Volts maximum (datasheet available in Appendix D).

Although it is satisfying the requirements of vibrating perpendicularly at fixed frequency and able to vary the voltage and unidirectional vibration, however, the range of frequency in which LRA motors are available is limited. LRA motor with a frequency less than 175 Hz is not available. The requirement of vibrating the motor at 100 Hz is not possible.

3.2.4 High displacement and low frequency tactor

High displacement and low frequency (HDLF) tactor (C2) is magnet linear actuator that has a frequency range of 60 – 160 Hz of mechanical resonance which provides high force and high displacement. It is designed in such a way that any of the frequency between 60 – 160 Hz is possible to set. Driving this motor is similar to that of LRA motor. When an electric signal is applied to the actuator, the contactor, as shown in Figure 3.9, oscillates perpendicular to the body.

Figure 3.9 : C2 HDLF vibration motor
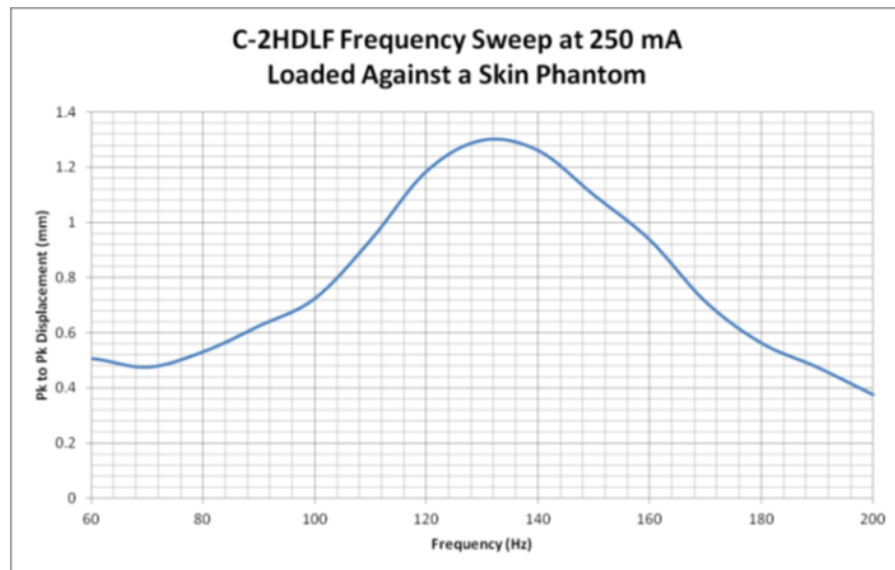
Figure 3.10 : Displacement Vs Frequency graph of vibration motor (C2HDLF 2017)

The displacement versus frequency graph is shown in Figure 3.10. If the frequency of vibration is fixed at 100 Hz, it is possible to obtain the maximum peak to peak displacement of 0.7 mm. Varying frequency will vary the displacement (see Appendix D).

C2HDLF benefits:

1. By varying the electric drive parameters, it is possible to change the vibration.
2. The frequency range provided by this tactor is from 60 – 160 Hz which is exactly matching the requirements and is possible to match with the neurothesiometer device.
3. Unlike neurothesiometer which always vibrates at fixed frequency, using this motor it is possible to adjust any frequency between 60 to 160 Hz.
4. The direction of vibration is perpendicular to accurately activate the required receptors.
5. The body weight of the motor is only 30 grams with a body diameter of 1.2" and height of 0.50", easy to mount on the required plate.

6. The main advantage of using this motor is that the applied vibration will be just focused on selected vibration site without affecting the mouting plate and the entire system.

Thus, from this discussion and comparing all these motors it is clear that C2 – HDLF tactor is the vibrator motor which is most suitable for providing required vibration stimulus to the body and therefore selected for the proposed device. However, the motor does not run on its own, a special circuit needs to be designed to operate at the required frequency and amplitude. Using this tactor, it is possible to overcome the design constraints as shown in Table 3.1.

Table 3.1 : Required parameters satisfied using C2 HDLF tactor

Parameters	Requirements	Satisfy or don't Satisfy
Vibration Direction	Perpendicular or in one direction	Satisfy
Vibration Frequency	Should be 100 hertz	Satisfy – Is even possible to set any frequency between 60 – 160 Hz.
Vibration amplitude(displacement)	≥250μ	Satisfy – at 100 Hz possible to achieve up to 350μ.
Compatible to use on proposed plate	Should be easily placed on the plate to provide vibration	Satisfy – Based on the body diameter, tactor is possible to fit on the plate.

3.2.5 Pressure monitoring using Force Sensitive Resistors (FSR)

For measuring the pressure, there are various technologies available which can be used for the device. The main objective of using pressure sensor is to monitor the pressure during the test. In Neurothesiometer, the vibration probe is applied on the skin surface without monitoring the pressure during the test. Because of this there is a possibility of human error. To overcome this limitation a pressure sensor (Force sensitive resistors) could be used on top of the vibrating motors.

Force sensitive resistors:
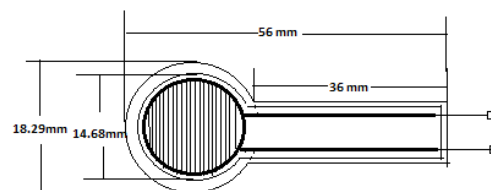
Figure 3.11 : Force sensitive resistors for pressure monitoring

The purpose of using the FSR in the device is to determine foot placement on the plate and to monitor the pressure during the test. FSRs are the special type of resistor consists of conductive polymer whose resistance changes by varying pressure on it. The active area of the sensor is ø14.68 mm and the thickness of the sensor is 0.46 mm shown in Figure 3.11. If the high pressure is applied, the resistance of the FSR decreases and when no pressure is applied the resistance remains the same. When these FSRs are connected to a microcontroller and pressure is applied, it shows FSR analog reading. The analog inputs of the microcontroller Arduino Uno are 10-bit which shows the analog readings between 0 to 1023 values. For example, if 100 grams of weight is applied on FSR then the FSR analog value is around 340. These values vary with varying pressure which has been calibrated using known weights set of $0 - 800$ grams. The inclination angle of the test plate is calculated by the formula $\alpha = \cos^{-1}\left(\frac{b^2+c^2-a^2}{2bc}\right)$, where b is the base length of the plate which is 33.3 cm at the initial position and increases by 0.1 cm per inclination from position 1 to 16 shown in Figure 3.13, c is the inclination plate length to place the foot which is 29.5 cm and a is the supporting plate length to which is 25 cm.
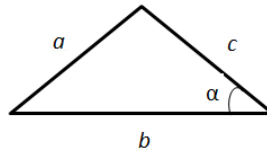
Figure 3.12 : Calculation of inclination angle
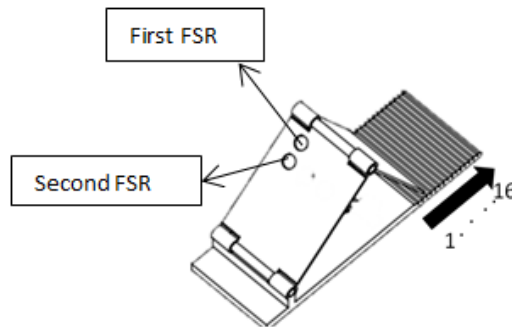
Figure 3.13 : Inclination changes from 1 to 16

When the constant weight of 100 grams is placed on the inclined plate then the weight on sensor can be calculated at each inclination as shown below:
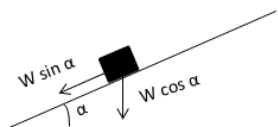
Figure 3.14 : Weight placed on an inclined plate

Where W is the constant weight of 100 grams, α is the inclination angle. Based on this the weight applied on the sensor is Wcosα and the graph of weight versus inclination angle is plotted as shown in the Figure 3.14.
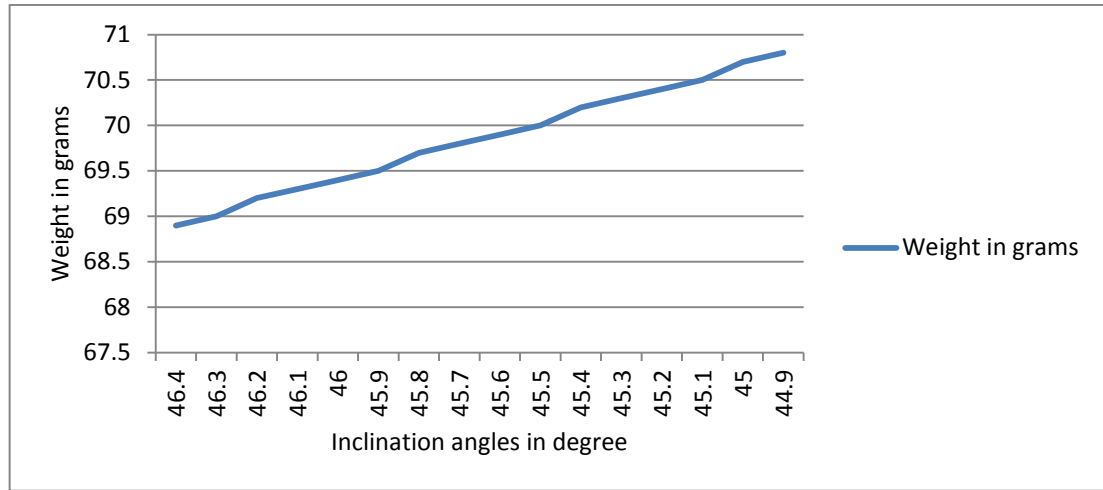
Figure 3.15 : Pressure change Vs inclinations

The relationship between the weight and inclination angle in degree shows that when the inclination decreases the weight increases. The same will be applied when the foot is placed on the plate, this weight is measured by FSR.

3.2.6 Electromyogram (EMG) to capture the muscle activity

(a)

(b)
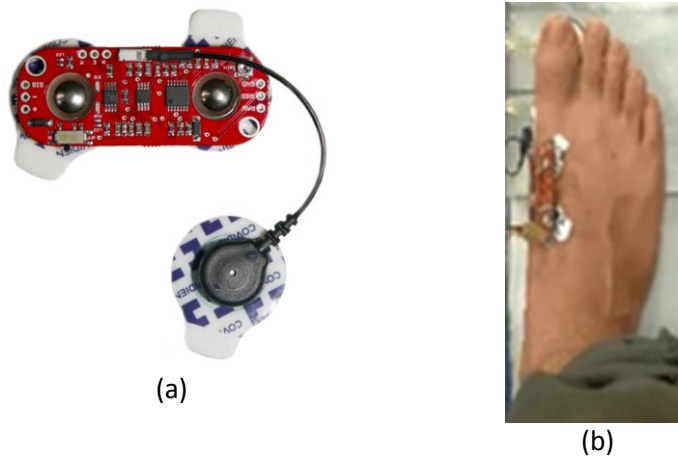
Figure 3.16 : (a) Myoware muscle sensor (Sensor 2017), (b) Myoware sensor on Extensor Hallucis Brevis muscle

For the proposed design, the setup also includes a feature of measuring the muscle activity during vibration stimulation using electromyogram (EMG) sensor. This may help in monitoring muscle activity when vibration is applied. For measuring the muscle activity it is important to select the appropriate muscle. Here in Figure 3.16 (a) shows the EMG sensor Figure 3.16 (b) shows its placement to the Extensor Hallucis Brevis muscle of the foot to measure its activity.

The main purpose to use this sensor is to capture the muscle activity when vibration is applied to the big toe. This is the extra feature which could be added to the device circuit to monitor the muscle activity to ensure that the subject is affected by vibration.

3.3 Integration of various components

Various components were used to make the electronic circuit of the device as shown in Figure 3.17. The components such as Arduino Uno, C2- HDLF tactor, FSR, Potentiometer, H- Bridge, Lipo Battery were used to design the device.

Figure 3.17 : Electronics components
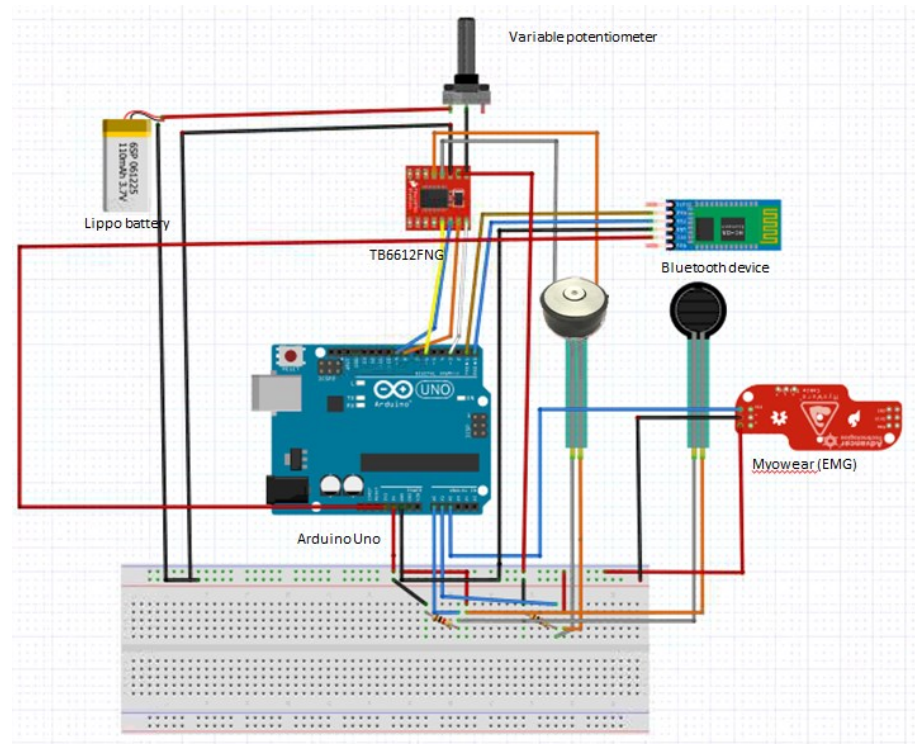
Figure 3.18 : Circuit diagram of the initial device
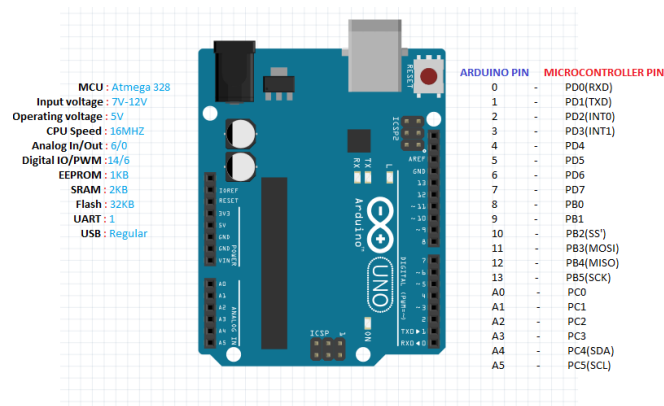
Figure 3.19 : Pin configuration of the Arduino Uno

Arduino Uno (Figure 3.19) is a microcontroller based on the ATmega328 operated on 5 voltage (Cheppali 2014). It has 14 digital input/output pins of which 6 are PWM output pins and 6 are analog inputs, a USB connection, 16 MHz crystal oscillator, an ICSP header, a power jack and a reset button are available. It can be connected to the computer using USB cable or wirelessly.

Force sensitive resistors are connected is such a way that one end is connected to 5 volts and another to the pull-down resistor of 10 KΩ value. The point between the fixed pull-down resistor and FSR is connected to the analog input (A1) of the Arduino Uno board. When force is applied the resistance decreases from 100 kΩ to 10 kΩ and current increases. As the force increase from 0 to 100 N, the voltage across the resistor changes from 0 to 5 volts. All six analog input of Arduino Uno is 10 bits. So according to the formula of 2^n where n is the slot that is 2^{10} is equal to 1024. The values changes from 0 to 1023 when pressure is applied. The values can be calibrated in terms of grams.
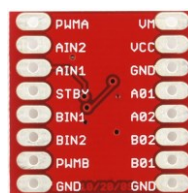
Figure 3.20 : Pin diagram of driver circuit – H Bridge

The Driver circuit is used as shown in Figure 3.20 to drive the motors on the circuit, there is two standard H-bridge on the chip (TB6612FNG 2017). It is capable of driving two motors at the same time. In the circuit one motor (tactor) is connected. The driver circuit is connected to the Arduino board. The signal supplied to the vibrator tactor is controlled from the microcontroller. As the microcontroller is not capable of providing enough current, an external battery of 4.1 Volts and 350mAh current is used. PWMA pin is connected to pin 3 PWM of Arduino. AIN1 and AIN2 of the driver circuit are connected to Pins 8 and 9 respectively. STBY is

connected to Pin 6 of the Arduino board. A01 and A02 pins of the driver circuit are connected to the motor. The Potentiometer is connected between the external battery and VM pin of the driver circuit to provide power to the motor.

Figure 3.21 : HC-05 Bluetooth module

The Bluetooth Module: (HC-05) is designed for transparent wireless serial connection setup (Figure 3.21). It uses CSR Bluecore 04-External single chip Bluetooth system with CMOS technology and with AFH (Adaptive Frequency Hopping Feature). It has the footprint as small as 12.7mmx27mm. The range is approximately 10 meters. To make the system wireless, this Bluetooth is connected to the microcontroller board. Four pins of the Bluetooth module as TX is connected to RX and RX of Bluetooth module is connected to TX of the microcontroller. Rest of the 2 pins are connected to 3.3 volts and ground of microcontroller board as shown in Table 3.2.

Table 3.2 : Arduino pins connection with all the modules

Arduino Uno Pins	Pins of modules	Module connected
A1	FSR 1	Force sensitive resistors
A2	FSR 2	
A3	EMG	Myoware sensor (EMG)
TXD	RXD	HC 05 – Bluetooth module
RXD	TXD	
3.3 volts	VCC	
Pin 3	PWMA	TB6612FNG
Pin 6	STBY	
Pin 8	AIN1	
Pin 9	AIN2	
5 Volts	VCC	TB6612FNG,FSRs,Potentiometer,EMG
GND	GND is common of all the devices	HC 05,TB6612FNG,Potentiometer,FSRs,EMG

3.3.1 Circuit diagram and working principle of the controller

1. The Arduino board requires 5V to switch ON, which is provided by the external power source. It is providing power to the integrated circuits containing H-Bridge (TB6612FNG), Force sensitive resistors and the Bluetooth module.

2. The microcontroller will read the sensor data at the baud rate of 9600 as per the installed program.

3. The programming of the microcontroller is done in C/C++ functions of Arduino Uno.

4. The Analog inputs of the microcontroller is 10 bit, it provides data in terms of 0 to 1023, once the data from the sensor is read, the analog signal has to be converted into a digital signal using A/D converter.

5. It could be possible to read multiple data from the FSR sensors.

6. As soon as the data is obtained in the Arduino, it is then read by MATLAB to plot the real time graph based on the force sensed from at sensor wirelessly using Bluetooth module. If no pressure is applied the graph in MATLAB is at reference 0 level when the pressure is varied, the graph shows pressure variations.

7. As the motor driver circuit is connected to the Arduino, the PWM signal which is generated by the microcontroller will be provided to the driver circuit i.e. generating PWM signal of 100 Hz using a microcontroller and applying to the PWMA pin of the driver circuit.

8. In this way, the same PWM signal is applied to the motor with signal strength of 4.1 voltages and 350mAh of current using an external battery. As per specifications of the motor, it requires 250mAh RMS to be driven.

9. Due to this a constant 4.1 volts is provided with the fixed frequency of 100 hertz and in order to vary the voltage from 0 to 4.1 manual potentiometer is used.

10. The whole set up is controlled wirelessly using Bluetooth through Graphic User Interface (GUI) which is developed using MATLAB framework.

3.3.2 Drawback of the circuit

The major drawback of the above circuit is the use of a potentiometer to vary the voltage of the motor. The amplitude was changing as per the requirement but the system was incapable of getting the value of the potentiometer in order to measure the varying voltage between 0 to 4.1 Volts. Because of this, it was not possible to capture the vibration perception threshold of the subject to interpret the results of the test.

To overcome this limitation the circuit was modified where the amplitude and frequency are handled through programming using PWM signals as shown in the circuit diagram in Figure 3.22.
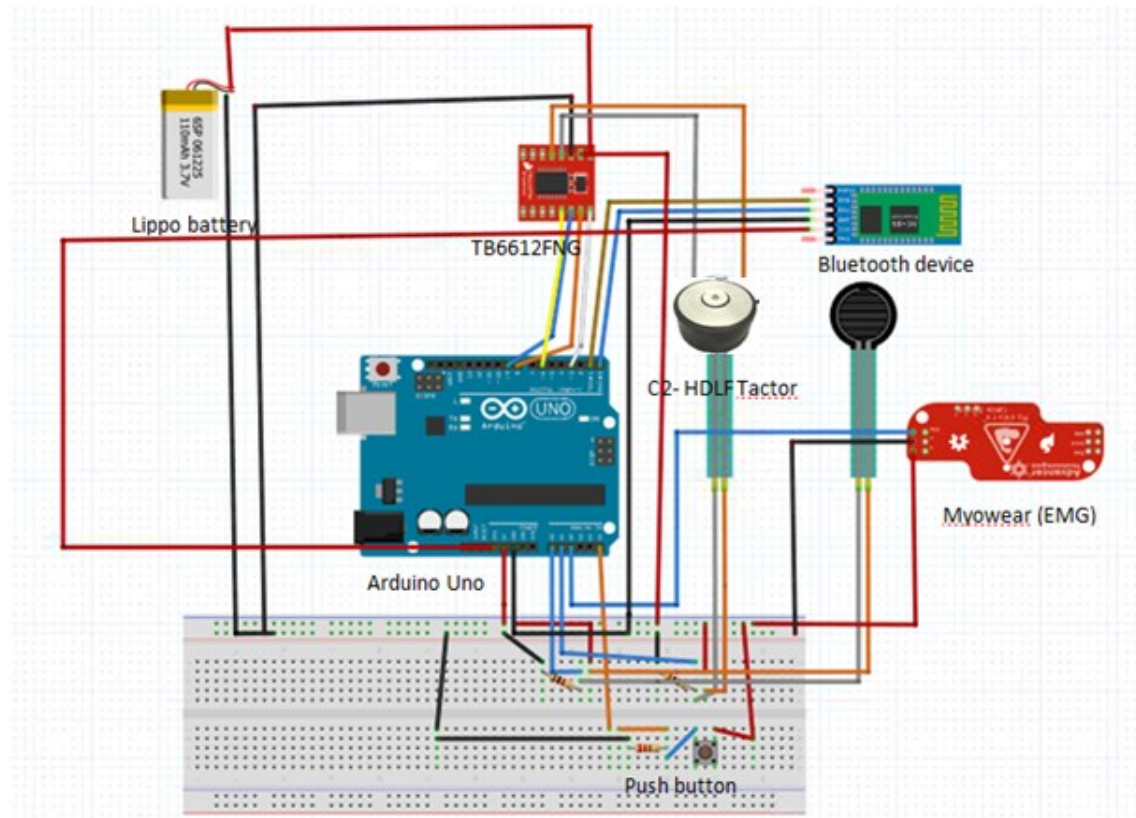
Figure 3.22 : Electronic circuit diagram – for version 2 of the device

The working of the modified circuit is mostly similar to the first one where the potentiometer is replaced and voltage is controlled by programming and the other advancement is the introduction of push button to make the system user friendly. The connection of the button is simple where one out of three pins is connected to ground, the second pin is connected to 5 volts and the third pin is connected to A5 the analog pin of the microcontroller board. When the push button is pressed the value 1 is captured in the microcontroller else it remains 0.

Potentiometer replaced by Pulse width modulation (PWM):

The Pulse width modulation is the technique to generate the analog signal through digital control. It consists of two components one is duty cycle and another is frequency. The duty cycle described as the amount of time the cycle is on high (ON), state the percentage of the total time taken to complete the one full cycle. The *frequency* is described as the time taken by the PWM to complete one cycle which can be measured in cycles per second. The *constant voltage* can be obtained by cycling a digital signal on and off at a fast rate and with a certain

duty cycle. The aim is to drive the vibration motor at 100 Hz i.e. 100 cycles per second with the varying voltage. In the zero duty cycle the pulse width is almost zero (see Figure 3.23).
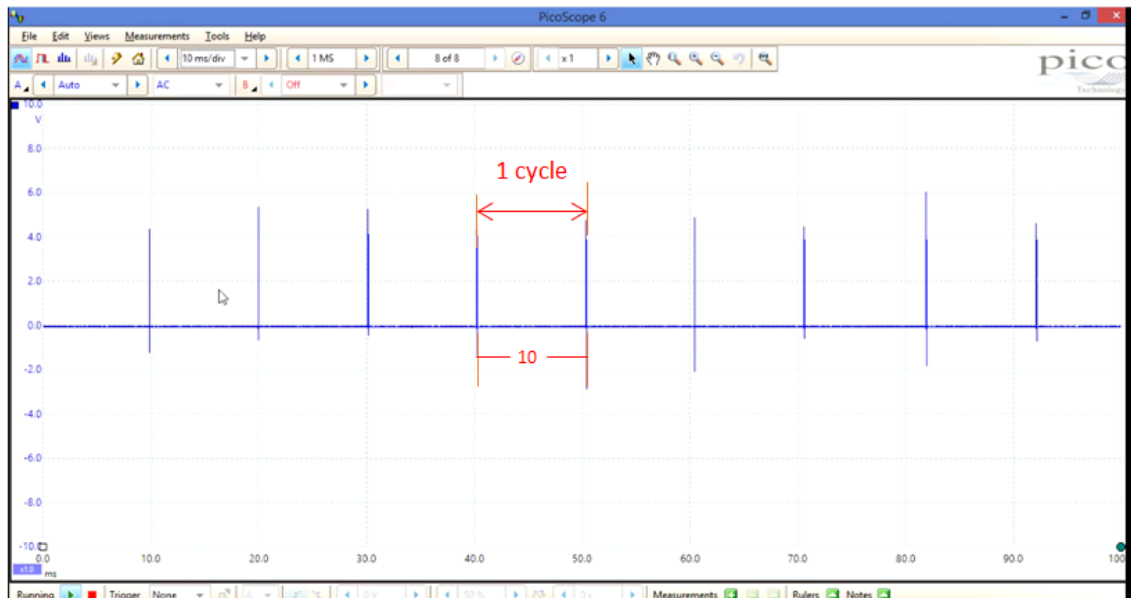
Figure 3.23 : PWM input signal to the h bridge with 0% duty cycle
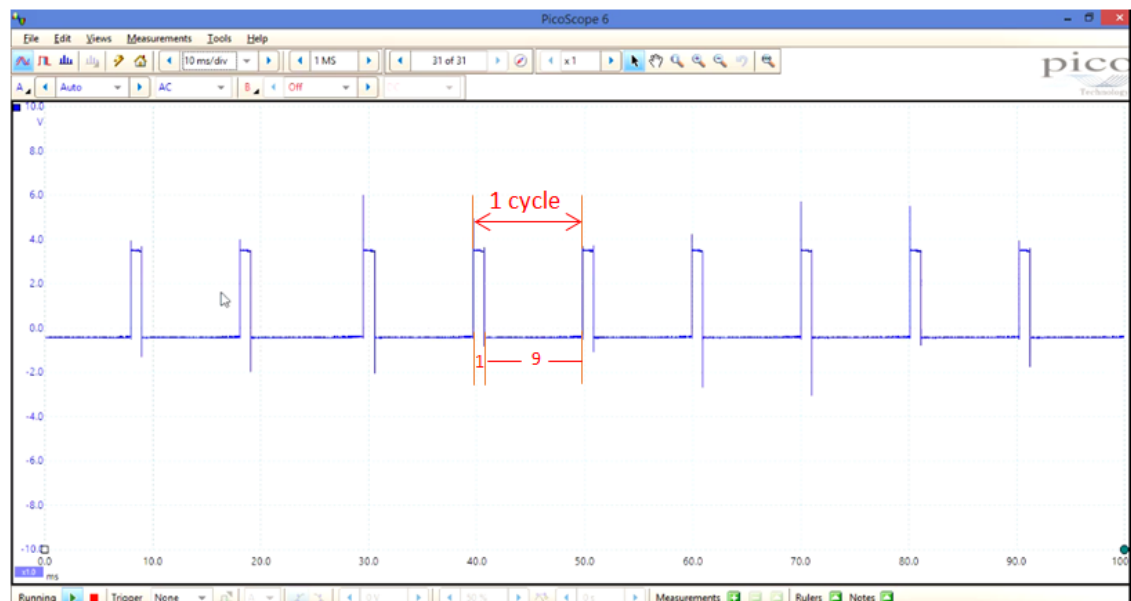
Figure 3.24 : PWM input signal to the h bridge driver with 10% duty cycle

As per the specification of the C2HDLF tactor (vibration motor), it is recommended to provide maximum up to 10% of the average duty cycle. If the digital signal is cycled fast, then the voltage seen at the output will appear as average voltage. The average voltage can be calculated by multiplying the digital high voltage with the duty cycle. That means 10% of the duty cycle can be calculated as 4.1×0.1 = 0.41 V. Similarly duty cycle of 5% will be 0.205 V. In order to varify the voltage change at every duty cycle the test has been performed where the

duty cycle is increased from 0 to 10% and the voltages are measured using multimeter shown in Figure 3.24.
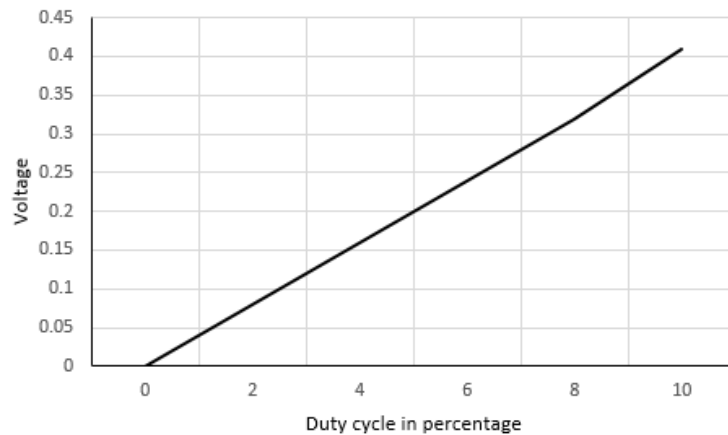
Figure 3.25 : Voltage versus Duty cycle

For creating the frequency of 100 cycles per seconds, the time period should be 10 milliseconds (1/10ms = 100 Hertz). PWM of 0% duty cycle with 100 cycles per seconds is created which is shown in Figure 3.23 and PWM with 10% duty cycle with 100 cycles per seconds created (Figure 3.24) in which 1 ms is the ON cycle and 9 ms is the OFF cycle creating the 10% of duty cycle gives the fixed frequency of 100 cycles per second (1/(1+9)). During the test, the vibration is provided from 0 V and is gradually increased up to 0.41V with the time interval of 500 milliseconds.

3.4 Graphic User Interface (GUI) development

Figure 3.26 : Front page for patient details

The graphic user interface(GUI) is developed for running the device using MATLAB software. The first page of GUI, asks for patient details (Figure 3.26). Once the details are provided the next page starts the test for detection of diabetic neuropathy (Figure 3.27).
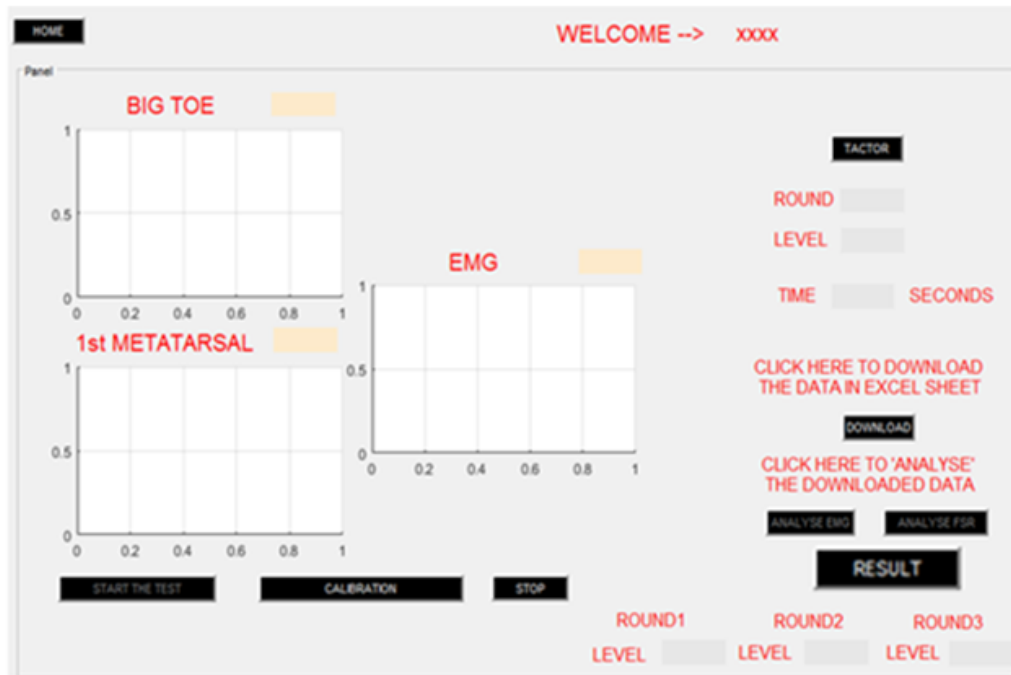
Figure 3.27 : Main page of the GUI

This is the main page for detecting VPT. Here three real-time graph for displaying the values of FSRs at the Big toe, 1st metatarsals and EMG signal are shown (Figure 3.27). Once the subject places foot on the plate a real time graph is displayed on all three windows (Figure 3.28). The button named *<Tactor>* available on the GUI is used to start the vibration motor. The proposed system is designed to run the test for three times and an average of all test rounds is calculated to display the result, once the *<result tab>* is pressed. The switch button is pressed and the vibration is applied to the foot, during each test round the subject is allowed to press the push button when they sense the vibration. Based on the current round the number will be displayed on *<Round tab>* and as per the level of vibration, the level will be displayed on the *<level tab>*. The duration of the whole test is displaced on the *<time tab>* in terms of seconds. When the switch is pressed by the subject, vibration will be stopped and the level is captured to display from the Round 1 tab, similarly, the levels will also be captured for Round 2 and Round 3 to complete the test, Pressing the *<Stop>* button finishes the test. Press the *<result tab>* to obtain VPT.

Figure 3.28 : User friendly graphic user interface (GUI)

The above figure shows the actual interface available to the user. The Force Sensitive Resistors are used to measure the real time pressure during the test. In the experiment two FSRs are used and placed on two points of the platform in such a way that when the subject places his/her foot on the plate, the force distributed at the planter surface of the foot at big toe and 1st metatarsals will be recorded and displayed at the same time.

3.4.1 Procedure to conduct the test

First, the subject is asked to sit on a chair comfortably and once he/she is ready, the subject is asked to remove the shoes and socks for conducting the test. The subjects are asked to place their right foot on the platform with attached Electromyogram sensor as shown in Figure 3.28. The rest of the procedure is described as below:

1. The command to start the test is provided through the GUI.
2. Once the test is started, pressure distributed at the big toe and 1st metatarsals will be captured and displayed real-time on GUI in order to make sure that the pressure remains constant.
3. Once the pressure is constant the vibration will be provided by pressing the tactor button on the GUI.
4. The vibration will be provided where the vibration frequency will be constant and amplitude will increase from 0 to 0.41 Volts automatically and will be displayed as *Level* on GUI.
5. The time interval between every vibration stimulus is kept fixed as 1000 milliseconds (this can be adjusted as per the requirement).

6. The subject will be holding the switch and the subject will be asked to press the switch when the vibration is felt.

7. Once the switch is pressed by the subject, the level of the vibration will be stored in round 1 and vibration will be stopped, to start the next round, tactor button should be pressed again.

8. This procedure should be repeated three times and the average of the three rounds will be taken to determine the vibration perception threshold. In the above example, if the *Level* displayed on the *rounds* i.e. Round 1, Round 2, and Round 3 are 2, 3 and 3 respectively so the average is 2.6.

9. Once the test is finished, *Download* button displayed on the page will be enabled and the user is able to download the data of FSRs, EMG with respect to time in a spread sheet for further analysis

10. Based on the average value of the captured level, presence of diabetic neuropathy could be determined.

3.4.2 Testing flow Chart
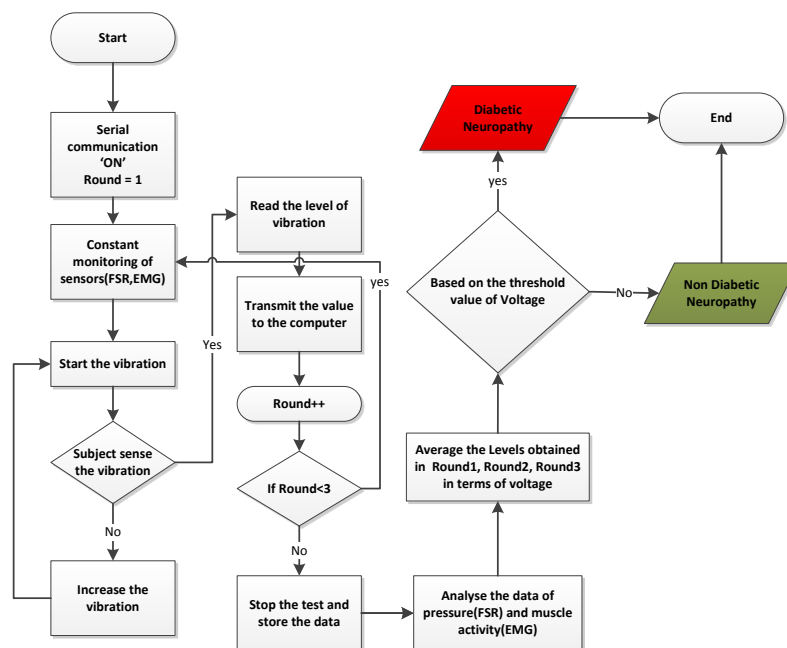
Figure 3.29 : Test procedure and data capture

The complete procedure in the software is shown in the flowchart (Figure 3.29). It shows the way the programming is done to operate the electronic circuit. Here based on the average value of the voltages level of diabetic neuropathy could be determined i.e. out of total 0.41 Volts (V), if the threshold value is ≤ 0.25 V then subject is non diabetic neuropathy and if greater than 0.25 V then subject is neuropathic in the simplest form.

3.5 Device evaluation

After developing the software as well as the hardware, it is very important to perform the evaluation of the device. For this purpose the current version of device is analysed on the following basis:

1. **Hardware evaluation:** The hardware developed for the device, has several limitations:
   - It can be used only for left leg.
   - There is no need of changing the plate inclination for every test.
   - During the test, it was found that while applying vibration stimulation, significant amount of vibration was transmitted through the test plate due to which the whole assembly vibrated unevenly.
   - This leakage was examined using accelerometer (Metawear CPRO) by placing it on the top of the vibration motor. It was found that if the applied vibration amplitude is 50μm then plate vibrates with the amplitude of 18μm i.e. around 36% of leakage.

2. **Electronic circuit evaluation:** There are several drawbacks which need to be upgraded:
   - The electronic circuit used for the device is capable of driving only one vibration motor. For driving two motors the circuit needs to be upgraded.
   - For EMG module, it was found that there is no evidence of muscle activity during the test; however this is an additional feature of the device which can be used for auto diagnosis from muscle activation.

3. **Software evaluation:** There are several drawbacks in the software:
   - The software developed was capable of operating only one vibration motor at a time.
   - The time taken to perform the test was high because subject needed to wait until they sense the vibration stimulus which increases gradually from 0 to 0.41 V.
   - For every incremented vibration it takes 5 seconds and to cover the whole range, it requires 250 seconds. This needs to be repeated for 3 times to obtain the mean value of the VPT so it could take as much as 750 seconds which is almost 12 minutes.
   - The output of the device varies from 0 to 0.41 Volts and due to this it is not possible to compare with any existing devices. This needs to be addressed by mapping to standard outcome (either by calibrating the output in terms of 0 to 50

Volts same as the Neurothesiometer), so that it can be easily interpreted by clinicians.

As in the device, FSRs were used for big toe and first Metatarsals, however in order to justify their significance, experiments were performed by placing these FSRs at various positions as shown below:

Case 1:
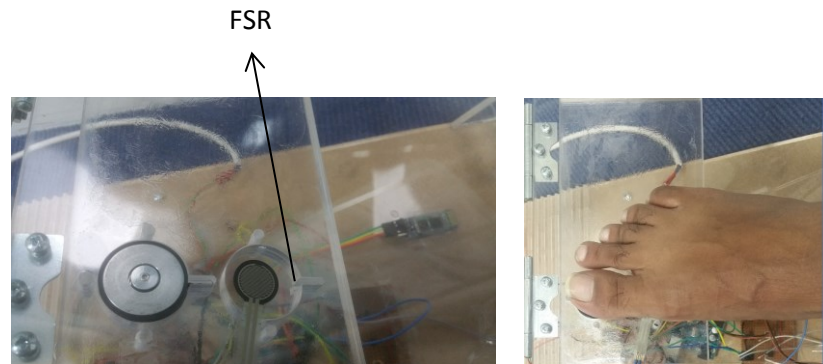
Figure 3.30 : FSR placed below the vibration motor

- The FSR is placed below the motor on the plate as shown in the Figure 3.30, so when the foot is placed on the plate, the pressure exerted by the first Metatarsal is recorded.

Using this position of FSR, their pressure remains constant as first Metatarsals will be at the same place throughout the test. It is not possible to identify the placement of big toe and monitor the pressure.

Case 2:

In this case, the placement of the FSRs is shown in the Figure 3.31 and the vibration stimulus is applied to the big toe.

FSRs

Figure 3.31 : FSRs placement at 1st Metatarsals and heel during the test

- As shown in the above Figure 3.31, out of two FSRs, first FSR was placed just below the motor on the plate and second at the centre of the plate so that when the foot is

placed on the plate, the pressure exerted by the first Metatarsal and heel of the foot can be recorded.

- The pressure exerted by the heel was greater than that of the first Metatarsals.

Similarly, as the size of the foot vary among the subjects, it could be difficult to maintain the distance of the FSRs. In this scenario too, when the vibration stimulus is applied to the big toe, it is not possible to identify the placement of big toe and monitor its pressure.

Case 3:
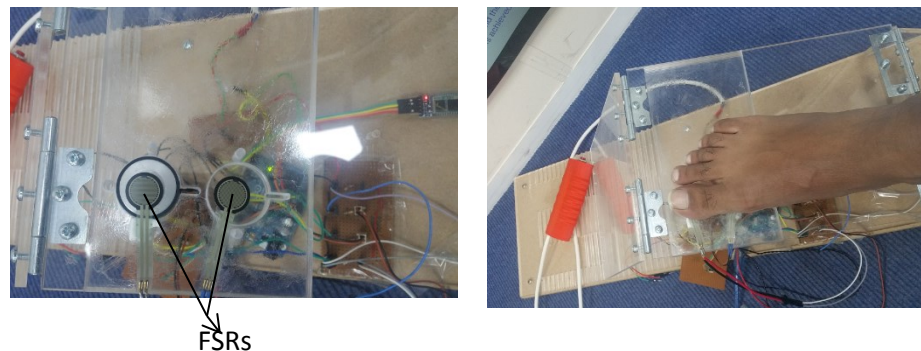
FSRs

Figure 3.32 : FSRs placement on great toe and 1st metatarsals of foot during the test

- Two FSRs were used to perform the experiments, in which the first FSR was placed on the top of the vibration motor and another was placed just below the motor as shown in the Figure 3.32.
- The pressure exerted by the first Metatarsal is greater than the big toe.

With this setting it is possible to track the position of the big toe and can monitor the pressure during the vibration application. However, there is no change in the pressure on the first Metatarsal which seems that use of the second FSR at first Metatarsal is not significant and can be ignored.

Case 4:

FSR
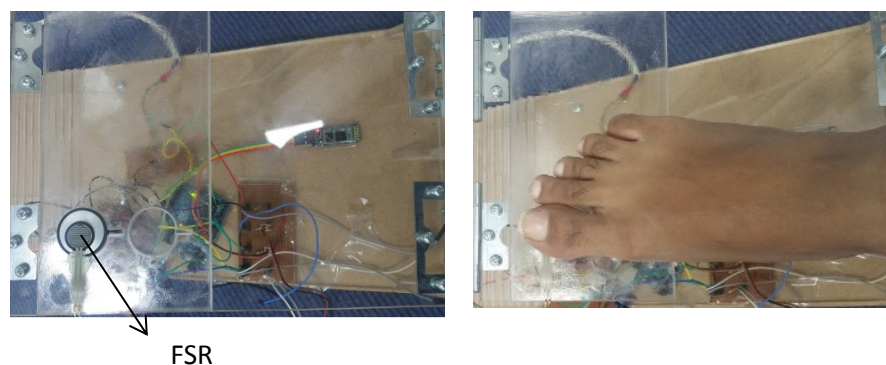
Figure 3.33 : FSR placed on the top of the vibration motor

- With this setting it was possible to track the position of the big toe and can monitor the pressure during the vibration stimulus and hence this placement of FSR was considered as the best location for conducting the test.

In order to address all these limitations in the device, there was a need for developing advanced version of device. This evaluation can help in developing a user-friendly, accessible to both feet, for a smart device.

3.5.1 Redesigning of the device

For addressing all the limitations of the previous version of the device, redesigning the device was considered for achieving the aim of developing the screening tool for diabetic neuropathy.

(a) Front view

(b) Left view

(c) Top view

(d) Isometric view
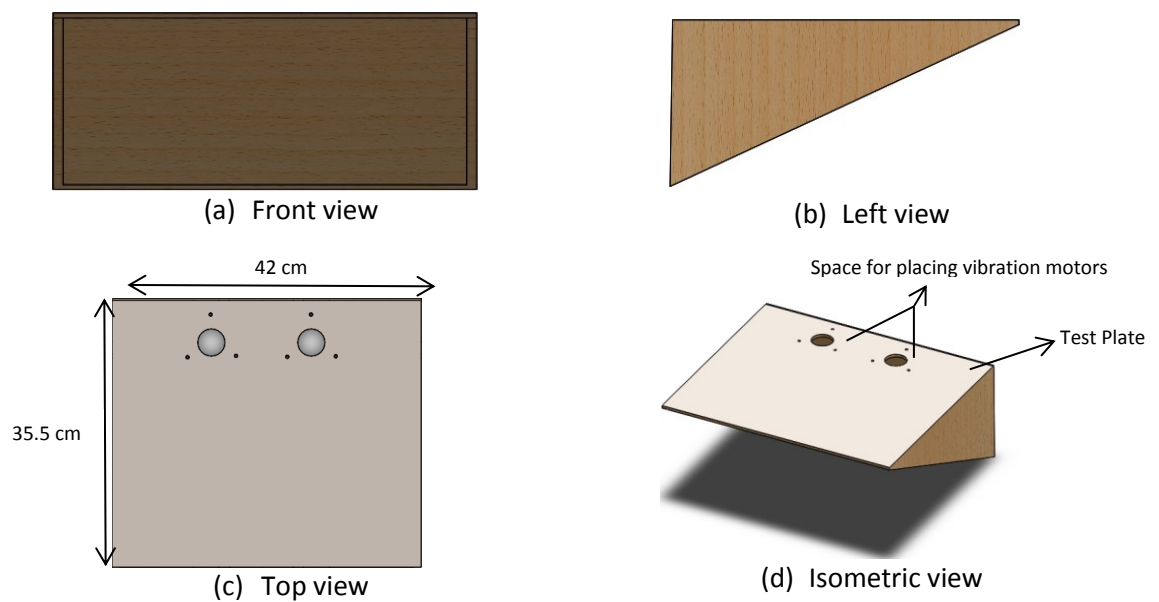
Figure 3.34 : Design of the latest device

The redesigning of the device is started by using software tool Solidworks through which device model was developed as shown in Figure 3.34. The length of the device is kept to 35.6 cm and width as 42 cm. The inclination angle of the test plate is kept constant at 36 degrees. The test plates consist of two holes to place the vibration motors. The diameter of both the holes was Ø3.6 cm as the diameter of the vibration motor is Ø3.17 cm. If the vibration motors are connected directly to the test plate then the whole plate will vibrate similar to the previous version of the device. To overcome this limitation the vibration motor needs to be isolated from the test plate. For that, an additional design feature is added to the test plate.
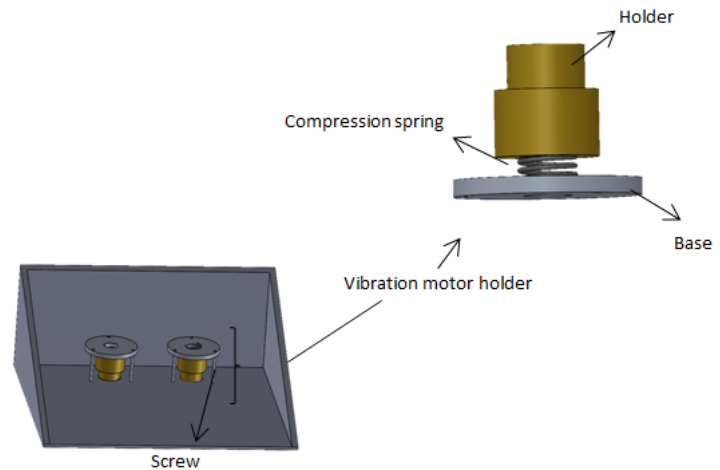
Figure 3.35 : Back view of the device

The bottom view of the test plate consists of vibration motor holder for each motor. It consists of a holder, compression spring and a base with three screws. The weight of the brass holder is kept nearly 10 times higher than that of the vibration motor. The compression spring is used between the holder and the base and the aluminium base plate has three screw holes so that it can be easily attached to the test plate. This design was finally used for developing the device.

Materials:
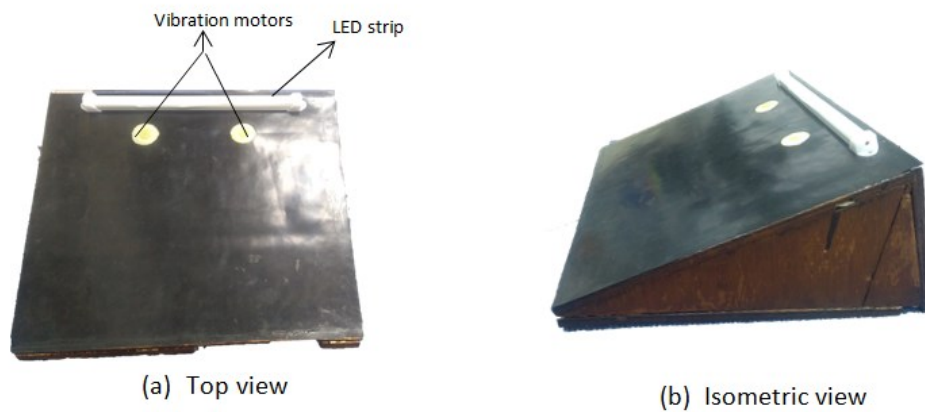
Figure 3.36 : Top and isometric view of the device

The whole device box is made up of wooden plate and it is completely covered from all sides. The vibration motor holder is made similar to the design shown above. It consists of brass holder as the vibration motors are electromagnetic in nature; so that the holder does interfere with the motor. The compression spring is used with the stiffness of 4.837 N/mm which is made up of steel. The base plate is made up of aluminium plate. The whole assembly of the vibration motor holder is fixed with the test plate using three screws such that both the

vibration motors are placed inside (Figure 3.36). Two FSRs are placed on the top of the motors to avoid direct contact with skin surface to the FSRs, it is covered by a thin natural latex sheet of 0.20mm. The test plate is fully covered by solid neoprene black colour rubber sheet of 1 mm thickness having fire - resistant benefits with good insulating property. It acts as an anti-slip for the feet placed on the plate. The LED (light emitting diode) strip is attached on the top of the plate which is covered by the white plastic cover for giving traffic light type of indication of neuropathy. On the back side of the box, there is a room for placing all the electronic circuits along with the battery which will be connected to the vibration motors, LED strip and FSRs.

3.5.2 Vibration isolation design

Vibration isolation is the technique of isolating the part of the equipment from the source of the vibration. Vibration propagate in the form of mechanical waves and due to some mechanical linkages, there is a possibility of vibration conduction. Passive isolation is commonly used where a certain type of materials are used to absorb or damp these extra mechanical waves. Sensors and actuators produce the interference to cancel the incoming vibration known as active vibration isolation. Mainly mechanical spring or rubber pads are used for passive vibration isolation.
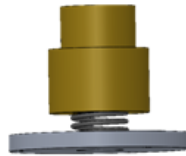
Figure 3.37 : Holder for isolating the vibration

In this case, the vibration motors can be taken as the source of the vibration. If the vibration motors are directly attached to the plate then vibration can propagates easily. To avoid this, a proper isolation technique should be implemented i.e. either passive or active. Passive vibration isolation technique was implemented, so using the mechanical spring.

The transmitted force from the vibration unit to the rest of the plate is given by:

$$F_T = F_a * \frac{1}{\pm\left[\left(\frac{\omega}{\omega_n}\right)^2 - 1\right]} \tag{1}$$

Where, F_T is the transmitted force,

F_a is the applied force,

ω is the frequency of the applied force.

ω_n is the natural frequency of the spring which can be given as $\sqrt{\dfrac{k}{M}}$,k is the stiffness and M is the mass placed over spring.

After several iterations, a spring with the stiffness of 4.837 N/mm was found suitable which can nullify the transmitted force to the device body.

Putting all the structural parameters the value of $\dfrac{F_T}{F_a} = \dfrac{1}{15}$, showing the transmitted force significantly reduced compared to the applied force.
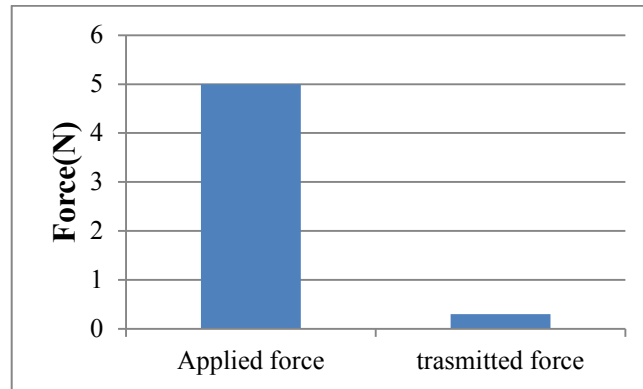
Figure 3.38 : Applied force versus transmitted force

Figure 3.38 shows the comparison between applied forces of the vibration to the transmitted force by using the holder design shown in Figure 3.37. Using this design, the vibration stimulus can be applied directly to the skin surface with negligible vibration leakage to the contact surface.

3.5.3 Electronic circuit design
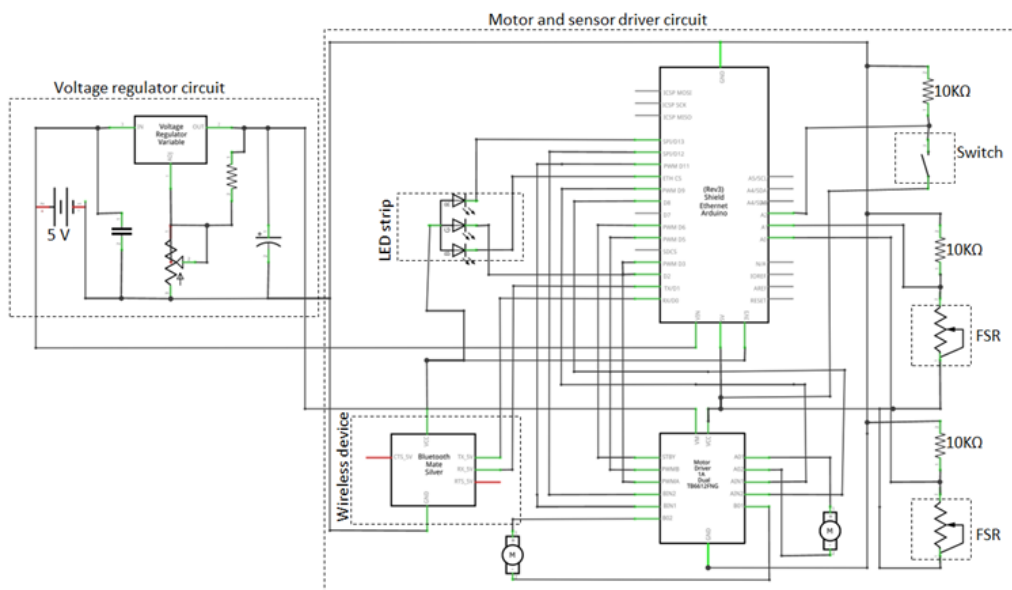
Figure 3.39 : Schematic diagram of the electronic circuit

All the electronic components mentioned in the previous version of the device were used expect EMG module. Few modifications like one more vibration motor (C2HDLF) is added,

addition of LED strip and battery of 5 Volts is used instead of Lipo battery. The connection of all the components is shown in the schematic diagram (Figure 3.39).

1. The circuit consists of 5 volts of battery with two output terminals.

2. It consists of two circuits, one is the voltage regulator circuit and another is the motor and sensor circuit.

3. Voltage regulator circuit consist of variable voltage regulator IC to vary the voltage from 0 to 5 Volts.

4. One output terminal of the battery is provided to the circuit as an input signal, the output of the signal will provide a constant output voltage to drive the vibration motors via H bridge. The potentiometer is used to vary the voltage which is provided to the motor driver circuit. However, the voltage provided to the driver circuit should remain constant and is set to 4.1 Volts.

5. The second output terminal of the battery which provides 5 Volts is connected directly to the Arduino.

6. The motor and sensor circuit is operated by Arduino programming via graphic user interface developed in the MATLAB framework that enables H bridge, Bluetooth, force sensitive resistors sensors and LED strip as explained in section 3.4.

3.5.4 Graphic User interface for the device
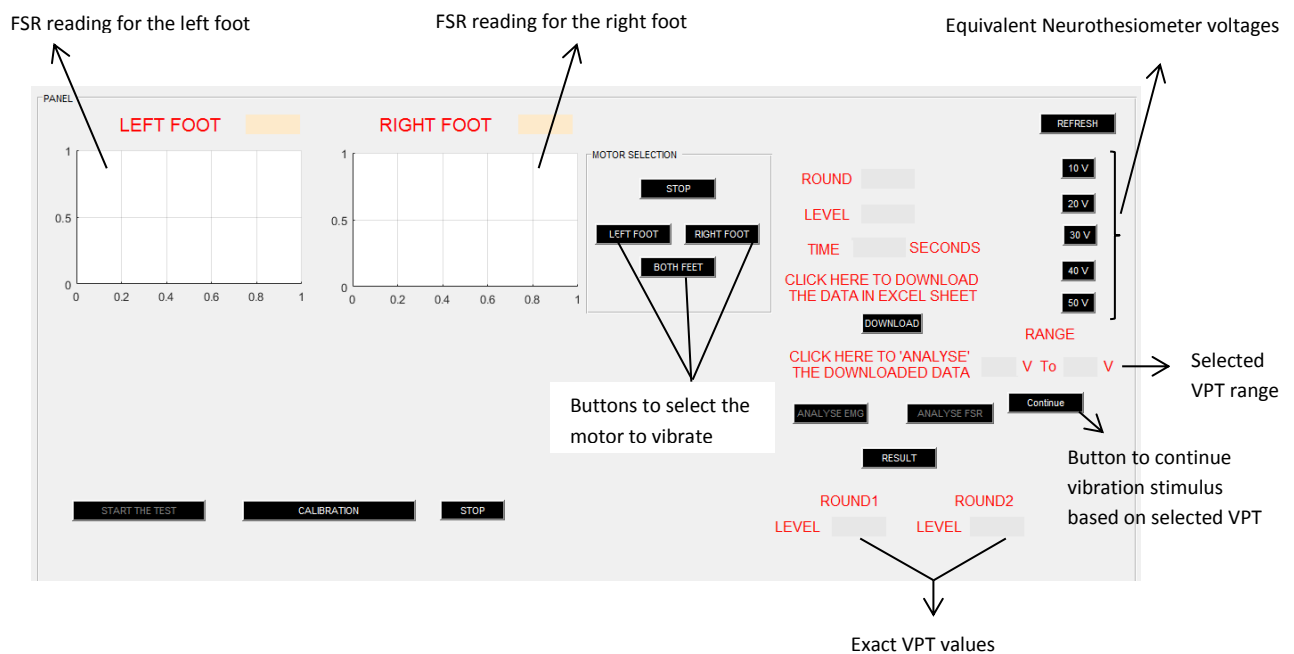
Figure 3.40 : Upgraded GUI for the latest version of device

The upgraded version of the GUI is shown in Figure 3.40. The main purpose of upgrading the GUI is to make it user friendly, easy and quicker to conduct the screening on both feet for determining diabetic neuropathy.

1. It consists of two graphs to show the real-time pressure value of the FSRs placed on the top of the vibrator motors.

2. The readings of the FSR placed on the left motor will be displayed on the left side graph and readings of the FSR on the right motor will be displaced on the right side graph.

3. In the motor section, there are three switches to select the vibration motor. Once the <LEFT FOOT> button is pressed the left side motor should be enabled. Similarly, when <RIGHT FOOT> button is pressed right side motor should be enabled. And while selecting <BOTH FEET> button both the motors should be enabled.

4. After selecting the motor, five buttons are available (10V to 50V) to select the vibration amplitude.

5. The range will have the value of the selected VPT range.

6. Press <Continue> button to start the motor from the selected vibration amplitude range as mentioned in step 5.

7. The exact VPT based on the rounds and levels of the vibration amplitude is captured in the window shown in Figure 3.40.

By enhancing this Graphic user interface, as there is a possibility of selecting the vibration amplitude of the motors, has become quicker in terms of the previous version of Graphic user interface. Once the range is selected, vibration should increase gradually for next 10 levels. Each level will take 5 seconds to move to the next level and whole process should be repeated for two times. The total time calculated will be just 20 seconds for one foot. So for both the feet it should take only 40 seconds to conduct the test.

Discussion

The development of the device is almost completed and it can be used for the both feet for measuring the VPTs of the subjects. There are important advancements in the latest version from the initial version of the device. The initial version of the device was capable of measuring VPT for only one foot and was also vibrating the whole platform resulting into noise. There was an option for selecting the inclination of the test platform which was removed in the later version because once the inclination of the test platform is fixed; there

was no need to change it. Initially, the force sensitive resistors were placed on the top of actuator and one on the first metatarsal but later realised that FSR on the first Metatarsal is not required. The major drawback about this initial version of device is it was taking longer to conduct the test approximately (12 minutes). Again the graphic user interface could only be able to determine whether a subject is neuropathic or non-neuropathic. Looking at all these drawbacks this version of device was updated where it was capable for measuring VPT of both feet. The placement of FSRs was also fixed which is placed on the top of the left and right actuators. The problem of vibration leakage was also solved by using passive vibration isolation technique. The updated GUI was capable of capturing real time pressure from both the feet along with the options of selecting the foot for VPT measurement. Here the idea of providing the vibration from 0V to 50V (as same as the Neurothesiometer voltage range) with 5 divisions is interesting as it can save time, but at the same time the threshold levels of each voltage (i.e. 10V to 50V) should be precisely set. This limitation can be overcome by precisely measuring the displacement at each voltage of device and comparing with the Neurothesiometer displacement for the whole vibration amplitude range to set the exact threshold values. This comparative study needs to be performed which will be discussed in the next chapter.

Chapter 4 Experimental evaluation of the developed device

In this chapter the first thing to understand is the vibration characteristic of Neurothesiometer device. Measurement of vibration characteristics includes measurement of frequency and amplitude. This is important to know in order to fix the same thresholds for the latest version of device. For this purpose, inductive sensor was used to measure the frequency of Neurothesiometer vibration probe by gradually increasing its vibration amplitude using manual rotating knob. For measuring the displacement of the vibration, a calibrated digital microscope was used. The measurement of vibration displacement was performed for whole range of vibration amplitude (i.e. 0V to 50V) which is discussed in the chapter.

Once the frequency of the Neurothesiometer is known, the same frequency should be set for the vibration actuator of the device using PWM signal. Similarly the displacement of the vibration actuator was measured using the same digital microscope till it reaches the maximum vibration amplitude of Neurothesiometer vibration probe (i.e. at 50V) which is investigated in the chapter. In order to obtain the device voltage range, equivalent to Neurothesiometer voltage range, a **curve fitting method** is implemented. This will help in calibrating the device voltage in terms of equivalent Neurothesiometer voltage for comparison purpose.

4.1 Comparison of the device with Neurothesiometer
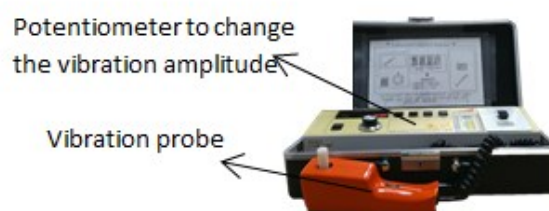
Figure 4.1 : Neurothesiometer

The latest version of the device which is developed could be used as a screening tool for diabetic neuropathy once it is compared and evaluated with the established techniques. This can be achieved only when the vibration amplitude and the frequency of the device has the same vibration characteristic of the existing devices. For comparison purpose, it is necessary to know the vibration characteristics of Neurothesiometer probe to compare and calibrate the device.

Vibration Frequency of Neurothesiometer:
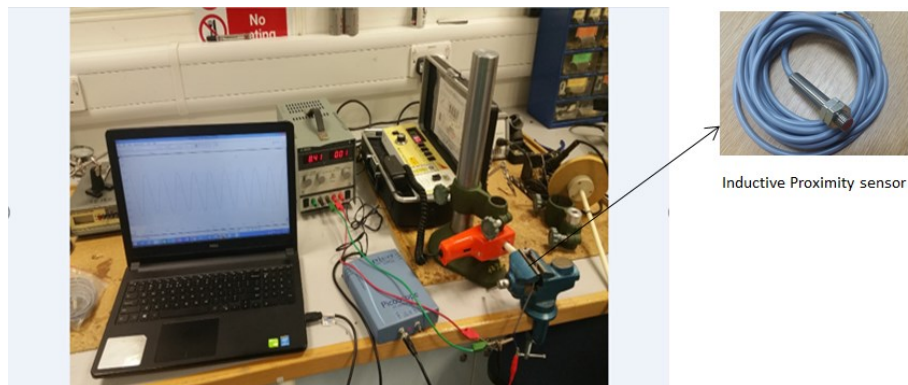
Figure 4.2 : Experiment setup for Neurothesiometer

An inductive proximity sensor is used for the experiment as shown in Figure 4.2. They are used for non-contact detection of metallic objects. Their operating principle is based on a coil and oscillator that creates an electromagnetic field in the close proximity of the sensing surface. The vibration probe is placed very near to the tip of the sensor (less than 1mm distance). There are three outputs of the sensor where one of the output is connected to the power supply to provide the voltage of 6V and another is connected to ground and the third one is connected to the digital oscilloscope to obtain the readings for frequency on the computer.

The manually controlled potentiometer is used to gradually increase the vibration. Based on the vibration intensity, the sensor will sense the intensity in terms of voltage. The vibration frequency at 0V, 10V, 20V, 30V, 40V and 50V are measured using the inductive proximity. After conducting this experiment, it was clear that the vibration frequency of the Neurothesiometer remains constant at 102 hertz at every voltage from 0 to 50V.

Vibration amplitude measurement of Neurothesiometer:

The vibration amplitude of the Neurothesiometer probe was measured using a digital microscope, however before using a digital microscope, it was important to calibrate it for measuring the accuracy of the results. Digital microscopes allow for the rapid acquisition of a high-quality image which can be precisely quantified or calibrated (Davis and Freeman 1998). The captured image can be analyzed for accuracy and stored for later use.

Calibration of Digital Microscope:

To ensure the accurate measurement and quantification of data using image analysis precise calibration is important. Typically images are captured by using a specific zoom or objective

lens to determine the overall magnification. The magnification of the microscope is from 50X to 500X. The calibration is set at 50X. First, the image of a physical scale is captured as shown in Figure 4.3.
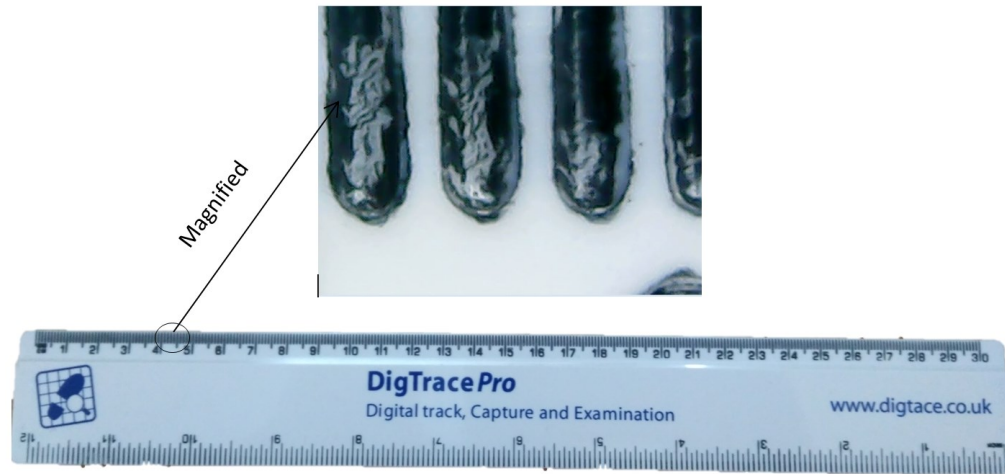
Figure 4.3 : Image captured using a digital microscope

It has been verified on the physical scale as seen in Figure 4.3. As the distance between each thread of the scale is 0.1 cm i.e. 1mm, the pixels for the selected distance is measured as 185 pixels as shown in Figure 4.4. This means that 1mm distance is equal to 185 pixels for 50X magnification. Similarly, for all the zooming range for the digital microscope (50X to 500X), the distance can be calibrated using the same method. This calibration (1mm= 185 pixel) can be added to the software such that it can be used to precisely measure the displacement.

Figure 4.4 : Distance measured in terms of millimetre and pixel

The experiment has been performed to measure the vibration amplitude of the Neurothesimeter vibration probe. The vibration amplitude is increased manually from 0 to 50 voltages using the potentiometer.
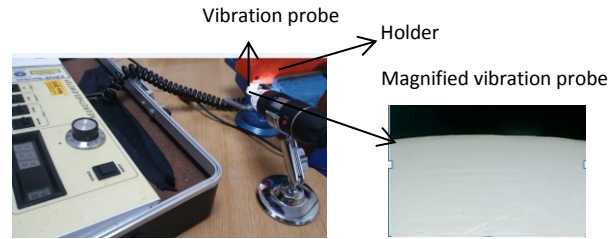
Figure 4.5 : Experimental setup for measuring Neurothesiometer vibration amplitude

As shown in Figure 4.5, the digital microscope was connected to the laptop in order to get the magnified image. The vibration probe of the Neurothesiometer was adjusted using the holder in such a way that it is presented on the front of the digital microscope. The distance of the digital microscope and the vibration probe was maintained throughout the experiment. Once the setup is ready, Neurothesiometer was switched ON and the voltage was kept at 0 Volts. Gradually the voltages of the Neurothesiometer probe was increased using the potentiometer (vibration knob) and the images were captured for almost every voltage. The Measured displacement was in mm as shown in Table 4.1 and graph Figure 4.6.

Table 4.1 : Experimental results of amplitude measurement of Neurothesiometer

Serial number	Voltage (V)	Measured amplitude (mm)
1	0	0
2	6	0.01
3	9	0.015
4	11	0.02
5	13	0.025
6	15	0.03
7	17	0.035
8	19	0.04
9	20	0.045
10	22	0.054
11	24	0.068
12	26	0.073
13	28	0.084
14	30	0.092
15	32	0.1
16	34	0.108
17	36	0.119
18	38	0.133
19	40	0.143
20	42	0.165
21	44	0.175
22	46	0.187
23	48	0.208
24	50	0.224
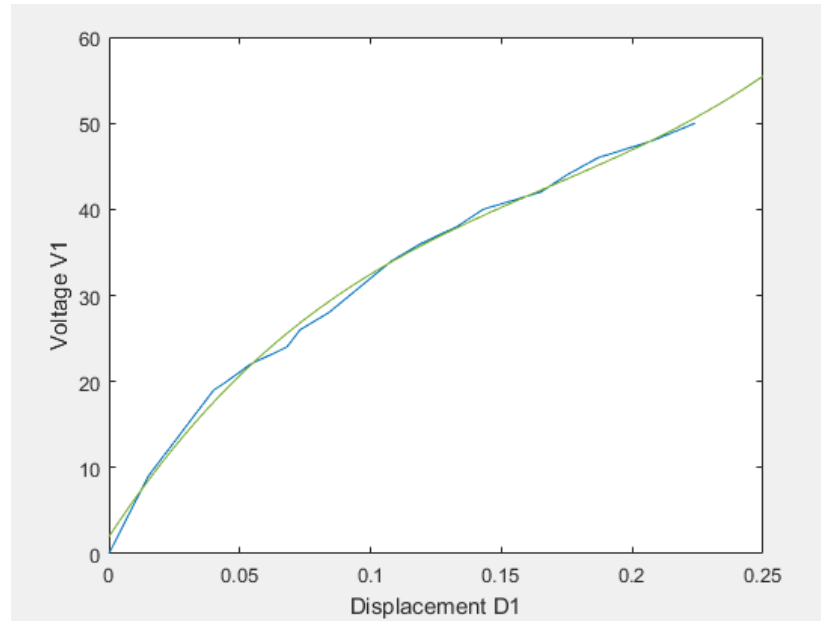
Figure 4.6 : Voltage and displacement relationship of Neurothesiometer

Figure 4.6, shows the relationship between Neurothesiometer voltages and vibration displacement. The equation for the above graph can be given as F (D_1) = V_1.

$$V_1 = 3.9e + 3D_1{}^3 - 2e + 3D^2{}_1 + 4.6e + 2D_1 + 2 \qquad (2)$$

Here, V_1 is the Neurothesiometer voltages and D_1 is the measured displacement of the vibration probe.

Vibration amplitude measurement for device:
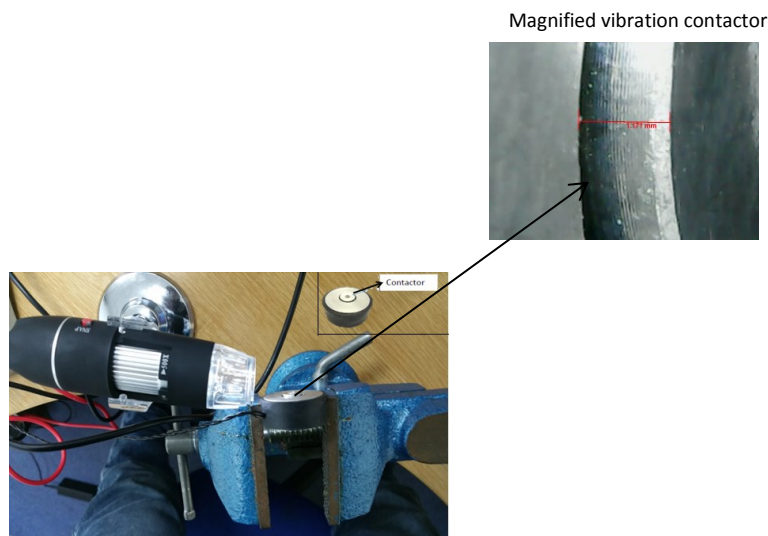
Figure 4.7 : Measuring displacement of the vibration motor

For measuring the vibration amplitude of the motor, the vibration motor needs to be enabled using GUI as discussed in section 3.6.4. The digital microscope was adjusted in such a way that the contactor of the motor should be in focus to get its magnified image as shown in Figure 4.7. Similarly, the distance between the microscope and vibration motor is maintained constant throughout the experiment. The motor will vibrate from 0 volts i.e. 0 mm until it reaches the amplitude of 225 mm similar to that of the Neurothesiometer maximum voltage. As discussed before vibration frequency of the motor was kept constant at 100 hertz throughout the experiment. All the readings of the vibration displacement were measured in mm. The readings are displayed in Table 4.2.

Table 4.2 : Vibration amplitude measure for vibration motor of the device

Serial number	Voltage	Displacement(mm)
1	0	0
2	0.04	0.015
3	0.08	0.025
4	0.12	0.043
5	0.16	0.053
6	0.2	0.07
7	0.24	0.08
8	0.28	0.086
9	0.32	0.107
10	0.36	0.113
11	0.4	0.129
12	0.44	0.145
13	0.48	0.151
14	0.52	0.162
15	0.56	0.172
16	0.6	0.183
17	0.64	0.194
18	0.68	0.205
19	0.72	0.218
20	0.76	0.232
21	0.8	0.237
22	1.2	0.247
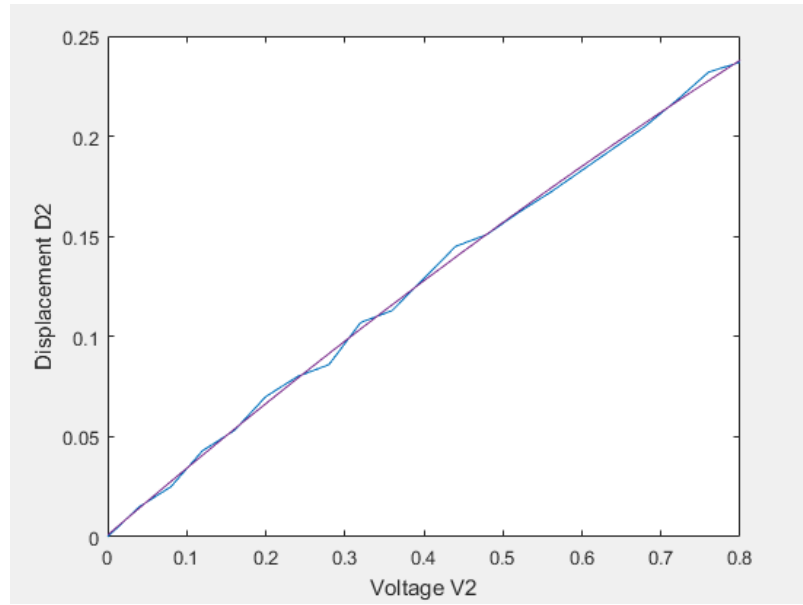
Figure 4.8 : Voltage versus displacement relationship of vibration motor of device

Figure 4.8, shows the relationship between Vibration motor voltages and the vibration displacement. The equation for the above graph is given below, where F (V_2) = D_2.

The Quadratic equation has been derived from the above graph such as:

$$D_2 = -0.05{V_2}^2 + 0.34V_2 + 0.0014 \hspace{2cm} (3)$$

Where, V_2 is the device voltage, D_2 is the measured displacement.

As the vibration amplitude range is the same in both the devices i.e. D_1 = D_2, it is possible to replace the value of D_1 in equation 2 by value of D_2 of equation 3 to get the relationship between Neurothesiometer voltage V_1 and out device voltage V_2 such as V_1 = F (V_2). The relationship graph is plotted as shown in Figure 4.9.
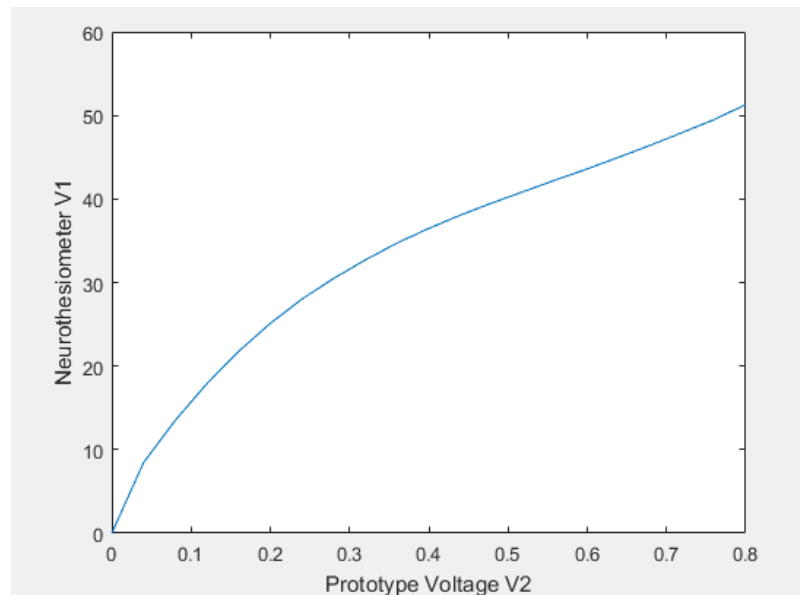
Figure 4.9 : Device voltage V2 versus Neurothesiometer V1

Thus, the relationship between the voltages of Neurothesiometer and the proposed device has been developed. The vibration stimulus is applied to the subject based on the selected voltage. For example, the voltage applied to the subject using Neurothesiometer and the subject sense the vibration at 15 Volts of the Neurothesiometer then the VPT of the subject is determined as 15 Volts. The advantage of establishing the relationship between Neurothesiometer and device is, when vibration stimulus is applied by the device; the determined VPT can be expressed in terms of equivalent Neurothesiometer voltage.

The derived equation is implemented in GUI to get results of VPT in terms of Neurothesiometer voltage range from 0 to 50 Volts.
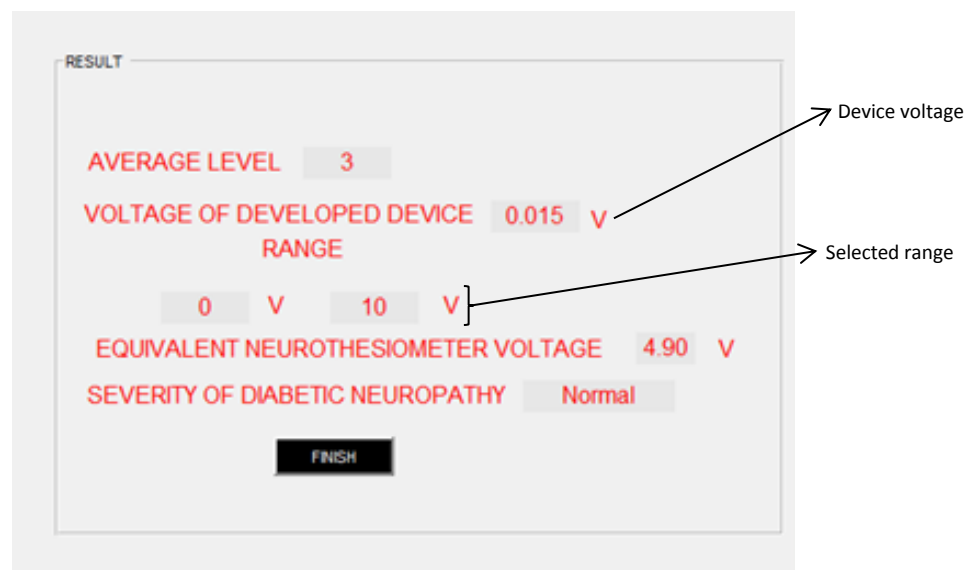
Figure 4.10 : Result expressed in GUI

In Figure 4.10, the average level i.e. 3 shows the average VPT measured by selecting the range. The average level is used to determine the actual voltage of device which is calculated as 0.015 V in the above case. The selected range is shown as 0 to 10 Volts which means that the subject has sensed the vibration stimulus within this range. The equation derived in the above section is used to obtain the Equivalent Neurothesiometer voltage showing 4.90 volts. The obtained VPT is used to determine the severity level of VPT and expressed the results as **'Normal'** in the above case.

4.2 Design summary

In the latest model, the progression is finished in terms of device design as it is conceivable to test the vibration sensation on both feet. When the vibration stimulus is given to one foot the second foot can lay easily on the same platform and this provides for adjustment during the test. Due to vibration isolation technique, the vibration will be relatively isolated from rest of the device body and is possible to provide vibration stimulus to the skin surface only.

With the upgradation in electronic circuit, it is now possible to operate any of the vibration motors or both the motors at the same time if required. It is capable of operating LED strip, switch, FSRs along with the wireless control using Bluetooth module.

By upgrading the software programming, it can now control the vibration motors. It gives the provision of selecting the vibration motors as per the user's need. The Graphic user interface is much more fexible for users to perform the test. In a way it allows the user to independently operate the device where results could be autonomously interpreted. With all these advanced features of device based on the vibration perception threshold, the device has been named as **'VibraScan'** (Dave et al. 2018)

4.2.1 Procedure for conducting test with VibraScan
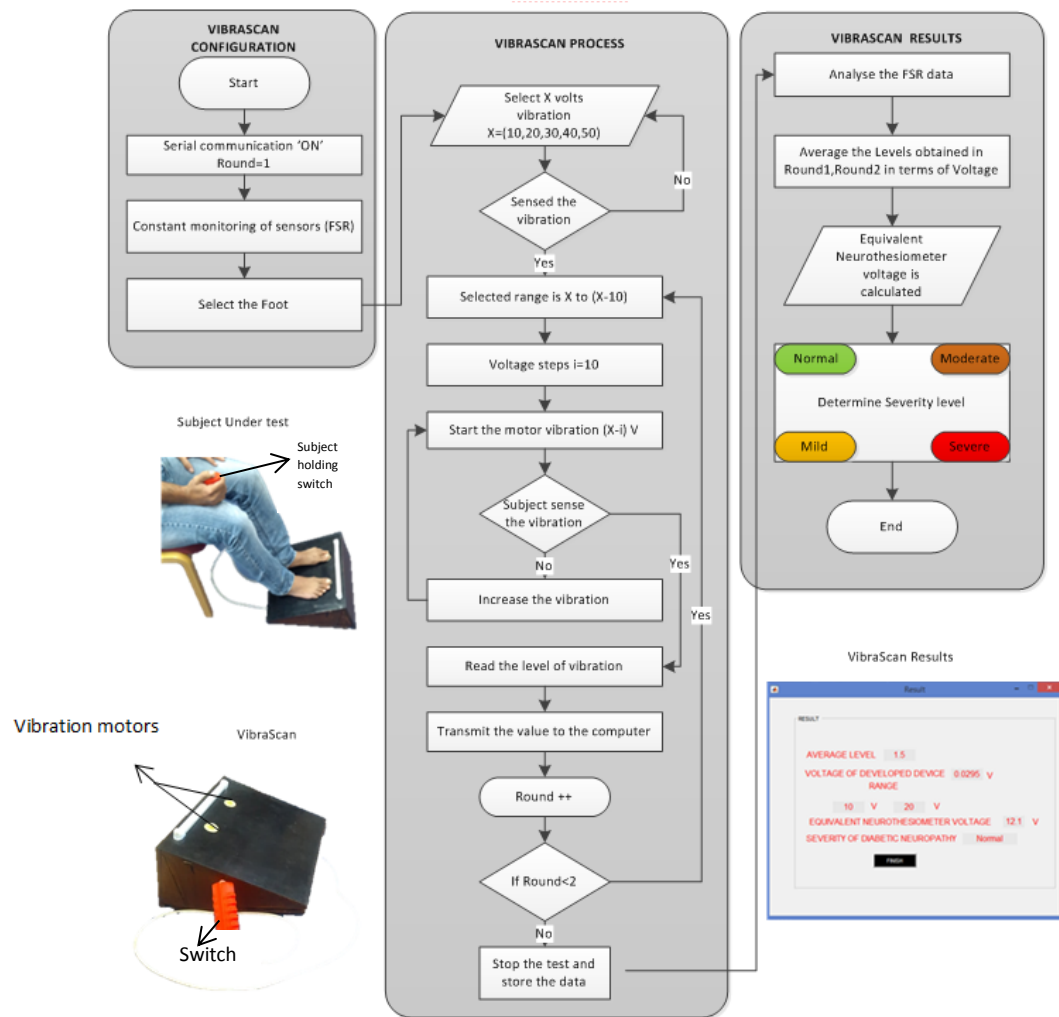
Figure 4.11 : Procedural screening tool of VibraScan

The detailed procedure of using VibraScan is shown in Figure 4.11. It consists of VibraScan device, method of operating VibraScan and the entire flow of the information which will be displayed in the form of the results.

1. For conducting the test, VibraScan should be first placed on the floor in front of the user chair.

2. All the time, test should be performed in the same ambient temperature that could be 25 degree centigrade.

3. VibraScan needs to switch ON to establish the serial communication with the Arduino microcontroller.

4. Once the connection is established, user needs to provide the credentials in the GUI and check for the FSRs data receiving on the GUI via Bluetooth.

5. The Pressure sensor data should be captured on the Left and right graph once everything is activated.

6. Now the subject needs to sit on the chair comfortably and put his/her feet on the plate as shown in Figure 4.11.

7. The great toe should be placed exactly on the top of the motor.

8. The subject needs to hold the switch during the test as shown in Figure 4.11.

9. After this setup, once the subject is ready for the test, the vibration motors should be selected from the GUI to provide the vibration stimulus.

10. Select <Left foot> button from GUI to enable left side motor (similarly, selection of <right foot> button or <both foot> button from GUI will enable right side motor or both the motors respectively).

11. For selecting the correct range of the vibration stimulus, press <10V> button to provide vibration amplitude equivalent to 10 Volts to the subject.

12. If the subject does not sense the vibration, provide vibration stimulus of 20 Volts, likewise increase the voltage until subject sense the vibration.

13. Subject is asked to press the switch at the point of vibration sensation. Once the switch is pressed, the vibration will stop automatically and range will be selected.

14. For example, if the subject presses the switch at 20 Volts, then 10V to 20V range should be selected.

15. After that <continue> button should be pressed to proceed for providing the vibration sensation that starts from 10 Volts and gradually increases until it reached 20 Volts.

16. The subject is asked again to press the switch to measure the exact VPT.

17. The procedure should be repeated twice by following the step 15 and step 16 to calculate the mean VPT.

18. Based on the mean VPT, the actual voltage of the VibraScan is captured to calculate the equivalent Neurothesiometer voltage shown in the result part in the Figure 4.11.

19. At the time of showing the outcome, the severity of the condition will be displayed as Normal, Mild, Moderate and Severe depending on the level of VPT, at the same time colour of the LED also changes from Green, Amber, Dark orange to Red respectively.

The procedure of conducting the test using VibraScan is straightforward and quick where results are interpreted automatically. VibraScan can be used as a screening tool for diabetic neuropathy and has the potential of replacing Neurothesiometer.

Discussion

The vibration characteristics of the Neurothesiometer probe are successfully measured. By using inductive sensor and the frequency was estimated as 102 hertz for the whole range of vibration amplitude. Using calibrated digital microscope the displacement of the vibration probe is estimated as (0V to 50V ≈ 0.2 mm) where 25V is equivalent to 0.07 mm. Similarly in VibraScan device the similar range of displacement was set from 0 mm to around 0.2 mm for comparison purpose. Using the curve fitting technique, equation is developed which gives the relation between VibraScan and Neurothesiometer voltages.

This shows how VibraScan has been evolved from concept to smart device. It is important to perform trial using VibraScan on human subjects to analyse its performance with respect to Neurothesiometer. For this purpose, both the tools (VibraScan and Neurothesiometer) should be applied on the human subjects to determine VPTs and perform the comparative study, this is discussed in the next chapter.

Chapter 5 Experimental study on Human subjects

This chapter will demonstrate the experiments performed on human subjects using both the Neurothesiometer and VibraScan devices. The purpose of the comparative study is to examine how well VibraScan is working when applied on subjects. The study will also ensure whether the outcome of VibraScan is acceptable by comparing it with Neurothesiometer.

To fulfil these requirements 20 healthy volunteers were invited to undergo the test using both the device after their prior consent. The procedure of conducting the test will be explained in the following sections. After conducting the test, a statistical analysis was performed. To assess the strength of the relationships of the measured VPTs (both right and left foot), **correlation coefficient method** was implemented. However, to check the level of agreement between both the devices **Blend's and Altman test method** was used which will be discussed in this chapter.

Ethical approval was given by Bournemouth University's Research Ethics committee (as shown in Appendix A) for conducting this test.

5.1 Criteria for selecting the subjects

1. The subject should be non- diabetic.
2. Should be more than 18 years old.
3. Should not have any injury or ulcers on the sole of the foot.
4. Should not have any problem with foot movement.

5.2 Experimental methodology

1. All 20 participants were tested using VibraScan and Neurothesiometer alternately.
2. Calculate the mean VPT using VibraScan for each subject and maintain the pressure throughout the test.
3. Calculate the mean VPT using Neurothesiometer for the same subjects.
4. Measure VPT for both feet of each subject for comparison.
5. Calculate the correlation coefficient between two measurements of left foot.
6. Calculate the correlation coefficient between two measurements of right foot.
7. Use the difference plots (i.e. Blends and Altman plot) for two measurement of each foot and examines the agreements between the two measurement techniques.

Procedure followed to conduct test using VibraScan

For conducting the test using VibraScan the following steps were used:

Figure 5.1 : Screening test using VibraScan

1. Subject needs to remove shoes and socks to perform the test.

2. Subject was asked to sit on the chair and place their feet on the VibraScan test plate.

3. Needs to hold the switch as shown in Figure 5.1.

4. When subject places the feet on the platform, FSR readings for both feet were continuously captured and displayed on the screen (Figure 5.1).

5. Any foot can be selected and vibration stimulus applied.

6. The vibration amplitude was measured from minimum to maximum, where subject was asked to press the switch for selecting the range.

7. Once the range of vibration was selected, vibration stimulus was provided again based on the selected range.

8. In the above example, if the selected range was from 0 to 10 volts, then the vibration stimulus was started from 0 and gradually increased to 10 volts.

9. The subject was asked again to press the switch when the vibration sensation was felt and was repeated to get the mean VPT.
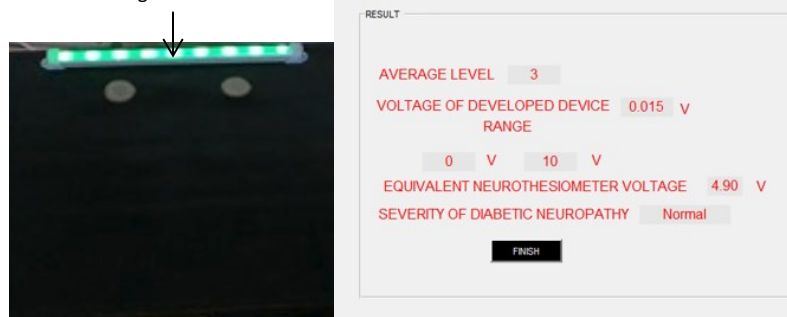
Figure 5.2 : Result displayed on VibraScan colour board

10. For the above example, the result was shown as 'Normal' and green LED light was displayed as shown in Figure 5.2.

11. Similarly, vibration stimulus was provided to another foot and all the above steps were repeated after selecting the correct foot to obtain VPT.

Procedure used to conduct test using Neurothesiometer:

After conducting the test with VibraScan, the same subject was tested using Neurothesiometer to determine VPT.

Figure 5.3 : Conducting test using Neurothesiometer

1. Subject was tested on both the feet one by one.

2. The subject was asked to keep their leg comfortably as shown in Figure 5.3.

3. Vibration stimulus was applied to the subject by holding the vibration probe.

4. The operator was allowed to control the amplitude of the vibration using vibration knob.

5. The subject was asked to say 'Yes' when vibration was felt.

6. The vibration amplitude ranges from 0 to 50 Volts, and the vibration started from 0 Volts and progressively incremented until subject felt the sensation.

7. The time at which the vibration sensation was felt was noted and the voltage showed on the Neurothesiometer determines the VPT of the subject. These were repeated thrice and mean VPT was calculated.

8. Similarly, VPT was obtained for another foot by following all the above steps.

Results were obtained for all the twenty subjects following the above method. The mean VPT obtained using both methods were compared with each other.

After conducting the test for all the twenty subjects, mean VPT for both feet were calculated using VibraScan and Neurothesiometer. For comparing both the methods correlation ceoefficient was calculated for each reading.

5.3 Correlation Analysis

Correlation analysis is carried out to measure the strength of the relationship between the pair of variables. The correlation coefficient is a statistical method used to compute the strength between the relative points of the two variables. The correlation coefficient r varies between -1 and +1. For interpreting the value of r there are various ranges set as follow:

r = 0 shows the absence of linear relationship.

r = +1 shows as a perfect positive linear relationship in which there is a positive increase in one variable when there is an increase in another variable.

 r = -1 shows there is a perfect negative linear relationship in which there is a positive increase in the one variable when there is a decrease in another variable.

0 > r > 0.3 shows a weak positive (or negative) linear relationship.

0.3 > r > 0.7 shows a moderate positive (or negative) linear relationship.

0.7 > r > 1 shows a strong positive (or negative) linear relationship (Ratner 2009).

If the value of r is between 0 and 1 then it reflects partial correlation which may be significant or may not be significant. For example, if the value of r is 0.70 that means 1 variable related to variable 2 is 70%. The only correlation that is significant at $p < 0.05$ or 0.01 needs to be considered. In order to have always positive value in some cases, squared value of r is calculated which is given as r^2 is also called coefficient of determination and denoted by R^2. R^2 indicates the percentage variation in one variable explained by another variable. Linear regression is like linear correlation where one variable depend on another independent variable. Linear equation $Y = AX + B$ is used to show the linear regression equation which is produced by using least difference between line point and the actual data point. Here the Slope A is measured from the ratio of $Y_1 - Y_0 / X_1 - X_0$ of the line. The correlation coefficient is scaled to fit between 0 and 1.

Calculated Correlation coefficient:

If A and B are the two variables then correlation coefficient can be calculated after getting standardised values as cA and cB of A and B respectively i.e. mean of cA and cB will be 0 and standard deviation (SD) will be 1. This can be expressed as:

$$cA_i = A_i - mean(A)/SD(A) \hspace{4cm} (4)$$

$$cB_i = B_i - mean(B)/SD(B) \hspace{4cm} (5)$$

The correlation coefficient can be given as the mean product of cA_i and cB_i shown as below:

$$r_{A,B} = \text{sum of } [cA_i \times cB_i]/(n-1) \tag{6}$$

Where n is the number of samples.

Left foot VPT measurement analysis:

Here the VPT of Left foot was measured using both the devices and shown in Table 5.1. Twenty subjects were tested. The central value of the data is expressed as the mean and the variation is expressed as the 95% confidence interval (CI). The CI shows the data distribution would differ significantly from each other based on the estimates. The lower bound of 95% CI is calculated by the equation 7:

$$Lower\ bound = mean - 1.96(SD/\sqrt{n}) \tag{7}$$

The upper bound of 95% CI can be calculated as $mean + 1.96\left((SD\big|\sqrt{n}\right)$ where n is the number of measurements and the CIs provides reliability of the data i.e. any measurements outside this limit consider the data from other distribution. The mean with 95% CI was calculated for VibraScan (Left foot) as 4.76 ± 0.60 V and similarly, the mean VPT of Neurothesiometer (Left foot) was calculated as 4.53 ± 0.65 V.

Table 5.1 : VibraScan and Neurothesiometer readings for Left foot

Series Number	VibraScan Left foot mean VPT (V)	Neurothesiometer Left foot mean VPT (V)
1	4.9	5
2	3.4	4.5
3	3.4	3
4	5.26	4
5	4.9	6.16
6	4.53	4.6
7	4.9	4.8
8	6.7	8.16
9	3.4	3.16
10	3.4	4
11	5.63	5.16
12	4.16	5.3
13	3.4	5
14	7.74	5.5
15	4.53	5
16	3.02	4.16
17	5.63	6
18	7.05	7.6
19	5.99	4.8
20	3.4	3.5

Here for the above measurements of the left foot, VibraScan score of VPT is compared with the Neurothesiometer VPT scores for all the twenty subjects as shown in Table 5.1. In order to get the relationship between the measurements, the correlation coefficient was calculated. Based on the value of the correlation coefficient strength of the linear relationship was obtained.
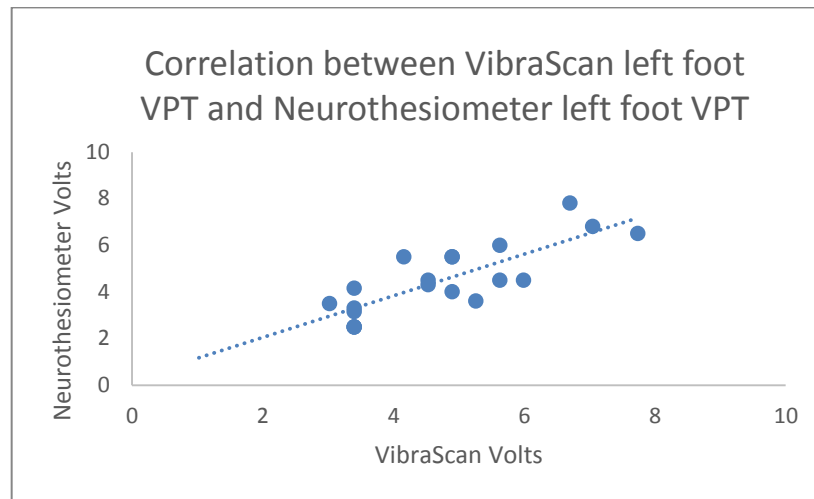
Figure 5.4 : Correlation between Neurothesiometer and VibraScan (Left foot), r = 0.816

Here correlation coefficient for both the individual measurements was calculated as r = 0.816 significant at $p < 0.001$ showing the large positive relationship as per Figure 5.4. As the points fall close to the line it has a close correlation between the measurements and as one variable increases, another variables also increases showing a positive relationship. The equation of the line is given by:

$$Y_1 = 0.8922X_1 + 0.2779 \qquad\qquad (8)$$

Where, Y_1 is the Neurothesiometer voltage,

X_1 is the VibraScan Voltage

0.8922 is the slope of the line.

Right foot VPT measurements

Table 5.2 : VibraScan and Neurothesiometer readings for Right foot

Series Number	VibraScan Right foot mean VPT (V)	Neurothesiometer Right foot mean VPT (V)
1	4.9	5
2	3.4	4.5
3	3.4	3
4	3.4	4
5	7.05	6.16

Series Number	VibraScan Right foot mean VPT (V)	Neurothesiometer Right foot mean VPT (V)
6	4.9	4.6
7	4.9	4.8
8	8.9	8.16
9	3.4	3.16
10	4.16	4
11	5.63	5.16
12	4.53	5.3
13	5.26	5
14	5.99	5.5
15	4.9	5
16	5.63	4.16
17	5.63	6
18	8	7.6
19	6.7	4.8
20	3.78	3.5

Here for the above measurements of VPT, the right foot VibraScan score of VPT is compared with the Neurothesiometer VPT scores for all twenty subjects as displayed in Table 5.2. In order to get the linear relationship between the measurements, the correlation coefficient was calculated.
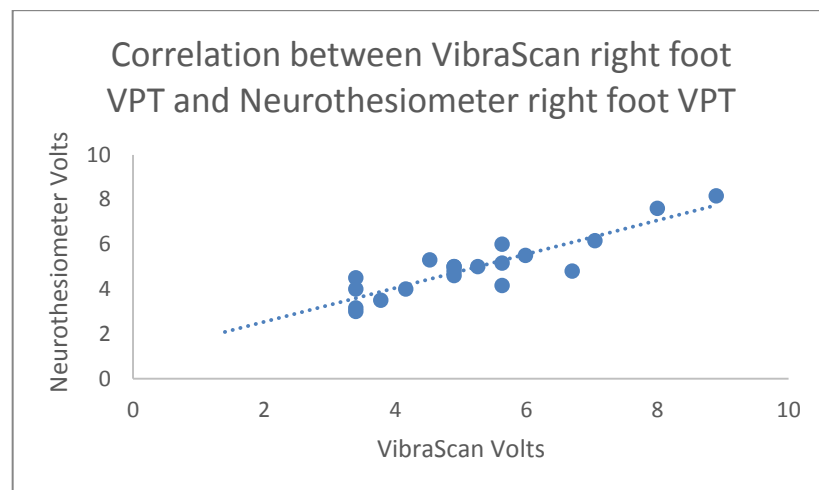
Figure 5.5 : Correlation between Neurothesiometer and VibraScan (Right foot), r = 0.893

Here, the correlation coefficient for both the individual measurements was calculated as r = 0.893 significant at $p < 0.001$ showing the large positive relationship as shown in Figure 5.5. In in this case also points fall close to the line so has a close correlation between the measurements and as one variable increases, another variable also increases showing a positive relationship. The equation of the line is given as:

$$Y_2 = 0.7543X_2 + 1.0303 \tag{9}$$

Where, X_2 is the Neurothesiometer voltage,

Y_2 is the VibraScan voltage,

0.7543 is the slope of the line.

5.4 Bland and Altman plot

There is a close linear relationship between the test scores of both feet. Although the correlation which is calculated is considered a way of paring the two instruments, the measured VPTs may correlate but not agree. Strong correlation may lack the agreement between measured scores. In order to find it out whether both the instruments are agreeing with each other, Bland and Altman method was applied to verify this (Bland and Altman 1986).

Bland and Altman's method was used to obtain the limit of agreement between the VPT scores. It is also known as the difference plot which is a graphical method to compare two measurement techniques. In this method the difference between the test scores $(X - Y)$ are plotted against their average value$([X + Y]/2)$. Through this plot, it is easy to evaluate the scatter of the values, level of different and measurement error. It also shows how much data is different from the mean value. Secondly, it shows the relationship between size of mean value and random error. Thus, this method might be used to figure out the level of random error if VibraScan VPT measurement is still acceptable to be used as an alternative to the Neurothesiometer measurement.

Results:
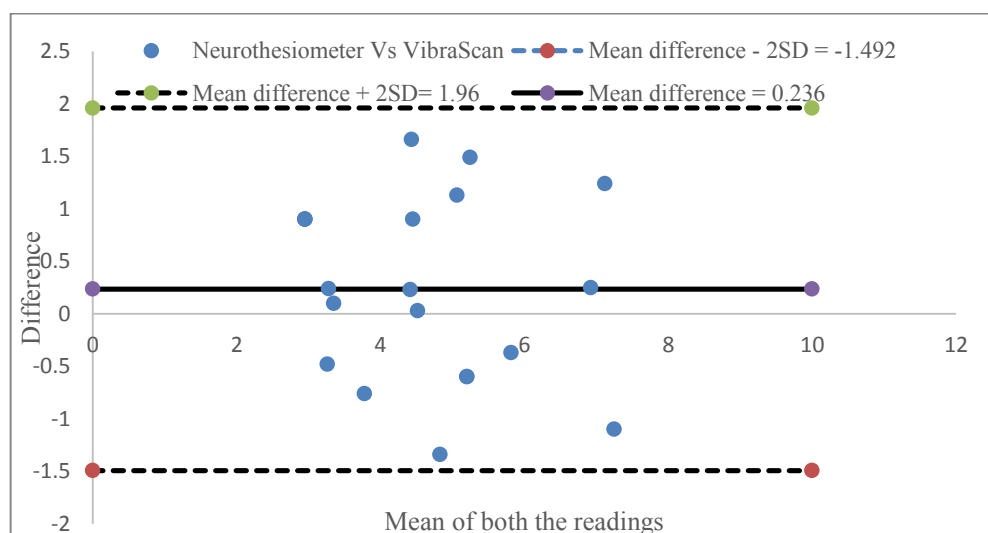
Figure 5.6 : Bland and Altman plot (left foot VPT measurements)

Bland and Altman's method was used to plot the difference of VibraScan and Neurothesiometer VPT measurement of left foot against the mean of two measurements shown in Figure 5.6. The plot also has the benefit of showing the variations in the results. The limits of agreement are indicated by the black broken lines that are the interval of two standard deviations of the estimation differences on either side of the mean difference (0.236). This shows that the 95% of subjects will have a difference in VPTs between the limits of agreement on the Bland – Altman plot for the left foot. It is important to see whether the range of the limit of agreement is large or small with respect to the range of values. As limits of agreement are small, the two measurements methods could be interchangeable.
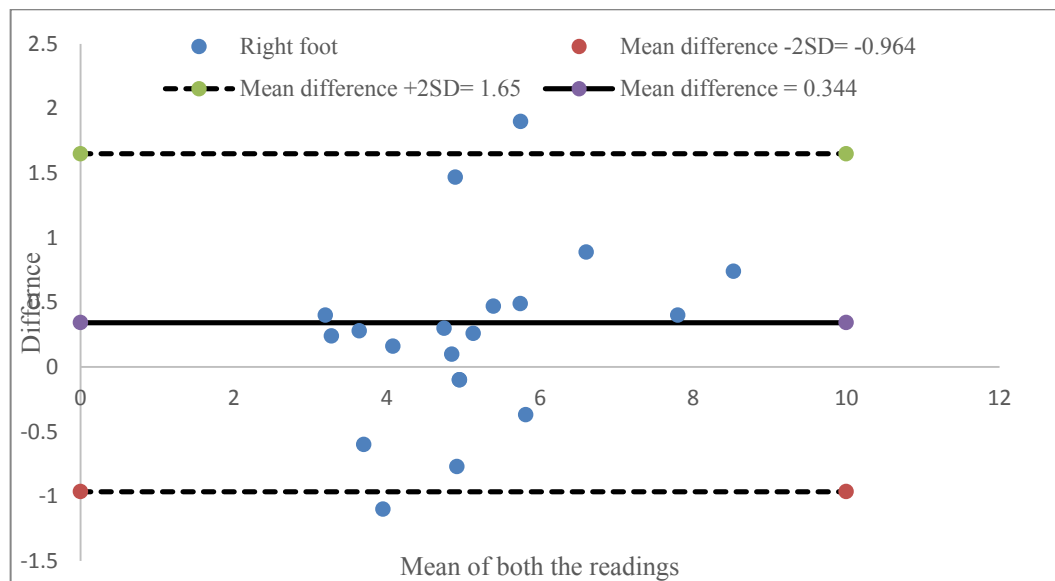
Figure 5.7 : Bland and Altman plot (right foot VPT measurements)

Bland and Altman's method was used to plot the difference of VibraScan and Neurothesiometer VPT measurement of right foot against the mean of two measurements shown in Figure 5.7. The limits of agreement are indicated by the dark broken lines that are the interval of two standard deviations of the estimation differences on either side of the mean difference (0.344). This shows that the 95% of subjects will have a difference in VPTs between the limits of agreement on the Bland – Altman plot for the right foot as well (Dave 2018)

Discussion

After testing the subjects using VibraScan and Neurothesiometer, the measured level of agreement proves that both these methods are consistently measuring similar VPTs when vibration stimulus is alternately applied on both feet. This shows that even the method of conducting the test is totally different, VibraScan behaves almost similar to Neurothesiometer

in terms of measuring VPT. The technique of independently measuring VPT, automatically interpreting the severity level of complication, programmable and an additional feature of monitoring pressure during the test makes VibraScan, an advanced tool for measuring diabetic neuropathy. The limitation of this study is at present, the outcome is based on twenty healthy subjects covering the normal range of VPT, however this study can be further extended to apply on many diabetic neuropathy patients and cover the whole range of VPT from 0 to 50 Volts for analysis purpose.

Chapter 6 Risk assessment Tool of VibraScan

In this chapter, the development of the tool that allows automated assessment of neuropathy based on the clinical history of subjects has been discussed. The flow chart below provides the overview of this chapter. This chapter will start with an introduction that explains the reason for developing VibraScan risk assessment tool. The risk factors associated with diabetic neuropathy were identified in this research study. The summarised patient data collection, it's pre-processing are explained in the data collection and data preparation sections. This chapter also covers the need and implementation of Box-Cox transformation and ordinary least square method to get an idea of potential risk factors in the summarised patient data.

The focus is mainly to find the best fitting methods and algorithms for solving the data analysis problem. Firstly, a standard artificial neural network (ANN) classifier was selected for the data analysis. The ANN classifier section starts with introduction, architecture and its implementation using complete set of attributes (attributes are the risk factors available in the data) and using only set of potential attributes for comparison purpose. Various classifiers such as ordinal logistic regression, discriminant functional classifier are implemented by using only potential attributes of the summarised patient data. The need for generating simulated patient data along with the implementation of the classifiers such as standard neural network classifier, discriminant functional analysis, ordinal logistic regression and neural network based proportional odds model (NNPOM) are also discussed. At last, the reason for selecting NNPOM method is explained for developing the risk assessment tool of the VibraScan by showing some examples.

Structural overview of the chapter
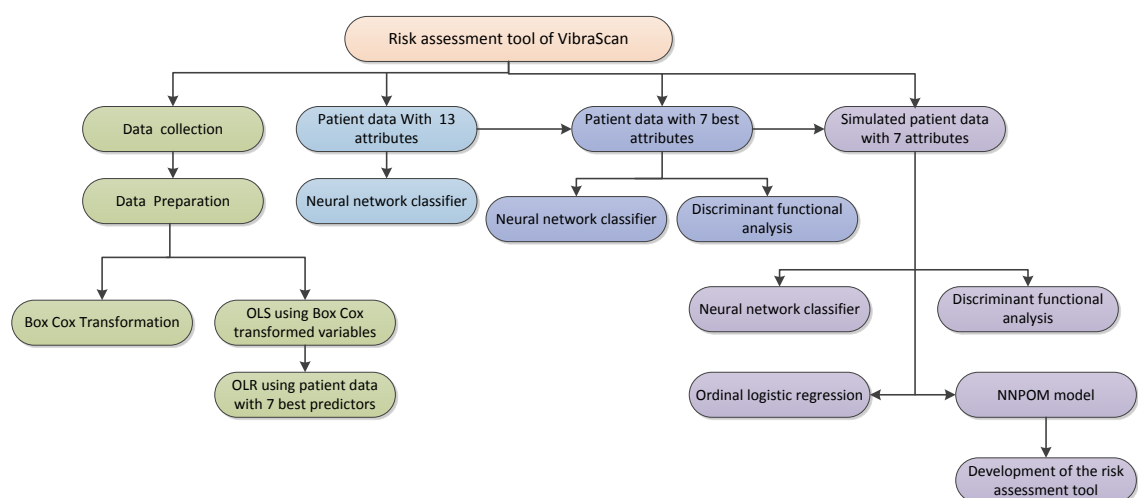
6.1 Introduction

Diabetic neuropathy (DN) is the serious neurological manifestation in diabetes. If neuropathy is not treated at the early stage it may increase the risk of foot ulceration and amputation (Adler et al. 1997). A novel VibraScan device was developed to assess DN based on vibration perception as discussed in the previous chapters. This entails that disease will be assessed only by vibration perception however, if one can consider the clinical characteristics of the subject, then DN can also be diagnosed based on clinical aspects of patients. This has given us the motivation for developing an automated tool for predicting VPT which can help in determining DN. This tool will help in getting better understanding of the disease progression by analysing the clinical data. There are many research studies available which have identified the risk factors associated with diabetic neuropathy. It has been observed that age was directly related to painful symptoms of diabetic neuropathy in large UK diabetes populations (Abbott et al. 2011b). There are several studies that shows there is a direct relationship between the duration of diabetes, increased age, obesity and diabetic neuropathy (Abbott et al. 2011b; Jambart et al. 2011) ; (Boulton 2008). Many studies have shown that there is no significant relation of gender in the diabetic neuropathy whereas in some studies it was shown that painful symptoms of diabetic neuropathy are more prevalent in females than in males (Abbott et al. 2011b). The study shows that age, insulin use, sex and duration of diabetes independently increased the risk factors of DN (Franklin et al. 1994). Likewise, not only demographic data but anthropometric and metabolic data could also play an important role in the prevalence of diabetic neuropathy. Existing devices like Biothesiometer/Neurothesiometer can perform screening test based sensation loss; however, risk factors of diabetic neuropathy were not taken into account. None of these existing tools considered both these possibilities (early symptoms and associated risk factors) to assess diabetic neuropathy. Taking this opportunity, the VibraScan risk assessment tool can be used as the independent tool for diagnosing DN from a set of risk factors for assessing diabetic neuropathy.

6.2 Risk factors for diabetic neuropathy

It will be interesting to know the common risk factors of diabetic neuropathy. Many research articles based on the onset diabetic neuropathy were studied. There are several independent risk factors that were significantly associated with diabetic neuropathy. The major risk factors of DN such as duration of diabetes, age, height, HbA$_1$c, cholesterol, sex, weight and BMI are discussed in this section.

Duration of diabetes: Duration of diabetes is one of the major factors of diabetes (Young et al. 1994). Based on the population selection and applying different methodology the exact prevalence of diabetic neuropathy differs, however the duration of diabetes association with DN was considered significant (Ziegler et al. 2014a).

Age: Age is considered to be one of the risk factors of DN. Several groups have demonstrated an independent effect of age, leading to a significant increase in diabetic neuropathy prevalence (Young et al. 1994; Abbott et al. 2011a).

Height: Height gives the measure of nerve fiber length, there are studies performed for both the types of diabetes where it was shown the association of height with diabetic neuropathy (Tesfaye et al. 1996b). According to one study (Papanas and Ziegler 2015), it was shown that there was 36% increase in the prevalence for every 5 cm increment in height in the population study in Mauritius.

HbA$_1$c: Glycosylated haemoglobin (HbA$_1$c) level is the important factor which needs to be considered to get the assessment of glycemic control, however in addition to HbA$_1$c, glycaemic variability could be considered as the independent risk factors of diabetes complication. HbA$_1$c variability had a significant association with diabetic neuropathy in type 2 diabetes (Lin et al. 2013).

Cholesterol: According to the study in 1996, it was found that there is a significant correlation between increasing level of cholesterol and diabetic neuropathy (Tesfaye et al. 1996a).

Sex: In one of the research study it was reported that the prevalence of diabetic neuropathy was more in males (30%) compared to females (18%) (Jaiswal et al. 2017), however, Abbot et al. have reported opposite that there was a higher prevalence in females (38%) compared to males (31%) (Abbott et al. 2011a).

Weight: As per the study carried out with 452 participants to obtain the risk factors of diabetic neuropathy, by linear regression models, weight was considered as one of the factors associated with DN (odds ratio [OR] 1.20 [95% Confidence Interval of 1.10;1.31]) per 5 kg (Andersen et al. 2018).

Body mass index (BMI): BMI is considered as an independent risk factor for diabetic neuropathy. According to the study (Xu et al. 2014), it was reported that BMI was the independent risk for the complication using multivariate regression analysis. This analysis is

mostly used to predict the value of one or more responses from the set of predictors where predictors can be continuous or categorical or a mixture of both.

Therefore, in most of the studies, the above-mentioned risk factors are commonly identified which were strongly associated with diabetic neuropathy. In these studies, different numbers of patient data were collected for which diabetic neuropathy assessment either using Michigan Neuropathy Screening Instrument (discussed in Chapter 2), using Neurothesiometer/ Biothesiometer by measuring VPT, or by Nerve conduction studies to determine the diabetic neuropathy patients and to identify the risk factors associated with it.

In order to determine the risk factors associated with diabetic neuropathy, there is a need to collect medical data where DN is assessed by vibration perception threshold.

6.3 Medical data collection

To perform this study, a summarised patient data was collected from the clinical database. In the summarised data, foot examination was assessed by Neurothesiometer, where vibration was provided at the great toe, the amplitude of the vibration was increased gradually and, subjects were asked to say 'yes' whenever they felt the vibration. Thus, the voltage at which the vibration was felt determines the vibration perception threshold (VPT). As per the VPT score, severity levels of diabetic neuropathy can be determined. The summarised patient data has patient's average measurements for the last 28 years which contains around 5158 subjects. In various studies almost same types measurements were followed to analyse independent risk factors for DN. These measurements can be used as the risk factors and need to analyse its effect for the prevalence of diabetic neuropathy. The main aim of using this data is to get a point estimate of VPT by giving the set of point measurements of some potential predictors. To achieve this aim, first data needs to be processed and used by the classical statistical technique for identifying the potential predictors.

6.3.1 Data preparation and statistical analysis

These variables in the data were measured once a year or are average of a small number of measurements within a year which was continued for 28 years, this longitudinal data was measured as an outcome repeatedly over time for the same subjects. There could be a possibility of unintended missing data or loss to follow-up which commonly occurs in longitudinal trials. The data can be analysed using multilevel modelling, however the output of these models may be less helpful so there is a need of baseline analysis, the output of which could be helpful for neural network modelling. For performing any statistical analysis of the

collected data, data needs to be further processed. First, the collected data were averaged over 28 years. The VPT measurements should be taken for both feet of each individual whereas in the collected data all the subjects did not have both the measurements for which statistical averaging technique was performed. These manipulations created a summary which conveniently eliminates missing measurements over time and over both feet as symmetrical neuropathy is the commonest among diabetic neuropathy (Bansal et al. 2006), thus maximising the number of patients with non-missing values for further analysis. Averaging is commonly used statistical technique which helps in identifying the trends and relationship within and between the datasets. After averaging the data, a summary of data count in each of the clinical measurements was calculated.

Table 6.1 : Summary of patient data

Variables	Observations	Mean	Std. dev.	Min	Max
VPT	5158	17.815	11.129	1.500	50
HbA1c	5143	08.728	1.295	4.766	14.4
High density lipoproteins (HDL)	4864	01.352	0.859	0.420	27.886
Low density lipoproteins (LDL)	4815	02.636	0.880	0.450	10.8
Urine albumin to creatinine ratio (ACR)	3886	7.152	18.355	0	293.830
Random Blood Glucose (RBG)	5078	11.573	3.779	1	38.3
Age	5158	57.733	18.450	7	98.0
Weight	5156	83.422	19.676	32.766	192.2
Height	5111	168.672	10.058	81	207.0
BMI	5107	29.286	6.426	14.583	104.77
Triglyceride	4928	02.072	1.292	0.3	22.6
Cholesterol	4852	03.998	1.193	1.43	18.7
Sex	5117	01.561	0.496	1	2
Duration of diabetes	5158	10.632	6.750	1	28

As shown in Table 6.1, it has been identified that out of 5158 data, 3691 subjects were having all the clinical measurements as required and rest of the missing data rows can be neglected for the analysis. Although a summary of patient data is achieved by averaging the data, however, to deal with longitudinal trends and skewness in the data there is still a need for statistical transformation to obtain information like relationship between the variables and to identify significant predictors. There are traditional types of transformation available such as logarithmic transformation, square root, inverting and reflecting that belong to power transformation, but for choosing the right type of power transformation which transforms the data in a way that its distribution better fits some target distribution, is a challenge. Therefore, an option of using transformation from Box-Cox family was taken into consideration, instead of just using a logarithmic transformation that makes the result normal and linearly related to covariates. Box-Cox transformation belongs to the power transformation family which can be used to identify the optimal normalising transformation for each variable (Box and Cox 1964).

6.3.2 Box-Cox transformation

Box Cox transformation was performed on all the individual variable and purpose was to find the behaviour when set of variables were used collectively by Box Cox regression model. This was found using Stata statistical software. For transforming the data set, the same mathematical operation or a transformation parameter should be applied to each data point of the set. Box-Cox transformation is defined by y^λ where y represents the data and λ is the power to which data is raised. The original form of the transformation is given as:

$$\left. \begin{array}{l} y(\lambda) = \frac{y^\lambda - 1}{\lambda}, \lambda \neq 0, \\ \\ y(\lambda) = \log(y), \lambda = 0. \end{array} \right\rbrace \qquad (10)$$

The value of λ is from -5 to 5, and to obtain the value of λ that best fit the data, transformation examines the values of it. Here, in the current data set the transformation was applied on both sides of the equation i.e. logarithmic transformation on the left-hand side and Box-Cox transformation on the right-hand side of the equation.

Box-Cox Right-hand side model (RHS only)

In the right-hand side model, all the independent variables were transformed using the parameter λ, which can be given in the form of equation 11 as below:

$$y_i = \beta_0 + \beta_1 x_{ij}^{(\lambda)} + \beta_2 x_{2j}^{(\lambda)} + \cdots + \beta_k x_{kj}^{(\lambda)} + y_1 z_{ij} + y_2 z_{2j} + \cdots + y_l z_{lj + \in_j} \qquad (11)$$

Where y is the dependent variable, $x_1, x_2, x_3 \dots x_k$ are the independent Box Cox transform variables with parameter λ and $z_1, z_2, z_3 \dots z_k$ are the independent variables without any transformation.

Hence the equation of the patient data can be expressed as natural logarithmic transform of dependent variable VPT as the function of independent transformed variables as age, height, weight, body max index (BMI), glycaemic control (HbA1c), High-density lipoprotein (HDL), Low-density lipoprotein (LDL), Urine albumin to creatinine ratio (ACR), Random Blood Glucose (RBG), Triglyceride, Cholesterol and duration of diabetes except variable sex.

After applying the analysis the results of the model is as presented in Table 6.2,

Table 6.2 : BoxCox right-hand side only model

Log Transformed VPT		Coefficient	Standard Error z P>|z|	[95% Conf. Interval]	
/λ		1.106	.0667	16.54 <0.001 .975	1.237
	Coefficient	R test statistics	p-values for LR tests	The degree of freedom of LR test	
Without transformed variable					
Sex	**.003**	**.019**	**0.89**	**1**	
Constant	**-1.40**				
Box Cox Transformed variables					
Duration of diabetes	.002	7.092	0.008	1	
Age	.019	2908.180	<0.001	1	
Height	.006	26.445	<0.001	1	
Weight	.004	12.576	<0.001	1	
BMI	-.004	1.874	0.171	1	
HbA1c	.032	34.914	<0.001	1	
HDL	.007	1.086	0.297	1	
LDL	.017	2.483	0.115	1	
ACR	.002	35.889	<0.001	1	
RBG	.002	1.088	0.297	1	
Triglyceride	-.002	0.096	0.754	1	
Cholesterol	.023	7.693	0.006	1	
λ Constant	1.106372				
Sigma Constant	**.428**				
N	**3691**				

The estimated value of λ is 1.106372 and is seen that the maximum likelihood estimate of the transformation parameter is positive and significant at 1%. Out of all the transformed variables, duration of diabetes, age, height, weight, glycaemic control (HbA$_1$c), ACR and cholesterol are significant predictors.

6.3.3 Ordinary least squares using Box Cox transformed variables

The maximum likelihood method is useful as the convenient route to the transform. Running the more familiar linear regression using the transformed variables provides additional information about model fits, linear relationship and about important predictors in more familiar terms. To get the additional fit estimates ordinary least squares regression is implemented. Basically ordinary least squares (OLS) regression method was used to detect the linear relationship between the natural logarithmic transformed dependent and Box-Cox transformed independent variables by using the formula as :

$$BoxCoxVariable = (Variable)^\lambda/\lambda \qquad (12)$$

Where λ = 1.106372

The calculated coefficient of determination (R^2) value of the whole test is 0.656 and the adjusted R square is 0.655 shows that all the independent variables shows 65% of the variability of the dependent variable as presented in Table 6.3. As per the analysis results out of all the 13 variables, duration of diabetes, Age, Height, Weight, glycaemic control (HbA1c), ACR and cholesterol are statistically significant predictors as the *p*- value is less than 0.05. However, sex, BMI, LDL, RGB, Triglyceride variables are not statistically significant as the *p*-value is greater than 0.05.

Table 6.3 : Ordinary least squares performed on all BoxCox transformed variables

	Coefficients	t- statistics	95% confidence limits	
Box Cox transformed variables except sex			**Upper bound**	**Lower bound**
Sex	0.002	(0.14)	-0.036	0.041
Duration of diabetes	0.002**	(2.72)	0.001	0.004
Age	0.020***	(73.21)	0.019	0.021
Height	0.006***	(5.57)	0.004	0.009
Weight	0.004***	(3.55)	0.002	0.006
BMI	-0.004	(-1.38)	-0.011	0.002
HbA1c	0.032***	(6.01)	0.022	0.043
HDL	0.006	(1.04)	-0.006	0.019
LDL	0.016	(1.58)	-0.004	0.037
ACR	0.002***	(6.17)	0.001	0.002
RBG	0.002	(1.04)	-0.002	0.005
Triglyceride	-0.002	(-0.31)	-0.016	0.011
Cholesterol	0.023**	(2.78)	0.007	0.039
_cons	-1.398***	(-4.55)	-2.001	-0.80
Observations	3691			
R^2	0.656			
adj. R^2	0.655			

t statistics in parentheses
* $p < 0.05$, ** $p < 0.01$, *** $p < 0.001$

In order to simplify this interpretation, OLS was performed again using only significant independent variables and dependent variable VPT. The analysis has been performed and results have been shown in Table 6.4.

Table 6.4 : Ordinary least squares performed on significant BoxCox transformed variables

Box-Cox transformed risk factors	Coefficients	t-statistics	95% confidence limits	
			Upper bound	Lower bound
Age	0.020***	(73.39)	0.019	0.020
Height	0.007***	(15.54)	0.006	0.008
Weight	0.002***	(9.24)	0.002	0.003
HbA1c	0.033***	(7.03)	0.024	0.042
Acr	0.002***	(6.01)	0.001	0.002
Cholesterol	0.018***	(3.71)	0.009	0.028
Duration of diabetes	0.002*	(2.52)	0.001	0.004
_cons	-1.524***	(-12.02)	-1.772	-1.275
Observations	3788			
R^2	0.646			
adj. R^2	0.645			

t statistics in parentheses
* $p < 0.05$, ** $p < 0.01$, *** $p < 0.001$

Table 6.5 : Significant predictors

	F - statistics	p-values	R^2	Change in R^2
Age	5148.12	<0.001	0.576	
Height	447.99	<0.001	0.621	0.045
Weight	133.04	<0.001	0.634	0.013
HbA1c	68.74	<0.001	0.641	0.007
ACR	45.62	<0.001	0.645	0.004
Cholesterol	11.53	<0.001	0.646	0.001
Duration of diabetes	6.34	0.012	0.646	0.001

As shown in Table 6.5, as expected all the variables are statistically significant as the *p*-value is less than 0.05 and can be considered as the risk factors for the development of diabetic neuropathy as per the analysis results. It shows age is the most significant predictor while duration of diabetes is the least significant predictor.

The advantage of applying this classical statistical method on the collected data is to get the hint of significant predictors in the collected data for getting classical information and can be useful to compare with the neural network predication success later on.

The original patient data set was pre-processed and information was extracted using required transformation of the variables where VPT was measured continuously. Now, this can be used to get the point prediction of VPT or VPT can be predicted with the confidence interval. If the confidence interval of predicted VPT is too large then it is less helpful to the user. In order to simplify the interpretation of the outcome variable (VPT) for both clinicians and subject itself, it was decided to interpret the VPT prediction in terms of cumulative risk levels. For solving this problem in terms of classification, the first step is to divide the data into specific categories based on VPT thresholds. By considering clinician's insight in the field of diabetic neuropathy it was decided to categories the dataset into three classes according to VPT measurement in voltages (V) as low risk (0 to 20.99 V), medium risk (21 to 30.99 V) and high

risk (≥ 31 V) diabetic neuropathy. To approach this dataset for further analysis where VPT was continuously measured, it is important to identify data's behaviour and its significant predictors for the categorical data set. To achieve this information, categorical data were analysed using ordinal logistic regression.

6.4 Ordinal Logistic Regression using summarised patient data

Ordinal logistic regression (OLR) is the statistical analysis method performed using SPSS statistical software to find the relationship between ordinal responsive (dependent) variable and independent explanatory variables (O'Connell 2006). The type of ordinal logistic regression implemented was the cumulative odds ordinal logistic regression with proportional odds that have cumulative categories. The ordinal variable is the categorical variable with the ordering of the category levels. As discussed before, the data is divided into three ordinal categories based on the VPT measurements along with the number of instances is presented as shown in Table 6.6. To analysis these categories after dividing the data, OLR was implemented. As per the case summary table, it shows a number of instances available in each level of the responsive variable. The total number of instances available in the data set is 2450, however, in two of these levels, there are fewer cases. SPSS does listwise deletion of cases if missing values are available in any of the variables.

Table 6.6 : Case summary of real patient data

Categories of the dependent variables	The range of VPT score in Volts (V)	No. of instances (2450)
Low risk	0 to 20.99	1696
Medium risk	21 to 30.99	459
High risk	31 onwards	295

In the model fitting information as shown in Table 6.7, the degree of freedom (df) is 7 i.e. 7 independent significant variables (age, height, weight, HbA1c, ACR, cholesterol and duration of diabetes) were used as determined from the previous analysis to OLR. Chi-Square is the difference between the two −2 log-likelihood values. The last row of the table presents the information that either all or some of the variables are statistically significant. In other words, added variables are statistically significantly improving the model compared to the intercept only (no added variables). As $p < 0.001$ means model predicts the dependent variable better than the intercept-only model.

Table 6.7 : Model Fitting Information

Model	-2 Log Likelihood	Chi-Square	df	Sig.
Intercept Only	4034.042			
Final	3223.445	810.597	7	< 0.001

As in Table 6.8, p < 0.05 (from the Sig. column) indicate model does not fit well with the data. Good models have large observed significance levels.

The model estimates from ordinal logistic regression are maximum likelihood estimated through an iterative process. As they are not calculated to minimise the variance, to evaluate the goodness of fit of logistic models, several pseudo R squared is calculated as displayed in Table 6.9. These pseudo R squares are like R square in terms of scale (but cannot be interpreted as OLS R square) i.e. ranging from 0 to 1, higher the value better the model fit.

Table 6.8 : Goodness-of-Fit

	Chi-Square	df	Sig.
Pearson	5399.082	4891	< 0.001
Deviance	3223.445	4891	1.000

Table 6.9 : Pseudo R-Square

Pseudo R-square	
Cox and Snell	.282
Nagelkerke	.349
McFadden	.201

There are coefficient, their standard errors, the Wad test and associated p- values (Sig.) and 95% confidence interval of the coefficient as available in the estimated parameter Table 6.10. The dataset has three level of a variable called <cat> (coded 1, 2, and 3) that are outcome variables. It can be used to determine the number of statistical significant independent variables on the dependent variable (VPT). Out of seven predictors age, weight and height were significant predictors while HbA1c, ACR, Cholesterol and duration of diabetes were not. As per the results, one unit increase in age (from 0 to 1), there can be 0.1 increase in the logarithmic odds of being a higher level of cat, with all the other variables in the model being constant. For weight variable, one unit increase in weight (from 0 to 1), there can be 0.02 increase in the logarithmic odds of being a higher level of cat, keeping other variables constant. For the height variable, one unit increase in height (from 0 to 1), there can be 0.05 increase in the logarithmic odds of being a higher level of cat, with other variables as constant as shown in Table 6.10.

This can be expressed in form of equation 13 as below:

$$y^* = x^T\beta + \epsilon \qquad\qquad (13)$$

Where y^* is the unobserved dependent variable, x^T is the vector of the independent variable, β is the estimated coefficient and ϵ is the error term.

And $y = \begin{cases} 0 & if\ y^* \leq\ \mu_1, \\ 1\ if\ \mu_1 < y^* \leq \mu_2, \\ 2\ if\ \mu_2 < y^* \leq \mu_3 \end{cases}$

Where x_i are the independent variables, μ_i are the set thresholds of the categories and using parameter vector β, the ordered logit technique will use the observations on y from y^*.

Table 6.10 : Parameter estimates

		Estimate	Std. Error	Wald	df	Sig.	95% Confidence Interval	
							Lower Bound	Upper Bound
Threshold	[cat = 1.00]	19.678	1.238	252.833	1	< 0.001	17.252	22.103
	[cat = 2.00]	21.202	1.251	287.450	1	< 0.001	18.751	23.653
Location	HbA1c	.013	.043	.099	1	.753	-.070	.097
	ACR	.004	.002	2.678	1	.102	-.001	.008
	Age	.111	.005	412.044	1	< 0.001	.100	.122
	Weight	.021	.003	54.160	1	< 0.001	.015	.027
	Height	.056	.006	90.113	1	< 0.001	.044	.068
	Cholesterol	.069	.042	2.668	1	.102	-.014	.152
	Duration of diabetes	.000	.008	.003	1	.958	-.016	.015

By comparing all the values of the responsive variable with the values of the predicted outcome, it is possible to calculate the classification success for each class. Using SPSS, the cross-tabulation (confusion matrix) was obtained as shown in Table 6.11 where data is presented for each of the classes in terms of true positive, true negative, false positive and false negative. It measures the percentage overall classification success estimated as 71.5%, in which low-risk category achieves classification success of 75.8%. This could be probably inflated by a large number of instances in category 1 i.e. 1629 is more probable by chance compared to the other classes.

Table 6.11 : Predicted Response Category Cross-tabulation

			Predicted Response Category			
			Low risk	Medium risk	High risk	Total
C A T E G O R I E S	Low risk	Count	1629	41	26	1696
		% within cat	96.0%	2.4%	1.5%	100.0%
		% within Predicted Response Category	75.8%	30.4%	15.8%	69.2%
	Medium risk	Count	344	50	65	459
		% within cat	74.9%	10.9%	14.2%	100.0%
		% within Predicted Response Category	16.0%	37.0%	39.4%	18.7%
	High risk	Count	177	44	74	295
		% within cat	60.0%	14.9%	25.1%	100.0%
		% within Predicted Response Category	8.2%	32.6%	44.8%	12.0%
Total		Count	2150	135	165	2450
		% within cat	87.8%	5.5%	6.7%	100.0%
		% within Predicted Response Category	100.0%	100.0%	100.0%	100.0%

Using this model, it gives an overview regarding significant predictors when the continuous data is categorised into three classes based on VPT measurement. These results were obtained from the conventional statistical methods; however, for developing a risk assessment tool, it

can be possible to use a classifier that can handle these data more precisely and accurately. Various research studies based on a clinical characteristic of the subjects were studied to get the idea for developing the tool.

6.5 Methods for developing a risk assessment tool

In one of the research study, assessment of DPN was performed using the Michigan Neuropathy Screening Instrument (MNSI) questionnaire examination. It was focused on the relationship between risk factors and the prevalence of diabetic neuropathy in youth with type 1 diabetes and type 2 diabetes. Out of 1734 youth, the prevalence of DPN was 7% in youth with type 1 diabetes and 22% in youth with type 2 diabetes. Older age, longer diabetes duration, smoking, increased diastolic blood pressure, obesity, increased LDL cholesterol and triglycerides, and lower HDL cholesterol are the selected risk factor for type 1 diabetes and older age, male sex, longer diabetes duration, smoking, and lower HDL-c were the risk factors for type 2 diabetes. It was found that the effect of the glycaemic control was getting poor over time with DN in youth with type 1 diabetes than another type (Jaiswal et al. 2017).

Another study was performed using 110 diabetic patients in which Michigan Neuropathic Diabetic Scoring (MNDS) was used to differentiate the cases among the normal and abnormal. In this study Nerve conduction study was used to assess diabetic neuropathy. It was found that age, duration of disease, gender, quality of diabetes control have a significant relationship with diabetic neuropathy and no correlation was found with risk factors like hyperlipidemia, high BP, cigarette smoking (Booya et al. 2005).

A study was performed to identify the risk factors associated with the prevalence of diabetic neuropathy by comparing the prevalence of diabetic neuropathy with known diabetes mellitus and with newly detected diabetes mellitus. In this study monofilament test, pinprick and vibration perception threshold was used to categories diabetic neuropathy into normal, mild, moderate and severe neuropathy. A total of 586 patients was identified with developed DN. Regression analysis was used to identify the risk factors associated with DN. It was found that age, dyslipidemia, alcoholic status, macro and microvascular complication significant risk factors for diabetic neuropathy (Bansal et al. 2014).

In most of the research studies, assessment of diabetic neuropathy was performed either by measuring vibration perception threshold or using various questionnaires to identify the risk factors of diabetic neuropathy. In most of the cases, data analysis was performed using conventional statistical methods to identify the significant risk factors of DN. To the best of

knowledge, there are no such tools available which make use of these risk factors for determining diabetic neuropathy of an individual which seems possible by analysing a large number of clinical data of DN. As discussed before, the focus is to develop the risk assessment tool to help the clinicians for analysing complex relationship between the risk factors and predicting the most likelihood level of DN. After getting the results from the classical statistical analysis and looking at the complexity and nonlinearity in the data, idea of using standard artificial neural network classifier was taken into consideration. The introduction of ANN showing capability of learning the data, structure, architecture, various methods, training the model and comparison with another classifier's result are discussed in the following sections.

6.5.1 Artificial neural networks

Artificial neural networks (ANN) technique is extensively used for prediction, forecast or classification. Capabilities of finding the pattern and recognising the relationship between the input variable is much faster than the other existing conventional methods for which ANN was widely used in medical (Yao and Liu 1999), ecology, cost estimation (Londhe and Deo 2004), forecasting (Ho et al. 2001), computer science and in physical sciences. ANN uses the intelligent mechanism similar to the human brain to solve the complex problems. There are different types of neural networks available based on the type of processes to be performed. Some of the neural networks are relatively simple and some are complex. The artificial neural network is used in performing various tasks like prediction, forecasting, pattern classification and clustering (He and Xu 2010). In the current study, pattern classification was used in ANN. However, by using the neural network classifier, it is important to get an idea of how well the neural network is working based on true predicted class for which loss function or cost function is used i.e. it maps the value of the variable with the real number to represent the cost associated with the event. To understand the working of the classifier and the way it learns the pattern of the data to perform classification, need to get into the basic theory behind the neural network. So the concept of neural network, neural network classifier, hyperparameter available to tune the network and its implementation needs are also discussed.

Biological Neuron and Artificial neuron:

Neural networks emulate the procedure used by the human brain to process the data that consists of learning the relationship between the data gathered and the data obtained. Here similarities in terms of structure and processing the signals are shown by comparing the Biological neuron and artificial neuron.
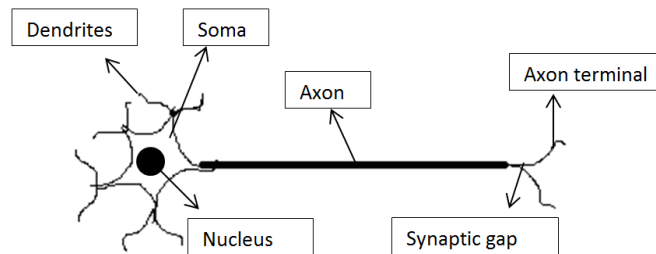
Figure 6.1 : The biological Neuron

For processing information in the human brain, it consists of a large number of neural cells. Each Biological neuron consists of three main components such as dendrites, axon and soma as shown in Figure 6.1 (Fausett 1994). The electric impulses as the input signal transmitted through the synaptic gap. The information is received by the dendrites which gather in the soma and deliver to the neuron's axon to the dendrites at its end. The information pass again if the certain threshold is crossed else would not pass further.
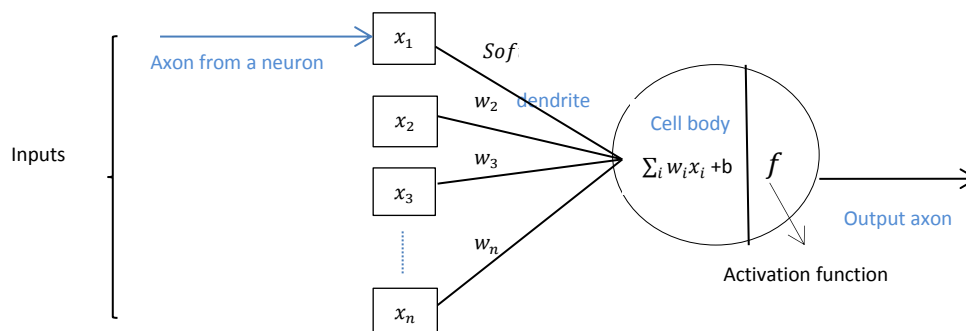
Figure 6.2 : The artificial Neuron

Similarly, an artificial neuron is a simple processing unit consist of three components shown in Figure 6.2 where a fixed number of inputs having activation from other neuron is connected with the neuron by weighted link w_i , neurons will sum up all the inputs and apply the activation function to get the output, this output will transmit the information to another neurons.

6.5.2 Classification using neural network

Depending on the number of class, neural network classification can be used. To start with first neural network binary classification is explained which is followed by multiclass classification.

Neural network Binary classification:
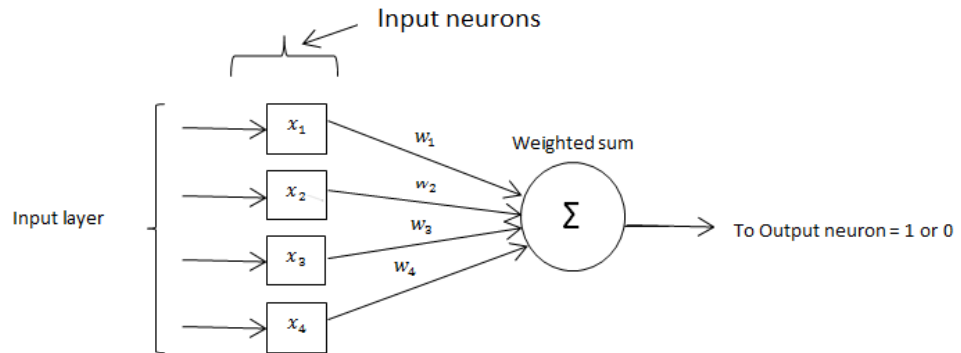
Figure 6.3 : A single layer perceptron

In the binary classification, there is an artificial neuron in which an input neurons layer is feed-forwarded to an output neurons layer as displayed in Figure 6.3. The inputs are directly connected to the output layer via a single layer of weights. Here the links are from each input to the output in one direction.

The initial weights are assigned randomly in single layer perceptron. Single layer perceptron is activated when the threshold reaches its maximum value. The threshold value is either 1 or 0. It is given as below:

$\Sigma w_i x_i > \theta$ => Output is 1

$\Sigma w_i x_i \leq \theta$ => Output is 0

The input is provided to the input layer to obtain the predicted output; if the predicted output is not equal to the desired or expected output then the weights will be adjusted to reduce the error. The process of adjusting the weights to obtain the expected results is known as **training** the network. If the predicted output matches the expected output there will not be any changes in the weights.

Single layer perceptron / binary classification networks can perform pattern classifications task to classify correctly into one or two classes. It is used to classify the objects according to their position in n-dimensional hyperspace (using n inputs) where the problem can be defined as a linear separable classification problem. It can be implemented on those patterns which are

only linearly separable patterns irrespective of non-linearity used. In the current scenario, there are three categories so more advanced neural network classifier should be used as described in the following section.

Neural network structure model (binary to multiclass classification):

Neural networks don't depend on pre-prepared program or mathematical equations to estimate the results. This complex nonlinear task can be achieved by neural network structure.
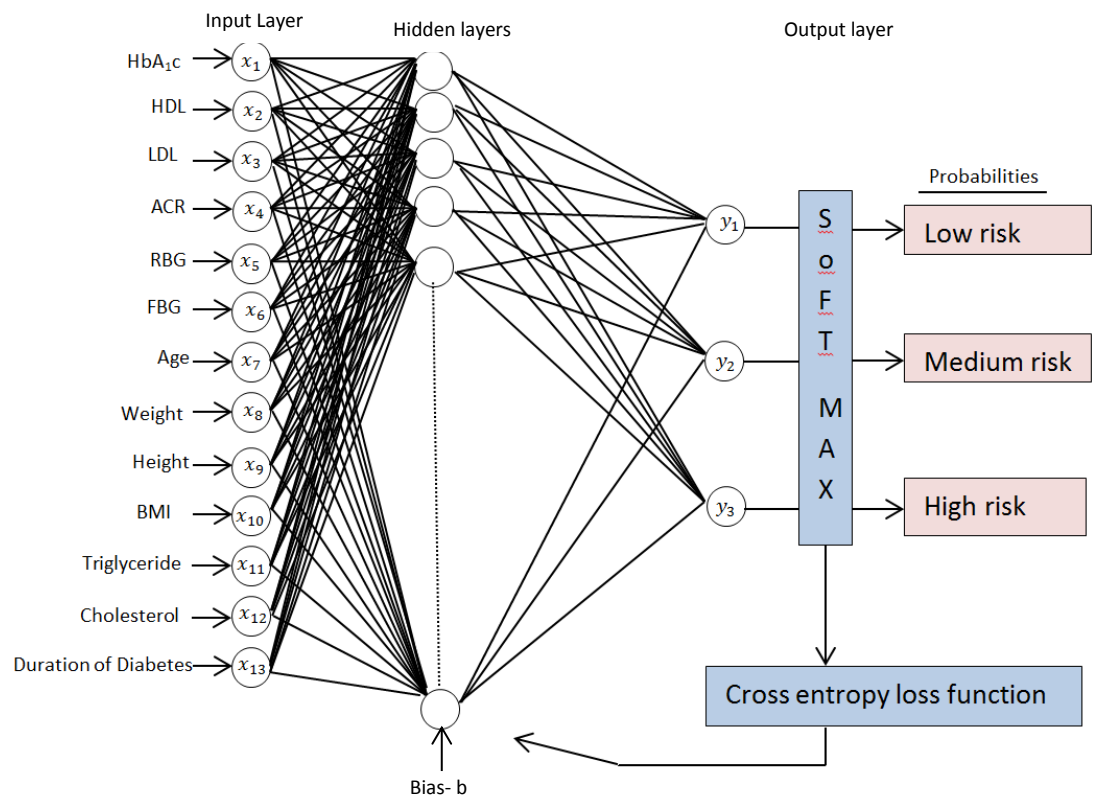
Figure 6.4 : Neural network structure for classification

This is the structure of the neural network classifier using feedforward learning algorithm as illustrated in Figure 6.4. It is a three layer feed-forward neural network which consists of the input layer, hidden layers and output layers. These layers having thirteen nodes in the input layer, N number of nodes in the hidden layer and three nodes in the output layer. Selecting a number of neurons in hidden units is a problem specific i.e. Number of hidden neurons may be appropriate for one model but may not work well for another dataset. The model might miss some of the minute details if selected neurons are less. If the neuron size is less or underestimated then it may lead to poor approximation and if excessive neurons are used then it may lead to a problem of overfitting. In the same way, hidden layers which consist of hidden units also need to be set. Increasing number of hidden layers also demands to specify the hidden units for each hidden layers. A number of hidden layers should be selected based

on the complexity of the data set. Selecting the number of hidden layers and neurons are an iterative process which needs to be properly assessed in terms of accuracy.

In the feed-forward architecture, the signal propagates from input to output and updating the whole cycle by obtaining the error value from calculated values and real values. This process is achieved when input values from the input layer propogates to the hidden layer node by multiplying the weight connecting the node. The entire training data set passes through a neural network is known as a number of epochs. The values of weights get updated in every epoch and associated error should get minimised with each epoch. If less number of epochs is set then there could be a problem of underfitting. Number of times the value of weight changes the graph can change from under fitting to optimal. A large number of epochs may result in overfitting of the curve. These weights and biases get updated in the direction depending on the types of training algorithms implemented in the network. To train the network various training algorithms are available, out of which resilient backpropagation algorithms and scaled conjugate gradient algorithm are fast and used for pattern classification of ANN (Mathworks 2018) (Sharma and Venugopalan 2014). Scaled conjugate algorithm (Trainscg) is fast because it does not require line search during each learning iteration step. Trainscg requires more iterations to converge than other algorithms, however number of computations decreases as it avoid each line of search (Hager and Zhang 2006). Resilience backpropagation (Trainrp) runs on the basis of eliminating the effects of the partial derivatives (Anastasiadis et al. 2005). Depending on the sign of the derivatives the direction of updating the weights will be decided; however there will not be any effect of magnitude of derivatives. After this, the hidden layer value is computed through the transfer function i.e. sigmoid function commonly used as the activation function provided in the following equation to get the output value.

$$F(X) = \frac{1}{1+e^x} \qquad (14)$$

It produces "**S**" shaped graph when plotted. There are two types of sigmoid functions log sigmoid function and tan-sigmoid function. The range of log sigmoid function is from 0 to 1 while the range of the tan-sigmoid function is -1 to 1. Preferably the tan-sigmoid function should be used due to its output range. The main advantage of this activation function is negative inputs will be strongly associated with negative output and zero inputs will be mapped near zero in the tan graph. Log and tan-sigmoid functions are commonly used in feedforward neural network. The neural network gets trained depending on selecting the value of the learning rate. Learning rate can be defined by adjusting the weights with respect

to loss gradient. Lower the value of the learning rate, it takes more time to learn. The advantage of using a low value of learning rate is, it will not miss any of the local minima but will take a longer time to converge.

At the output node, the softmax activation function is used yields the probability values of the classification provided by the nodes. The softmax usually takes the un-normalised vector and normalises in terms of probability distribution over predicted output classes. Here X is the input, where inputs are values of all the 13 attributes $= (x_1, x_2, x_3, \ldots, x_{13})$. Y is the output: Output of the classifier is 1 of the 3 classes' probabilities (1 to 3). $Y = (y_1, y_2, y_3)$. Each y_i represents the input values belongs to class i.

Softmax function is applied to output probabilities of multiple output class and can be given as the input X is multiplied by weights W and added to bias to generate activations.

$$y_i = softmax\left(\sum_j W_{i \, .j} x_j + b_i\right) \tag{15}$$

$$Softmax(x_i) = \frac{e^{z_i}}{\sum_j e^{z_j}}$$

In, $3-$ class classification problem with 3 output nodes, softmax normalise the 3-dimensional vector into the range of [1, 0] $\in$ R. Here $y_{i,}$ is the predicted probability. The input and output of the softmax function are both vectors defined in the equation. In order to evaluate how well the classifier is working, the loss function is used. Loss function of the model plays an important role in measuring the inconsistency between the predicted output and actual output. The loss function is known as the performance goal. Here cross entropy loss function is used to get the classification success given by the equation as below:

$$crossentropy(label, y) = -\sum_i label_i \log(y_i) \tag{16}$$

This model will be used to train the neural network as per the numbers of provided attributes.

6.5.3 Experimental methodology

Experiments were carried out on a window operating system with an i5 processor with 8 GB RAM. All the neural network implementations were achieved using pattern classification feature of neural network toolbox in MATLAB platform.

1. Pre-process the medical data to achieve the class balance before using a neural network for classification.

2. Follow the file format like (labels, attr1, attr2, attr3,… attrN) where labels should be encoded as [1,0,0], [0,1,0] and [0,0,1]. (where attr means attributes ----> risk factors of the DN)

3. Divide dataset into three sets as training (70%), testing 15% (unseen data) and validation sets (15%).

4. Adjust the important hyperparameters such as hidden neurons ϵ (10, 15, 25, 50), hidden layers ϵ (1), learning rate ϵ (0.1), iterations ϵ (1000) and measure the epochs.

5. Train the neural network using resilient backpropagation (Trainrp) and scaled conjugate gradient (Trainscg) algorithm.

6. Train neural network with 13 attributes using training, test and validation set. Select the model that gives optimal result by changing the values of required hyperparameters.

7. Confusion matrix is computed to assess the neural network performance.

8. Based on the classification success of training, testing and validation set, calculate overall accuracy for comparison.

9. Repeat steps 2 to 8 to train the neural network using 7 best predictors.

10. Compare the accuracies of the dataset with a different number of attributes.

Pre-processing of the medical dataset

Before selecting any of the classification models it is important to understand the property of the medical data. For training any of the medical data, the issues and challenges that are related to those data need to be carefully handled. As the medical data is collected directly from the medical database, possibly common issues can be identified as follow:

1. **A total number of variables:** It is essential to have relevant information in the data for any medical diagnosis. To perform any machine learning technique the complexities associated with these data is not linear. As the number of variables increases the complexities also increases. Another limitation of collected data is that it may have a specific number of attributes that may vary according to the patient's requirements. For research purpose, if the required number of attributes are more, this may not be fulfilled when the data is collected from the medical database.

2. **Missing data**: Medical database system does not have all the required data that are useful for research. In the clinical practice, it happens that patients do no fill all the details asked in the report because they feel it is not essential or in some cases, they are not in a position to record few of the attributes (Almeida et al. 2010). Because of

this reason, there are patients in the database who have missing data in some of the attributes. In the collected data total number of observations was around 5158. In this huge number of observations, there were missing values in few of the attributes. For neural network training, it requires full sets of input data. In this situation for getting full set of input data, those observations were discarded with the missing value in any of the attributes, due to that a set of 2450 observations were available having input values in all the attributes.

3. **Noisy data**: Data available in the medical database have noise which involves implicit errors introduced by the measurement tools or by the experts while gathering the data. Due to this there is a possibility of extreme values in some of the attributes, i.e. either very low value or very high values because of which the mean value of the attributes gets affected.

4. **Class Imbalance in medical data:** In most of the medical datasets, datasets are not balanced in terms of class labels. When the dataset is extremely imbalanced, classification method does not work well on the minority class. In the current medical dataset VPT scores of these observations were used to define class labels. The range of the VPT score is from 0 to 50 Volts. All the collected observations were associated with this VPT score. In this datasets, data were divided into three class labels such as Low risk, medium risk and high risk with the threshold value of 0 - 20 Volts, 21 - 30 Volts and 31 Volts onwards respectively. When the data is divided into these classes it was interesting to see the observations available in each class as shown in Table 6.12:

Table 6.12 : Class imbalance

Class labels	Number of instances – (Total number of instances is 2450)	Percentage distribution %
Low risk – class 1	1696	69.2
Medium risk – class 2	459	18.73
High risk – class 3	295	12.0

This shows that the dataset is highly imbalanced as the number of instances available in class 2 and 3 is very less. The percentage of instances available in class 1 is 69.2% called the majority class. The number of instances available in class 2 and class 3 are 18.73% and 12.0% respectively of the whole dataset called minority classes. If the classification algorithm is applied then more correctly classified will belongs to majority class only. Data sampling

techniques can be used to solve the problems with distribution of the dataset. This can be achieved by under-sampling the majority class or oversampling the minority class. The data available in class 1 is 1696 and if undersampling of the majority class is implemented then overall data will be reduced and so oversampling of minority class technique had been chosen for class balance. In this technique, it will not add any new information to the dataset but will reuse the existing data sample (Song et al. 2010). In order to balance both class 2 and class 3, it should have 1696 instances. This data sampling technique is applied using MATLAB software where the original data file is loaded in the workspace and instances were added in class 2 and 3 by replicating their sample data to balance the class.

Due to class sampling technique, all the classes were having the same number of instances as shown in below Table 6.13:

Table 6.13 : Class balance after data sampling

Class labels	Number of instances – (Total number of instances is 5088)	Percentage distribution %
Low risk – class 1	1696	33.3
Medium risk – class 2	1696	33.3
High risk – class 3	1696	33.3

This shows that now all the three classes are having an equal number of instances. Before using these data for performing the experiments as the input data range are different from each other in order to reduce the calculation time and obtain better results, all the input data of each variable (attribute) were normalized prior to neural network training (Sola and Sevilla 1997).

6.5.4 Results of neural network classifier using 13 attributes

An experiment was performed using 13 attributes and some of the basic hyper-parameters were kept fixed as shown below:

1. Max_epoch = 1000
2. Time = infinite
3. Minimum gradient = 1
4. Maximum_validation_fail = 20
5. Performance goal = 0

Table 6.14 : Neural network modelling using 13 attributes

	Training Algorithm	Hidden neurons	Hidden Layer	Epoch	Learning rate	Overall Classification %
1	Trainscg	10	1	191	0.1	61.6
2	Trainscg	15	1	248	0.1	63.7
3	Trainscg	25	1	188	0.1	64.2
4	Trainscg	50	1	226	0.1	66.9
5	Trainrp	10	1	164	0.1	60
6	Trainrp	15	1	261	0.1	62.2
7	Trainrp	25	1	345	0.1	65.1
8	**Trainrp**	**50**	**1**	**129**	**0.1**	**67.9**

The confusion matrix of the overall data set (consists of testing, validation, training sets) is shown in Table 6.15. The confusion matrix is the summary of prediction results on classification problems and presents the accuracy of the classifier. It will give correct classification as 'True positive' or 'true negative' as mentioned in green coloured boxes (diagonal of the square) and incorrect classification is listed by 'false positive' and 'false negative' as mentioned in red coloured boxes.

The row indicates how much each target class are classified into each output classes.

1. 1696 samples from class 1, 1139 samples were correctly classified as class 1,

2. 1696 samples from class 2, 1016 samples were correctly classified as class 2 and

3. 1696 samples form class 3, 1264 samples were correctly classified as class 3.

Each row of the matrix correlate to the predicted class and each column of the matrix correlate to an actual class. The accuracy has been calculated based on Equation 17 below:

$$Accuracy = \frac{\sum True\ positive + \sum True\ negative}{\sum Total\ number\ of\ instances} \qquad (17)$$

$$Accuracy\ of\ overall\ matrix = \frac{1139+1016+1264}{5088} = 67.2\%$$

Table 6.15 : Confusion matrix with a dataset of 13 attributes (hidden unit 50 with resilient backpropagation)
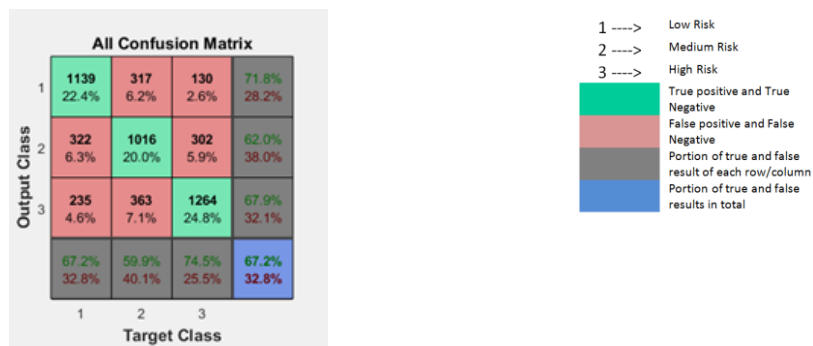
6.5.5 Results of neural network classifier using 7 best attributes

Neural network was trained using 7 attributes as shown in Table 6.16.

Table 6.16 : Neural network modelling using 7 attributes

	Training functions	Hidden neurons	Hidden layer	Epoch	Learning rate	Overall Classification %
1	Trainscg	10	1	134	0.1	58
2	Trainscg	15	1	47	0.1	60
3	Trainscg	25	1	172	0.1	60.3
4	**Trainscg**	**50**	**1**	**335**	**0.1**	**67.4**
5	Trainrp	10	1	90	0.1	57.7
6	Trainrp	15	1	426	0.1	62.7
7	Trainrp	25	1	144	0.1	61.1
8	Trainrp	50	1	53	0.1	58.3

Table 6.17 : Confusion matrix with a dataset of 7 attributes (hidden unit 50 with scaled Conjugate backpropagation)

As per the confusion matrix overall classification success obtained was 67.4% shown in Table 6.17.

The main purpose of applying NN classifier on both the datasets was to identify the difference in results using all the attributes and using only 7 attributes. Table 6.14 shows the comparison resilient backpropagation algorithms (Trainrp) and scaled Conjugate back propagation (Trainscg) algorithms using 13 attributes. Results show epochs varied from 188 to maximum 345 epochs this means that the training has stopped when it has stopped improving and reached the performance goal of 0. The maximum validation check has been set to 20, means that the training will stop when the validation subset error rate increases continuously for more than 20. Another important parameter is the learning rate, learning rate (LR) is the parameter which controls the adjustment of the weight with respect to the loss gradient. If the value of the learning rate is too low then it takes a long time to converge and if the value of learning rate too high that it might miss any local minima. Typically learning rate can be configured by an iterative process. The value has been tested for 0.1, 0.01 and 0.001. In Figure

6.5 (a), it shows that based on the choice of learning rate can affect the convergence of the algorithm.

(a)   Learning rate curves

(b)   Curve with LR equal to 0.1
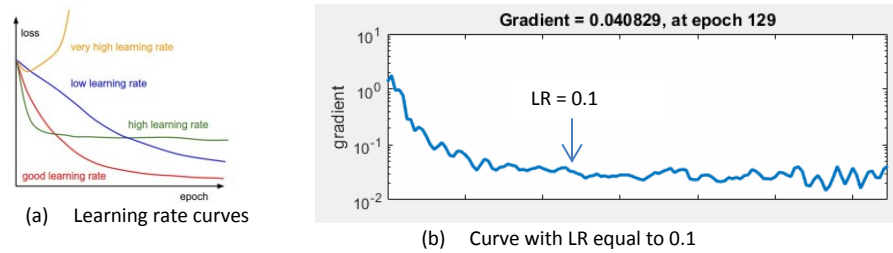
Figure 6.5: (a) showing the different effect of various learning rates (Fei-Fei Jan 2015) (b) Effect of leaning rate at 0.1

Figure 6.5 (b) shows the loss function over time, that by selecting the value of 0.1 it looks more satisfactory for the selected dataset. Because of this reason the learning rate has been kept fixed at 0.1. It shows that the error is decreasing over time as per the requirement and then becoming constant.

Similarly, using above mentioned algorithms neural network was trained with 7 attributes shown in Table 6.16. A dataset with 13 attributes was trained using resilient backpropagation algorithm with 50 hidden units and 1 hidden layer it provides optimal accuracy of 67.9%. In a dataset with 7 attributes, the scaled conjugate gradient algorithm with 50 hidden units and 1 hidden layer provides the maximum percentage of correctly classified data to 67.2%.

By comparing the results between these datasets, the range of accuracy varies from 60% to 67.9% in the dataset with 13 attributes while dataset with significant predictors in Table 6.14, the accuracy of the model varies from 57.7 to 67.4% in Table 6.16. It appears that there is no much distinction in accuracy, thus dataset with significant predictors can be used for further analysis.

These are the results obtained by comparing various models of neural network classifier; however, it is essential to compare the results using a conventional classifier to assess the neural network classifier performance capability in handling these data. For comparison purpose discriminant functional analysis was implemented.

6.6 Discriminant Function Analysis using summarised patient data

DFA is performed on the patient data in order to compare the results with the neural network model output using the same class balanced patient data. DFA builds the predictive model of group membership. It is composed of discriminant functions depending on the linear combination of the variables to obtain the best discrimination between the groups. Its main purpose is to separate the groups at maximum level. It is used to obtain the relationship

between all the independent variables groups and categorical labels. With this relationship, it is possible to predict the classification depending on how well these independent variables separate the categories in the classification. DFA is implemented using SPSS software with all the seven independent variables and three categories.

6.6.1 Results from DFA analysis
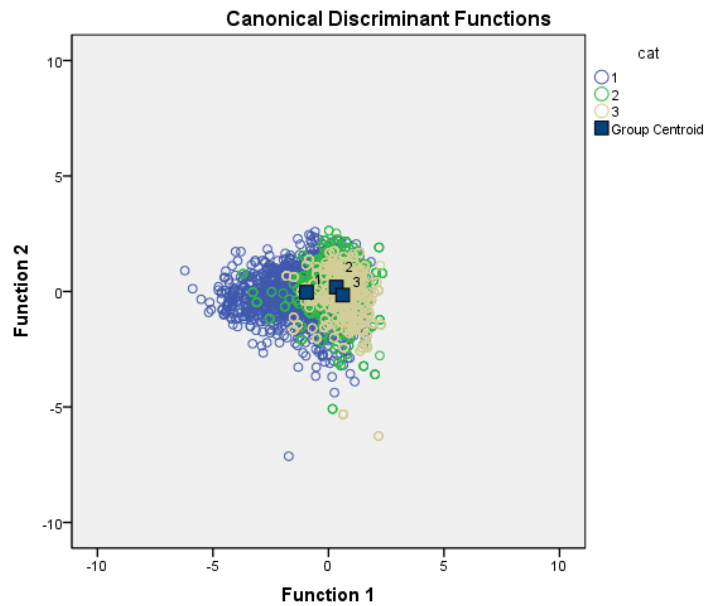
Figure 6.6 : Discriminant group of VPT categories (1-3) cat1 = Low, cat2 = medium and cat3 = high

The three group mean is fully explained in the two-dimensional space. The graphical representation of group's mean and the scatter of individual observations along with the centroid of each group in the discriminant coordinate system are shown in Figure 6.6. Function1 and Function 2 are calculated using standardized coefficients and the standardized variables as given below:

$Function1 = 0.17*zHbA_1c + 0.087*zACR + 0.966*zAge + 0.315*zWeight + 0.358*zHeight + 0.063*zCholesterol - 0.064*duration of diabetes$

$Function2 = 0.171*zHbA_1c - 0.417*zACR + 0.332*zAge - 0.748*zWeight - 0.009*zHeight + 0.429zCholesterol - 0.064*duration of diabetes$

Where $zHbA_1c$, zACR, zAge, zWieght, zHeight, zCholesterol and zduration of diabetes are the standardised variables multiplied by the magnitude of the coefficient. The magnitude of the coefficient can be used to indicate the impact on the discriminant score, so, for example, standardized coefficient of age in the first function is greater than the other coefficient which means age will have the greatest impact than other variables in the first discriminant score.

The separations between the groups are not clear. The closer the group centroids, it is likely to have more errors of classification. The samples available in each group are overlapping with each other in the discriminant space due to which it is difficult to achieve a good classification.

Table 6.18 : Confusion matrix of patient data

	Risk categories	Predicted Group Membership			Total
		Low	Medium	High	
Count	Low	1048	420	228	1696
	Medium	276	829	591	1696
	High	171	640	885	1696
%	Low	61.8	24.8	13.4	100.0
	Medium	16.3	48.9	34.8	100.0
	High	10.1	37.7	52.2	100.0

The error count can be calculated (or misclassified) for each observation as 38.2% (i.e. 24.8% + 13.4%) for low risk, similarly 51.1% for medium risk and 47.8% for high-risk categories as per Table 6.18. The overall correctly classified cases are calculated as **54.3%.** The classification of individuals into their original population varied from 48.9% to 61.8%. Among the three categories, the portion of correctly classified low-risk samples into their original population was the highest as 61.8% while a portion of correctly classified medium risk samples into their original population was the lowest as 48.9%.

Comparison between neural network classifier and conventional classifier has been performed to analyse the results. The percentage of correctly classified classes obtained using conventional classifier i.e. DFA is 54.3% while 67.4% accuracy was achieved using neural network classifier given in Table 6.16. This shows that neural network classifier is performing better than the conventional classifier.

By using DFA, we get an idea about the data distribution of each class in the discriminant space which were highly overlapped. In order to obtain higher accuracy, either data need to be collected precisely or need to process the data in a way to reduce the noise. Instead of choosing the prolonged process of collecting patient data again, the second option of increasing the predictor precision was taken into consideration by generating a simulated patient data.

6.7 Method of generating simulated patient data

For generating simulated patient data with similar property, real patient data's mean and covariance of each predictor were used with reduced standard error to increase the precision of data. The summarised real patient data (summarised patient data as discussed in section 6.3 is addressed as real patient data) consist of a number of observations, mean and standard error of all the seven significant predictors which were calculated as shown in Table 6.19. This simulated data were generated with real patient's mean and covariance's but with the reduced standard error. By this method, larger dataset can be obtained for improving predictor's precision. The simulated data was generated using R software where genCor Code simstudy package was used (Goldfeld 2018). It requires the mean, standard error, correlation matrix or correlation coefficient of real patient data to use.

Table 6.19 : Mean and standard deviation of the real patient data

Variables	Observations	Mean	Std. dev.	Min	Max
VPT	5158	17.82	11.13	1.5	50
HbA1c	5143	8.73	1.29	4.77	14.4
Urine albumin to creatinine ratio (ACR)	3886	7.15	18.35	0	293.83
Age	5158	57.73	18.45	7	98
Weight	5156	83.42	19.67	32.77	192.2
Height	5111	168.67	10.06	81	207
Cholesterol	4852	4	1.19	1.43	18.7
Duration of diabetes	5158	10.63	6.75	1	28

Using this function, it will generate multivariate normal data. If data is generated by using the same standard error of the real patient data then the spread of the data may remain the same for each predictor, therefore standard error was reduced for independent variables. Two data sets were generated wherein the first dataset; 50% of standard error and named as simulated patient data 1. For comparison purpose, another dataset was generated by 40% of standard error and named simulated patient data 2. Around 1 million data was generated for each set by this method. The summary of the real patient simulated data were compared with the real patient's summary in terms of range of each predictor. It was found that the tails in some of the predictors were far too long which means the values of the variable are outside the required limit. For example, as the range of the VPT from 0 to 50 Volts and in the generated data if the value is more than 50 Volts then the relationship of those values are unknown with the rest of the predictors and needs to be ignored. Similarly, for all of those variables whose data were out of the real patient data range were deleted from the simulated file to generate a more realistic simulated patient data set. After truncating data rows from the file, 757323 and 830365 numbers of observations in each attribute were available in which 50% and 40% of standard error as shown in Table 6.20 and Table 6.21 respectively.

Table 6.20 : Summary of the simulated data 1

Variables	Observations	Mean	Std. error.	Min	Max
VPT	757323	18.13	5.51	1.01	44.2
HbA1c	757323	8.75	0.64	5.54	11.85
Urine albumin to creatinine ratio (ACR)	757323	10.62	6.90	0	52.74
Age	757323	58.06	9.23	19.16	97.86
Weight	757323	83.70	9.79	37.17	128.13
Height	757323	168.65	5.03	142.15	193.18
Cholesterol	757323	4.01	.71	1.43	7.23
Duration of diabetes	757323	10.66	3.37	1	22.12

Table 6.21 : Summary of the simulated patient data 2

Variables	Observations	Mean	Std. error.	Min	Max
VPT	830365	18	4.43	1.5	37.89
HbA1c	830365	8.74	0.52	6.34	11.22
Urine albumin to creatinine ratio (ACR)	830365	9.33	5.80	0	42.47
Age	830365	57.95	7.40	24.04	93.69
Weight	830365	83.58	7.84	48.36	118.67
Height	830365	168.66	4.02	149.10	188.29
Cholesterol	830365	4.01	0.57	1.45	6.88
Duration of diabetes	830365	10.63	2.72	1.00	23.70

The comparison was made between summarised real patient data and simulated patient datasets (Table 6.19, 6.20 and 6.21), it was found that they compare pretty close in mean and the range of each variable, in correlation and covariance, however, variance and standard error is reduced to 50% in (Table 6.20) and 40% in (Table 6.21) of the patient data as expected.

This dataset were used for neural network modelling to calculate the percentage correctly classified class or accuracy.

6.7.1 Experimental methodology

1. Divide the simulated data into three categories based on VPT thresholds. (Low risk- 0 to 20.99, medium risk - 21 to 30.99 and high risk - ≥ 31)

2. Pre-process the simulated data or use a random sampling technique to achieve class balance for both the dataset.

3. Divide both dataset into three sets as training (70%), testing 15% (unseen data) and validation sets (15%).

4. Set important hyperparameters such as hidden neurons ∈ (10, 15, 25, and 50), hidden layers ∈ (1), learning rate ∈ (0.1), iterations ∈ (1000) and measure the epochs.

5. Train the neural network using resilient backpropagation (Trainrp function) and scaled conjugate gradient (Trainscg function) algorithm.

6. Train the neural network using simulated patient data 1. Select the model that gives optimal result by changing the values of required hyperparameters.

7. Train the neural network using simulated patient data 2. Select the model that gives optimal result by changing the values of required hyperparameters.

8. Compute Confusion matrices to assess the neural network performance.

9. Based on the classification success of training, testing and validation set, calculate overall accuracy for each trial for comparison.

10. Compare the accuracy of both the dataset to select the best.

Pre-processing the simulated patient dataset:

The dataset was divided into three classes based on the VPT scores same as the real patient data. After dividing the data into three classes, the number of instances available in each class for both the datasets was calculated.

Table 6.22 : Instances per class of simulated patient data 1

Class labels	Number of instances – (Total number of instances - 757323)	Percentage distribution %
Low risk – class 1	529294	69.8
Medium risk – class 2	220531	29.1
High risk – class 3	7498	0.9

As per the calculations it was found that class 1 is inflated with lot instances covering around 69.8% of the total data while class 3 is having least number of instances around 0.95% of the total data as shown in Table 6.22. This shows that data is highly imbalanced to be trained for any classifier.

Table 6.23 : Instances per class simulated patient data 2

Class labels	Number of instances – (Total number of instances - 830365)	Percentage distribution %
Low risk – class 1	623137	75
Medium risk – class 2	205842	24.78
High risk – class 3	1386	0.16

Similarly, simulated patient data 2, 830365 data was generated in which the same issue of class imbalance was recognised as shown in Table 6.23. In order to use this dataset for any of the classifiers it is important to undergo a class balance technique as implemented for the real patient data.

The benefit of using the simulated data is that large number of data can be generated as per the requirement. There are two options to adjust the class distribution of a dataset, one is either oversampling of the minority class as performed on real patient data or undersampling

of the majority class (Hernandez et al. 2013). As per the data available in class 3, it is possible to perform undersampling of majority class on both the datasets of simulated patient data.

As per the instances available in class 3, class 1 and class 2 were undersampled with the number of instance 7498. Undersampling was successfully applied and the updated number of instances available in each class is displayed in Table 6.24:

Table 6.24 : Class balanced for simulated patient data with 50% of standard error

Class labels	Number of instances – (Total number of instances - 22494)	Percentage distribution %
Low risk – class 1	7498	33.3
Medium risk – class 2	7498	33.3
High risk – class 3	7498	33.3

Similarly undersampling of the majority classes was performed in simulated patient data 2 as well. Here 1386 instances were obtained by undersampling the majority classes by using MATLAB function as presented in Table 6.25.

Table 6.25 : Class balanced for simulated patient data with 40% of standard error

Class labels	Number of instances – (Total number of instances - 4158)	Percentage distribution %
Low risk – class 1	1386	33.3
Medium risk – class 2	1386	33.3
High risk – class 3	1386	33.3

In order to get all the attributes in the comparable range, all the data available in each attribute was normalised. After pre-processing the data, it can be trained by neural network classifier to get the classification success.

6.7.2 Results

As the data been generated from the real patient data all the hyperparameters and specific training algorithms were used again for training this dataset. Some of the hyperparameters were kept fixed for both the data sets as mentioned below:

1. Max_epoch = 1000
2. Time = infinite
3. Minimum gradient = 1
4. Maximum_validation_fail = 20
5. Performance goal = 0

Table 6.26 : Comparison between training functions on simulated patient data 1

	Training Algorithm	Hidden neurons	Hidden Layer	Epoch	Learning rate	Overall Classification success %
1	Trainscg	10	1	95	0.1	65.4
2	Trainscg	15	1	62	0.1	65.4
3	Trainscg	25	1	111	0.1	65.4
4	Trainscg	50	1	113	0.1	65.1
5	Trainrp	10	1	52	0.1	65.3
6	Trainrp	15	1	92	0.1	65.5
7	Trainrp	25	1	55	0.1	65.3
8	**Trainrp**	**50**	**1**	**37**	**0.1**	**65.8**

As per the results obtained, it shows that by using all these training functions the achieved range of the percentage of correctly classified classes is from 65.1% to 65.8% (this is the overall accuracy which includes trained, test and validation set confusion matrix). This means that by changing hidden neurons there is no further increase in accuracy. It will be interesting to know the results by using the simulated patient data 2 i.e. dataset with 40% of standard error.

The results obtained using this simulated patient dataset 2 is as shown in Table 6.27.

Table 6.27 : Comparison between training function on simulated patient data 2

	Training functions	Hidden neurons	Hidden layer	Epoch	Learning rate	Overall Classification success %
1	Trainscg	10	1	59	0.1	68.3
2	Trainscg	15	1	47	0.1	68
3	Trainscg	25	1	59	0.1	68.6
4	Trainscg	50	1	48	0.1	67.1
5	Trainrp	10	1	54	0.1	68.6
6	Trainrp	15	1	34	0.1	68.3
7	Trainrp	25	1	43	0.1	68.6
8	**Trainrp**	**50**	**1**	**75**	**0.1**	**70.1**

As per the results obtained using dataset with a reduced standard error the range of overall percentage of correctly classified classes range varied from 68% to 70.1%. The resilient backpropagation with 50 hidden neurons with 75 epochs has provided the best result.

Analysis of the results using simulated patient data

First of all, by generating the simulated patient data from the real patient data by using means, covariance's of each variable it was possible to reduce the skewness of the data and that of the real patient data. By comparing the accuracy obtained using both the dataset, it can be

concluded that by reducing the standard error of each predictor the accuracy is definitely increasing. Based on the obtained results it can be concluded that simulated patient data 2 i.e. 40% of standard error can be used for further studies. However, for comparison purpose, the classifier outcome can be compared with the discriminant function analysis results as well. One limitation of reducing the standard error is, it could start affecting the range of the VPT. If the range of VPT is reduced more than the very less data or instances will be available in class 3 which may lead to extreme imbalance of the class distribution.

6.8 Discriminant Function Analysis using simulated patient data

For comparison purpose the conventional classifier called discriminant functional analysis (DFA) was also implemented using simulated patient data 2 with 7 attributes.

6.8.1 Results from simulated patient data
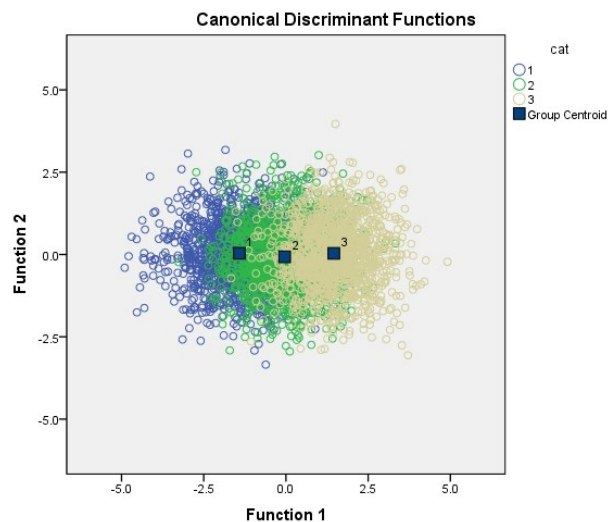
Figure 6.7 : Discriminant group of VPT categories (1-3) cat1 = Low, cat2 = medium and cat3 = high using simulated data

The three group mean are fully explained in the two dimensional space as shown in Figure 6.7. The function scores can be given as below:

$Function1$ = 0.041*zHbA$_1$c + 0.127*zACR + 0.965*zAge + 0.208*zWeight + 0.399*zHeight + 0.042*zCholesterol − 0.007*duration of diabetes

$Function2$ = 0.466*zHbA$_1$c - 0.503*zACR + 0.059*zAge + 0.057*zWeight - 0.535*zHeight + 0.298zCholesterol − 0.261*duration of diabetes

Where zHbA$_1$c, zACR, zAge, zWieght, zHeight, zCholesterol and zduration of diabetes are the standardised variables multiplied by the magnitude of the coefficient. The graphical representation of group's mean and the distribution of individual observations along with the

centroid of each group are shown in the discriminant coordinate system. The separations between the groups are much clearer than the real patient data. This clarity in the distribution shows that the simulated patient data is much more precise and accurate than the real patient data and definitely has the capability to gain more accuracy, since the portion of the data available in the classes are not much overlapped in the discriminant space when the dataset is divided into three categories.

Table 6.28 : Confusion matrix of simulated patient data 2

| | Cat | Predicted Group Membership | | | Total |
		Low risk	Medium risk	High risk	
Count	Low risk	1014	345	27	1386
	Medium risk	340	753	293	1386
	High risk	18	272	1096	1386
%	Low risk	73.2	24.9	1.9	100.0
	Medium risk	24.5	54.3	21.1	100.0
	High risk	1.3	19.6	79.1	100.0

The error count (or misclassification) for each observation was estimated as 26.8% for low risk, 45.6% for medium risk and 20.9% for high-risk categories. The overall correctly classified cases are calculated as **68.9%** [calculated as (73.2 + 54.3 + 79.1) / 3)]**.**

The classification of individuals into their original population varied from 54.3% to 79.1%. Among the three categories, the portion of correctly classified low-risk samples into their original population was the highest as 79.1% while a portion of correctly classified medium risk samples into their original population was the lowest as 54.3%.

Using neural network classifier accuracy of 70.1% was achieved. However, using DFA classifier gains accuracy of 68.7%. This shows that neural network classifier is more capable of handling the data than the conventional classifier (DFA). At this stage, it can be assumed that the neural network trained on the simulated data with 40% of standard error is performing at the best level and can be used for further analysis.

Limitations of using neural network classifier and DFA

The best-trained model is saved in the workspace of MATLAB and results were analysed. When new inputs are provided results were obtained in terms of three probabilities of risk levels. So in order to test the neural network model as trained using all the seven best predictors, the input should be provided as the vector of 7 inputs in the same sequence i.e. HbA_1c, acr, Age, Weight, Height, Cholesterol and duration of diabetes as followed during training procedure to get the expected output as shown in Examples 1 below:

Example 1:

Input variable	Output probabilities
HbA$_1$c - 8.9	Low risk - 96%
Acr - 13	
Age - 41	Medium risk - 4%
Weight – 82	
Height – 174	
Cholesterol – 3.6	High risk - 0%
Duration of diabetes -13	

Here the inputs were provided with all the best predictors as shown in the Example 1. The value of most significant predictor i.e. age is given as 41 years along with rest of the predictors and model predicted the outcome in terms of probability. The prediction shows that subject at **low risk** of developing diabetic neuropathy.

Example 2:

Input variable	Output probabilities
HbA$_1$c - 8.9	Low risk - 13%
Acr - 13	
Age - 65	Medium risk - 54%
Weight – 82	
Height – 174	
Cholesterol – 3.6	High risk - 32.2%
Duration of diabetes -13	

Looking at Example 2, here keeping all the other predictors as constant, age was increase to 65 and as seen the predicted probabilities changed as Low risk - '13%', medium risk - '54%' and high risk – '32.2%' which means subject is at medium risk of developing diabetic neuropathy. This reflects that based on the trained pattern, neural network is updating all the probabilities.

Example 3:

Input variable	Output probabilities
HbA1c - 9	Low risk - 30%
Acr - 13	
Age - 65	Medium risk - 26%
Weight – 88	
Height – 171	
Cholesterol – 5	High risk - 44%
Duration of diabetes -9	

Example 3 shows that based on the above mentioned inputs or predictors, the output probabilities were predicted by the model. This example shows that low risk is greater than medium risk and medium risk is less than high risk. In the practical scenario, we do not want to

get such kind of predictions where order is not maintained. This unordered prediction is due to the limitation of the data and also the type of typical softmax based neural network model which was used but does not explicitly maintaning the order.

This problem also persists while using discriminant function analysis, because DFA is normally applied when dependent variables are divided into two or more categories and these categories need to be mutually exclusive. So when DFA was applied using real patient data and simulated patient data, a test was performed to identify this type of unordered misclassification. It was found that using real patient data, the number of times class 1 predicted class 3 was 53 times and a number of times class 3 predicted class 1 was 8 times and using simulated data set no such cases were found. In the present dataset we have only 3 class labels; however, if there are more than 3 classes then this type of error may increase a lot and may create confusion. The problem was seen more in real patient data may be because a portion of data in each class highly overlaps with each other and also not having large dataset, while in the simulated dataset it is much less due to less class overlaps as shown in the discriminant graph (Figure 6.6 and 6.7).

Similarly, when neural network classifier was trained on real patient data, there was around 15 to 20% of misclassification. And when NN was trained on simulated data only 1 or 2 cases were found.

In fact, it shows that unordered misclassification is higher using real patient data than using simulated patient data. Perhaps the problem of misclassification may not occur once we have large enough dataset, however, in current scenario it is not possible to get more data, and therefore simulated patient data can be used for further analysis. Hence, ordinal logistic regression was implemented on simulated patient data 2 which will explicitly maintain the order of classification as shown in the next section.

6.9 Ordinal logistic regression using simulated patient data

Ordinal logistic regression is applied on simulated dataset to obtain the information about the significant predictors along with classification success using simulated dataset as given in Table 6.29.

Table 6.29 : Case summary

Categories of the dependent variables	Range of VPT score in Volts (V)	No. of instances (4158)
Low risk	0 to 20.99	1386
Medium risk	21 to 30.99	1386
High risk	31 onwards	1386

In the model fitting information as shown in Table 6.30, as per the degree of freedom seven independent variables were used in the data set for performing the analysis. The last row (Sig.) of the table presents the information that either all or some of the variables are statistically significant and the mean variables are statistically significantly improving the model compered to intercept only model (no added variables). As p < 0.001 means model predicts the dependent variable better than the intercept only model.

Table 6.30 : Model Fitting Information

Model	-2 Log Likelihood	Chi-Square	Df	Sig.
Intercept Only	9136.060			
Final	5602.161	3533.899	7	.000

In the goodness of fit table, large chi-square values indicate poor fit of the model. A statistically significant value (p < 0.5) indicates that model does not fit well. The first row that is Pearson means, Pearson chi-square statistic as well as Deviance chi- square have p > 0.05 (from the **Sig.** column) i.e. not statistically significant indicates that model fits well with the data. Pseudo R- squared presented in Table 6.32. The indicated pseudo R squared is higher than the Pseudo R squared of the real patient data seems that the model better predicts the outcome in this case.

Table 6.31 : Goodness-of-Fit

	Chi-Square	df	Sig.
Pearson	7015.429	8303	1.000
Deviance	5602.161	8303	1.000

Table 6.32 : Pseudo R-square

Pseudo R-Square	
Cox and Snell	.573
Nagelkerke	.644
McFadden	.387

There are coefficient, their standard errors, the Wad test and associated p- values (Sig.) and 95% confidence interval of the coefficient as available in parameter estimated in Table 6.33. The dataset has three level of variable called <cat> (coded 1, 2, and 3) which will be used as an outcome variable. It can be used to determine number of statistical significant independent variables on the dependent variable (VPT). Out of all the seven predictors / attributes HbA1c, ACR, age, weight, height are significant predictors while Cholesterol and duration of diabetes are not significant. So for HbA_1c variable, one unit increase in age (from 0 to 1), there can be 0.140 increase in the logarithmic odds of being higher level of cat, with all the other variables in the model are constant. For ACR variable, one unit increase in age (from 0 to 1), there can be 0.37 increase in the logarithmic odds of being higher level of cat, with all the other variables in the model are constant. For age variable, one unit increase in age (from 0 to 1), there can be

0.25 increase in the logarithmic odds of being higher level of cat, with all the other variables in the model are constant. Similarly for rest of the variables can be interpreted from the table.

Table 6.33 : Parameter Estimates

		Estimate	Std. Error	Wald	df	Sig.	95% Confidence Interval	
							Lower Bound	Upper Bound
Threshold	[cat = 1.00]	50.221	1.976	646.017	1	< 0.001	46.348	54.094
	[cat = 2.00]	53.066	2.002	702.941	1	< 0.001	49.143	56.989
Location	HbA$_1$c	.140	.070	4.058	1	.044	.004	.277
	ACR	.037	.006	37.443	1	< 0.001	.025	.048
	Age	.250	.006	1616.672	1	< 0.001	.238	.262
	Weight	.047	.005	80.779	1	< 0.001	.037	.057
	Height	.174	.010	287.566	1	< 0.001	.154	.195
	Cholesterol	.109	.066	2.772	1	.096	-.019	.238
	Duration of diabetes	-.001	.013	.008	1	.928	-.027	.024

By comparing all the values of the responsive variable with the values of the predicted outcome, it is possible to calculate the classification success for each class. Table 6.34 shows the cross tabulation (confusion matrix) of the model where data is presented for each of the classes in terms of true positive, true negative, false positive and false negative. It measures the percentage overall classification success estimated as 68.4%, where low risk category achieves classification success of 72%, medium risk category as 56.3% and high risk category as 77.1% .

Table 6.34 : cat * Predicted Response Category Cross tabulation

			Predicted Response Category			Total
			Low risk	Medium risk	High risk	
C A T A G O R I E S	Low risk	Count	998	367	21	1386
		% within cat	72.0%	26.5%	1.5%	100.0%
		% within Predicted Response Category	74.3%	25.3%	1.5%	33.3%
	Medium risk	Count	330	781	275	1386
		% within cat	23.8%	56.3%	19.8%	100.0%
		% within Predicted Response Category	24.6%	53.8%	20.2%	33.3%
	High risk	Count	15	303	1068	1386
		% within cat	1.1%	21.9%	77.1%	100.0%
		% within Predicted Response Category	1.1%	20.9%	78.3%	33.3%
Total		Count	1343	1451	1364	4158
		% within cat	32.3%	34.9%	32.8%	100.0%
		% within Predicted Response Category	100.0%	100.0%	100.0%	100.0%

By using ordinal logistic regression it is possible to obtain the overall classification success of 68.4% with five significant predictors out of seven independent variables. Using this analysis a hint regarding significant predictors, and on the other hand it treat the data into the set of ordered category i.e. (Low risk < medium risk < high risk) (Chu and Ghahramani 2005) . So the issue of considering these classes as nominal did not arise in the above used classifier. This means that ordinal regression analysis applied on the data set is better to use, however if he data is trained using neural network then it might work better than the conventional method. So if it is possible to use a neural network based model which can take care of ordinal categories and predict the outcome in terms of probability then it can be used for developing a risk assessment tool. The advantages of using artificial neural network based model are learning in both real time and in batch mode, training on very large data and providing good performance, better in handling non- linear data, rapid prediction and model can be optimised using trained and tested data (unseen data set) with various hyper parameters like hidden neurons, hidden layers, no. of iterations to obtain better results (Cheng et al. 2008). In order to use such a model for taking advantages of neural network, neural network based proportional odds model was implemented.

6.10 Neural Network based Proportional Odds Model

There are many classifiers available to classify or predict the numerical values from the labelled patterns while less consideration was paid on ordinal classification problems in which labels of the dependent variable or targets have a natural ordering. In the current scenario, as stated before, labels are ordered as (Low risk, medium risk and high risk). While working with the problems misclassification which has more error if the patient of low risk was classified as high risk than misclassified as medium risk. This encouraged us to use an ordinal classification model to carefully handle an ordinal labels. Ordinal regression models are commonly used in many research areas such as medical research (Jang et al. 2011), brain computer interface, age estimation and more (Gutierrez et al. 2016). To adopt a probabilistic framework, Neural Network based Proportional Odds Model (NNPOM) is considered which is proposed by Mathieson (Mathieson 1996; Gutiérrez et al. 2014). The model approaches ordinal classification by estimating the latent variable belonging to ordinal categories and the model will learn based on the set of thresholds discretising variable. NNPOM is also called as threshold model that has been seen to perform well when classes are defined from a discretised variable (Gutierrez et al. 2016).
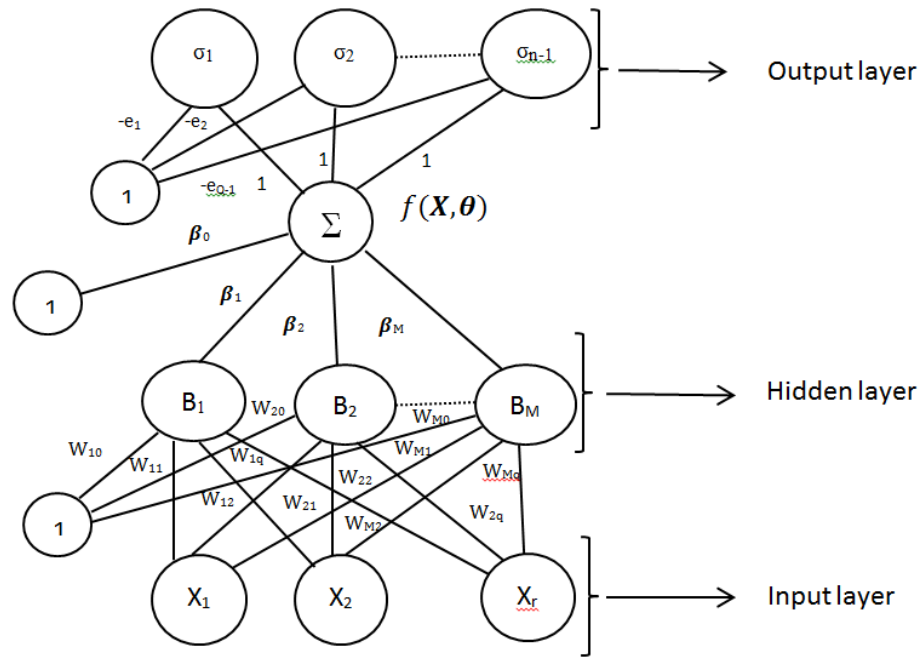
Figure 6.8 : Structure of the probabilistic neural network model (NNPOM)

The structure of the NNPOM model is shown in Figure 6.8. It consists of input layer; hidden layer and output layer same as the previously used neural network classifier. It has one input layer with 7 input nodes i.e. 7 best predictors given by variable **X** (X_1 to X_7). The input signal propagates through input layer by multiplying with weights **W**. It has one hidden layer where number of hidden neurons M can be arbitrarily defined and can be given as **B** (B_1 to B_M**).** The input of the hidden layer propagates by multiplying with weights $\boldsymbol{\beta} = (\boldsymbol{\beta}_1 \dots \boldsymbol{\beta}_M)$ and transmit to the output layer**.** It has one output layer consisting of one neuron with as many thresholds as the number of classes minus one. The thresholds of each class C_q are denoted by e_q where q is the number of thresholds. The main difference in the structure of NNPOM is standard softmax activation function in the output nodes used in traditional neural network classifier is replaced with a sigmoidal function as it will consider ordered partitions encoding instead of traditional encoding. Sigmoidal unit is define as $B_j(x_t, w_j) = \sigma\left(W_j^T \cdot (1, x_t)\right)$, $w_j = \{w_{j0}, w_{j1}, \dots, w_{jr}\}$, w_0 is the bias and r is the number of inputs. The whole parameter vector of NNPOM can be given as $K = \{\beta, \mathbf{W}, \boldsymbol{a_1}, \boldsymbol{a_2}, \dots, \boldsymbol{a_{Q-1}}\}$. The cross entropy loss function is optimised by iRprop[+] algorithm (improved resilient back propagation algorithm) to estimate the parameters of the model (Igel and Hüsken 2003). This model is adjusted and updates the weights by minimising cross entropy loss in every iteration *iter*. NNPOM is a linear combination of nonlinear basis functions i.e. hidden neurons (Pérez-Ortiz et al. 2018) given as:

$$f(X_t, \theta) = \sum_{j=1}^{M} \beta_j \, B_j \, (X_t, w_j) \tag{18}$$

Where θ is the weight given as $\theta = (\boldsymbol{\beta}, \mathbf{W})$ and $f(X_t, \theta)$ is the projection of the model for pattern X_t.

In NNPOM, probabilities can be estimated in the following equations (Pérez-Ortiz et al. 2018):

$$P(y_{t+s} = C_1 | X_t) = \sigma(f(X_t, \theta) - e_1,$$

$$P(y_{t+s} = C_q | X_t) = \sigma(f(X_t, \theta) - e_q) - \sigma(f(X_t, \theta) - e_{q-1}), \tag{19}$$

$$q \in (2, \ldots N - 1),$$

$$P(y_{t+s} = C_N | X_t) = 1 - \sigma(f(X_t, \theta) - e_{N-1}).$$

Where s is the input nodes, e_q is the threshold of class C_q and e_q can be defined as follow:

$$e_q = e_1 + \sum_{j=2}^{q} a_j^2 \tag{20}$$

a_j is the padding variable and is kept square to make the threshold positive.

NNPOM model can be adjusted by three hyper parameters as hidden neurons M, number of Iterations *iter* and value of lambda λ, where λ is the regularisation parameter that is used in the error function to avoid over fitting.

6.10.1 Experiment methodology

1. Use the categorical simulated dataset 2 with 7 best predictors (attributes).
2. Divide the data into two sets i.e. training set (75%) and testing set (25%) save as text files.
3. The format of the file should be (attribute1 attribute2 ....attribute7 label) where labels should be coded as [1, 2, 3].
4. Set the hyper parameter of such as hidden neurons M, number of iteration iter and regularisation parameter λ until the model achieve the optimal results.
5. Compute confusion matrices of both training and testing sets to get the overall classification success.
6. Compare the results with classical ordinal regression.
7. Save the best trained model to build the risk assessment tool of VibraScan.

6.10.2 Results

The training of neural network based proportion odds model was performed on MATLAB framework. The performance of the model may vary depending on number of attributes; the percentage partition of training and testing sets and number of instances in the data file. The summary of the dataset is shown in Table 6.35 as below:

Table 6.35 : Summary of the dataset

Categories of the dependent variables	Range of VPT score in Volts (V)	No. of instances (4158)	
		Training	Testing
Low risk	0 to 20.99	3188	970
Medium risk	21 to 30.99	3188	970
High risk	31 onwards	3188	970

The data files were loaded in to the MATLAB workspace and NNPOM model was trained with prior setting of all the hyper parameters. The range was explored using different number of hidden neurons $M \in \{10, 40, 60, 80, 85, 120, 130\}$, $iter \in \{1000, 1500\}$ and $\lambda \in \{0.01, 0.001\}$. The results obtained by using these range is given in Table 6.36. Accuracy of the model is calculated based on the percentage correctly classified class. The sum of training accuracy and test accuracy gives the total percentage of correctly classified class.

Table 6.36 : Performance evaluation

Number of hidden neurons M	Number of Iteration	Value of λ	Training accuracy %	Test accuracy %	Overall accuracy %
10	1000	0.01	68	68.7	68.25
40	1000	0.01	68.6	69.5	68.8
60	1000	0.01	69.1	69.1	69.14
60	1000	0.001	68.5	69.5	68.75
80	1000	0.01	68.9	68.9	68.9
60	1500	0.01	68.9	69.1	68.9
60	1500	0.001	63.6	63.7	63.6
85	1500	0.001	69.3	69.6	69.4
120	**1500**	**0.01**	**70.02**	**69.79**	**70.1**
130	1500	0.01	69.3	69.7	69.7

As per the results obtained in Table 6.36, various ranges of hidden neurons, iteration and value of lambda were used to select the optimal results. By increasing the number of hidden neurons the accuracy was increasing with lambda value equal to 0.01 and when lambda value was changed to 0.001 the accuracy was decreasing. By increasing the hidden units, training time increases. By changing these hyper parameters, results changes from 68.25% to 70.1%. By selecting $M = 120$, $iter = 1500$ and lambda value = 0.01 the highest percentage correctly

classified class was obtained as 70.1%. The overall confusion matrix (training and testing) of the whole data is displayed in Table 6.37 where the diagonal of the matrix is the truly predicted class used to calculate the accuracy (LR: Low risk, MR: Medium risk and HR: High risk).

Table 6.37 : Confusion matrix (M = 120, iter = 1500 and λ = 0.01)

	LR	MR	HR	Classification overall
Low risk(LR)	**1017**	344	25	1386
Medium risk(MR)	234	**831**	262	1386
High risk (HR)	16	303	**1067**	1386
Truth overall	**1267**	**1478**	**1354**	**4158**

This version of trained model with highest accuracy was selected to develop risk assessment tool for diabetic neuropathy.

6.10.3 Development of risk assessment tool of VibraScan

To make it user friendly and easy to use, an application was developed on MATLAB framework using the trained neural network model as shown in Figure 6.9.
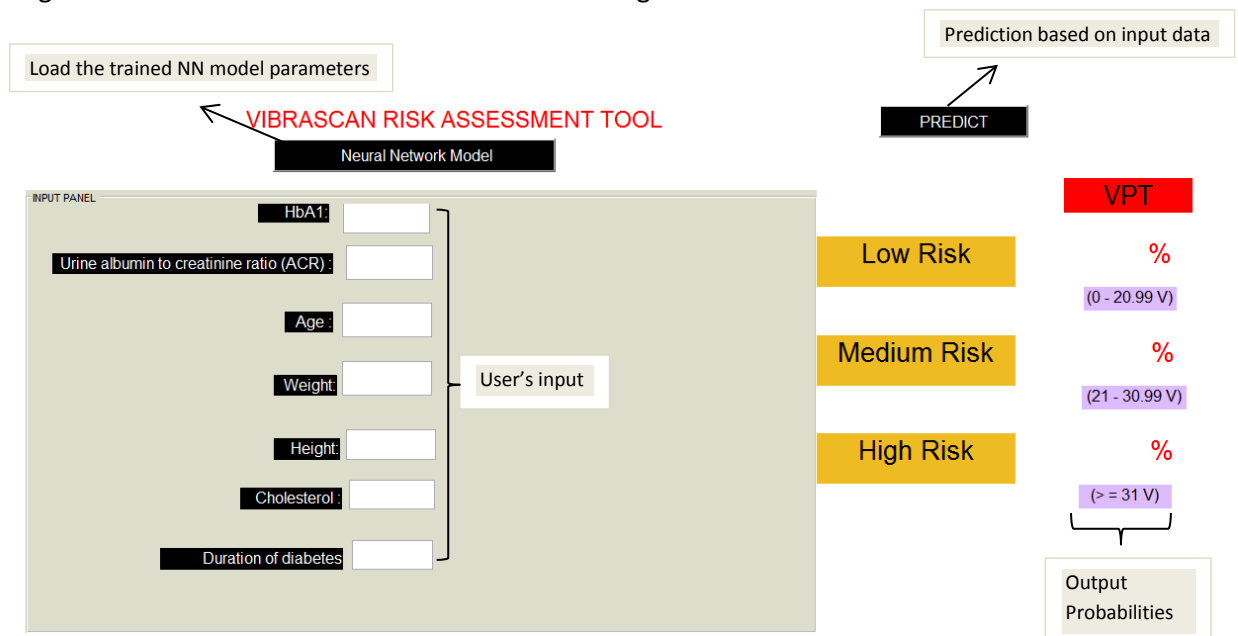
Figure 6.9 : Graphic user interface (GUI) of VibraScan risk assessment tool

There are several user friendly steps to follow for operating this application:

1. Open the Graphic User Interface on MATLAB platform.

2. The application will be displayed as shown in the Figure 6.9.

3. There is a button called <Neural network model> needs to be used to load all the necessary parameters like weights, output labels of the trained model as discussed before to predict the new outputs.

4. In the input panel, there are seven inputs needs to be provided by the subject as per the clinical results.

5. Use the button called <Predict> to obtain all the three predicted VPT level probabilities for low risk (0 - 20.99 V), medium risk (21 - 30.99 V) and high risk (≥ 31 V).

6. Out of the three probabilities, highest probability can be used to measure the risk level of the subject.

The following examples shown below were used to show case the usability of the tool and its advantages.

1. Subject has provided following inputs in the input panel as displayed in the Figure 6.10.

Figure 6.10 : VibraScan risk assessment tool prediction based on input variable (Example 1)

Based on the input values provided to the tool, VPT probabilities were predicted from the learnt model with 2% chance of low risk, 23% chance if medium risk and 75% chance of high risk. The result shows that the person is likely to have high risk of diabetic neuropathy according to their clinical characteristic.

Second example was test by keeping all the parameter as constant and just decreasing age by 10 years to determine the categories and observe the change in the risk level.

Figure 6.11 : VibraScan risk assessment tool prediction based on input variable (Example 2)

By keeping all the other inputs as constant other than age, it shows that when age is decreasing the risk level of diabetic neuropathy is reduces from high to medium risk showing approximate VPT level between 21 to 30.99 Volts. Thus, based on the combination and relationship between clinical inputs of the subject, tool can predict the VPT level to determine the risk level of diabetic neuropathy.

Discussion:

The risk assessment tool based on vibration perception thresholds is developed for the first time for easy and early diagnosis of diabetic neuropathy. The advantage of using this tool is to get the results in terms of probability and can be used as an alarm for progressiveness of this devastating disease. The study was started with the longitudinal data with the continuous measurement of VPT for which Box Cox transformation on all the independent variables with natural logarithmic transformation of dependent variable (VPT) was implemented to improve the skewness of the data. Then, ordinary least square method was used on this transformed variable to determine the significant predictors. Out of 13 variables, 7 variables were identified as the significant predictors. For easy interpretation of the risk level of DN, VPT was divided into three categories based on the VPT thresholds. For determining the significant predictors on this categorical VPT based dataset, Ordinal logistic regression (OLR) was implemented. OLR has achieved the accuracy of 71.5%. However, this high accuracy could be because category 1 was inflated with large number of data. Results of OLR have shown that age, weight and height as the significant predictors providing scope for further analysis. The determination of significant predictors using OLR is based on linear association; however, advanced model such as artificial neural network (ANN) can also learn non-linear association along with linear association from the

data. Due to this ability of ANN, we have considered all 13 variables for the training. At first multiclass neural network was implemented on the 2450 instance of summarised patient data. Due to data division, it has been identified that there is a class imbalance, for which oversampling of minority class was performed. The ANN was trained on 13 attributes and accuracy of 67.9% was achieved. The ANN trained on 7 best predictors an accuracy of 67.4% was achieved. This comparison is giving an indication of using only significant predictors rather than all the attributes. Another classifier called discriminant functional analysis was used and achieved an accuracy of 54.3%. It has shown the distribution of summarised patient data on discriminant space where data in each class were highly overlapped.

In order to improve the precision of summarised patient data, data with similar property was simulated using summarised patient's covariance and mean value but with reduces standard error. Simulated data with 50% of standard error (simulated patient data 1) and 40% of standard error (simulated patient data 2) was generated out of which simulated patient data 2 was considered for further analysis because of its higher precision. Due to class imbalance in the dataset, under sampling of majority classes was implemented. Neural network was trained on simulated data 2 and achieved accuracy of 70.1% and DFA classifier has achieved an accuracy of 68.7%. From this new dataset, DFA has shown the distribution of the simulated data in the discriminant space where data in each class were less overlapped showing more precise dataset. This improvement in accuracy is due to less class overlap, however some class overlaps still exist and size of data may not be sufficient to train the models. Therefore, neural network and DFA analysis have shown to struggle for maintaining the order during classification in few cases.

As ordinal logistic regression is capable of handling this order, so OLR was implemented again using simulated dataset 2 where accuracy of 68.4% was achieved and has identified five significant predictors. However, as we have stated earlier this cannot deal with nonlinearity of the data, so the efforts were made to implement model using neural network which can maintain the orders explicitly. This order based neural network is called Proportional odds model. Finally, NNPOM is trained on simulated dataset 2 where accuracy of 70.1% was achieved with seven predictors. This method is working as per the requirements and risk assessment tool of VibraScan has been developed.

Thus, the overall analysis of the data allowed us in getting the insight for selecting the right model as well as the importance of quality of the data. This limitation of quality of data is

handled by using simulated patient data the quality of data was increased by improving the precision of the variables. Hence, the achieved accuracy can be improved by collecting more patient data from the clinics specifically for the analysis purpose and can be trained using a suitable neural network model for early diagnosis of the disease. A futuristic framework of risk assessment tool is proposed in the concluding chapter using the VibraScan risk assessment tool with the advantage of collecting precise patient data and at the same time updating and improving the prediction over time.

Chapter 7 Conclusions

This chapter provides the conclusions derived from the designing and experimental analysis conducted in developing the risk assessment tool for diabetic neuropathy. These conclusions are discussed based on fulfilling the set objectives of this thesis. It also discusses the limitations and future scope of the risk assessment tool where VibraScan and artificial neural network based application can be used together to enhance the capability of diagnosing diabetic neuropathy.

7.1 Achieving the set objectives of the thesis

- **In order to detect diabetic neuropathy develop a smart, operator independent and user-friendly device, which is capable of generating a vibration stimulus with a required frequency and varying amplitude.**

  These conclusions are based on the literature survey conducted in Chapter 1, 2 and the developmental phase of device discussed in Chapter 3. In the literature survey, study related to types of diabetes (type 1 and type 2) and its related complications were discussed. Diabetic neuropathy is one of the serious complications of diabetes. It has been found that the rate of neuropathy in type 1 diabetes is higher than type 2 diabetes. Various types of diabetic neuropathy, its prevalence and importance of early detection of DN were studied. The detailed discussion of the currently available methods and devices for diagnosing diabetic neuropathy are conducted in Chapter 2. Devices based on vibration perception were generally considered as the gold standard for diabetic neuropathy, a 128-hertz tuning fork was the first tool used to assess the neuropathy based on vibration perception. Later more advanced device Biothesiometer was developed which was then replaced by Neurothesiometer. This works in the same way but with a self-contained power source. The method of conducting the test, generating vibration, vibration property such as a range of vibration amplitude and frequency of Neurothesiometer were carefully studied. By looking at the limitations, such as operator dependency, range of the vibration amplitude causing the ceiling effect, time is taken to conduct the test and manual interpretation of results in Neurothesiometer led to the idea of developing a smart device. Typically a Biothesiometer or Neurothesiometer vibrates at a fixed frequency and varying the vibration amplitude which is operator dependent was a major limitation. VibarScan can be used to measure VPT independently. It is developed as a platform based device where subject has to lay their feet on the device and provided a manual switch to capture VPT level. The device will automatically calculate the VPT level and display the results in the

form of severity of DN. The vibration actuator C2- HDLF tactor was used in VibraScan which is capable of generating the vibration with the required range of frequency and amplitude. Pulse width modulation technique was used for generating vibration of required fixed frequency and varying voltage, discussed in Chapter 3. The vibration applied using the vibration actuator is digitally controlled and is fully programmable. Thus, the objective of generating fixed frequency with varying voltage in VibraScan device is successfully achieved where neuropathy assessment is possible without the need of an operator.

- **To be able to robustly detect diabetic neuropathy, develop a vibration generating device which can effectively increase the vibration intensity, in order to detect the vibration perception threshold of the subject.**

 These conclusions are based on the modelling and simulation conducted in Chapter 4 and 5. The feeling of sensing the vibration is also based on the type of vibration motor and design of the test rig (discussed in Chapter 3). Using the Plate-form based device, the subject can comfortably place from their feet on the plate. Various vibration characteristics such as the nature of vibration, vibration site and safety measures during the test were analysed for developing the device. By selecting the platform based device it was necessary that vibration should be applied perpendicularly to the skin. Various vibration motors such as Eccentric Rotating Mass Vibration Motors (ERM), linear actuators and C2 - high displacement and low frequency (C2- HDLF) tactor were analysed to make selection criterion, C2- HDLF was selected as it was capable of generating the required nature of vibration. Using PWM signals, this vibration motor can be controlled easily for increasing the vibration amplitude covering the same range of Neurothesiometer vibration amplitude. Initially, a device was made for testing purpose for one foot where platform inclination is allowed to change from 44 to 26 degree. By successfully testing the first version of the device, it was redesigned for both feet with all necessary advancement. In the latest version of the device, based on the flexibility of the user, the inclination was kept fixed at approximately 36 degrees. The software was also upgraded to measure the VPT from both feet and results are automatically interpreted in terms of severity level of neuropathy. In the latest version, vibration isolation technique using spring was implemented to avoid the background vibration. To obtain the comparative range of the vibration amplitude with that of the Neurothesiometer, an experimental study was performed to measure the displacement of the vibration amplitude for each device. Curve fitting technique was used to develop the equation for finding the relationship between VibraScan and

Neurothesiometer. The comparative study discussed in Chapter 5, was conducted between VibraScan and Neurothesiometer using twenty healthy subjects after getting approval from the ethical committee of Bournemouth University. The VPT was alternately measured for each foot using both devices. To get the linear interdependency of both the measurements, correlation coefficient was calculated as r = 0.816, p < 0.001 for left foot and r = 0.893, p < 0.001 for right foot. Although there is a strong correlation between both techniques it is possible to say that both the techniques are agreeing with each other. To support this Bland and Altman analysis was used which showed that there is a close agreement between both the measurement techniques. Hence, the vibration stimulation applied to the subject/patient using VibraScan is made effective by careful designing of the device, by selecting the appropriate vibration motor (which is capable of generating higher vibration amplitude than Neurothesiometer vibration probe i.e. greater than 250 micrometer) and depending on the experimental results using human subject, VibraScan can be used an smart screening tool for diabetic neuropathy.

- **To develop a more reliable device by maintaining a constant pressure while applying vibration stimuli to the patient.**

These conclusions are based on the evaluation of the pressure measurement carried out in Chapter 3. By studying all the devices available for measurement of vibration perception threshold, it was found that none of these devices like Biothesiometer / Neurothesiometer are considering pressure measurement during the test. In these devices, vibration stimulus are applied to the subject by holding the vibration probe. So while conducting the test there could be a possibility of applying vibration with higher pressure which can result in activating the human skin receptors abnormally. To overcome this limitation, with the special design of VibraScan, it is possible to conduct the test at constant pressure by simply placing the foot on the device. However, there could still be a chance of pressure change if it is not monitored during the test. Therefore force sensitive resistors (FSRs) were used to capture any change of pressure during the test. Based on the experimental analysis, the placement of FSRs was decided i.e. on the top of the C2 - HDLF tactor where the great toe of the subject is placed. These FSRs were used to monitor the pressure and also verify the correct placement of the foot. A user-friendly graphic user interface (GUI) was developed on the Matlab framework to wirelessly control the device which captures and show the real-time pressure change during the test. The real-time pressure graph is useful for subjects for maintaining constant pressure during their assessment.

- **To develop the risk assessment tool that is capable of utilising the clinical characteristics of a patient to predict the risk level of Diabetic neuropathy.**

  These conclusions are based on the analysis conducted in Chapter 6. By developing VibraScan, diabetic neuropathy can be assessed by measuring vibration perception threshold; however, there is no consideration for clinical risk assessment of diabetic neuropathy. To help with the idea of assessing the disease through risk factors, summarised patient data were used. The data were analysed by classical statistical method using Box-Cox transform to get information related to significant predictors from the summarised patient data. Ordinal logistic regression was applied using Box-Cox transforms variable with output variable as logarithmic VPT to identify the significant predictors such as age, height, weight, urine albumin to creatinine ratio (ACR), HbA1c, cholesterol, and duration of diabetes. The analysis results from the classical statistics have given the direction of predicting VPT using these significant predictors. Predicting VPT in terms of the continuous variable was considered less helpful. As a result, VPT is divided into low risk (0 to 20.99 V), medium risk (21 to 30.99 V) and high risk (≥ 31 V). To increase the precision of the summarised patient data, simulated patient data was generated with the similar property of summarised patient data but with reduced standard error. Ordinal logistic regression was applied to get the best predictor set based on this categorical outcome. The information obtained from this analysis has helped in creating the baseline for this classification problem and focus was set to find the best classifier. Finally, a neural network based proportional odds model (NNPOM) was implemented using simulated patient data that could obtain the highest accuracy of 70.1%, slightly higher than the classical classifiers. A version of this model is used to develop the risk assessment tool of VibraScan.

Thus, VibraScan device diagnosis based on vibration perception and risk assessment tool of VibraScan using risk factors of the disease helps in providing a comprehensive assessment tool for diabetic neuropathy.

7.2 Limitations and Future scope

The VibraScan has been developed and was tested on healthy subjects. Although comparative study between Neurothesiometer and VibraScan has shown a strong agreement, but, the challenge was to access real patients for measuring VPT using VibraScan.

For the risk assessment of the VibraScan, the challenge was to deal with the summarised patient data in which VPT was measured continuously and was divided into categorised VPT. Due to this division, data sample available in each class was not equal; this was handled by sampling technique to obtain the class balance. Due to noise in the summarised data, the simulated patient data were used for developing the risk assessment tool to show the potential of the tool when clean patient dataset will be used in the future. The challenge was to get the large patient data which can be used to train the neural network for better prediction of VPT.

The futuristic Model

As VibraScan device is developed to measure the VPT of the subject and risk assessment tool is used to predict the VPT. Taking an opportunity of using both these features of the device, a futuristic framework has been proposed as shown in Figure 7.1.
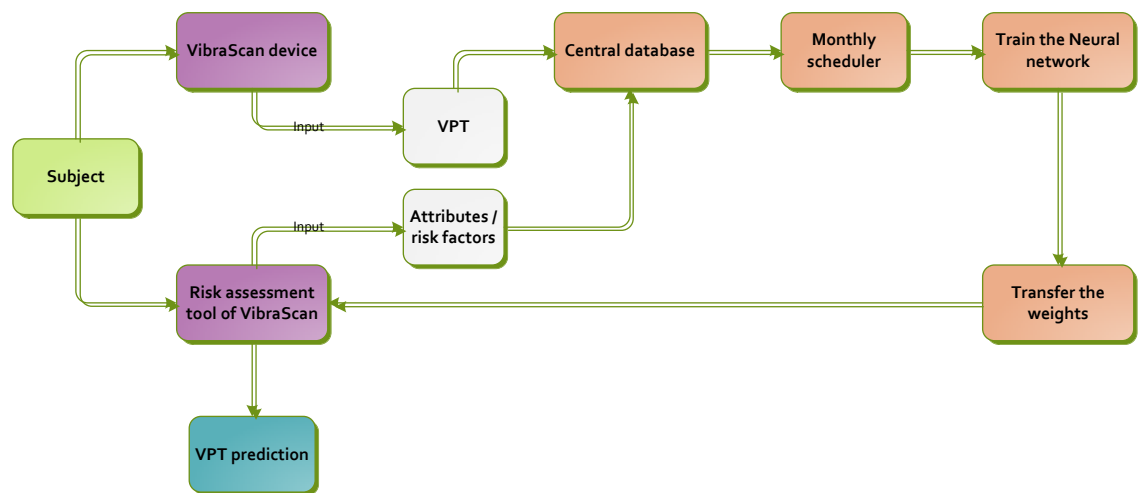
Figure 7.1: The futuristic model

This model involves both VibraScan device and risk assessment tool of VibraScan as shown in Figure 7.1. For collecting a large patient data, the first subject needs to be tested using VibraScan, the measured VPT value should be collected in the central database.

Secondly, subject should also use risk assessment tool so when they enter the values of risk factors i.e. age, height, weight, urine albumin to creatinine ratio (ACR), HbA1c, cholesterol, and duration of diabetes, it can be captured and transfered to the central database which is currently filled with simulated patient data. The format of collecting the data in the central database should maintain in the form of [attr1, attr2, attr3…. attrN, VPT] where *attr* is the

attributes/risk factors of diabetic neuropathy. The simulated patient data which is available in the central database should be replaced as per the VPT to maintain the categories with the fresh patient data as shown in the example below.

Simulated patient data	**sVPT 5V**	=	sAttr1	sAttr2	sAttr3	sAttr4	sAttr5	sAttr6	sAttr7
Patient data	**VPT 5V**	=	Attr1	Attr2	Attr3	Attr4	Attr5	Attr6	Attr7

Here sVPT is the simulated VPT present in the database. Likewise, all the simulated patient data will be replaced by real patient data gradually. The monthly scheduler should fetch the data from the central data-base and neural network should be trained using the newly updated dataset. Once the optimal classification accuracy is achieved the weights should be transferred to the risk assessment tool. This process can be continued until large patient data is collected. By using this model following advantages can be achieved as shown in Figure 7.2:
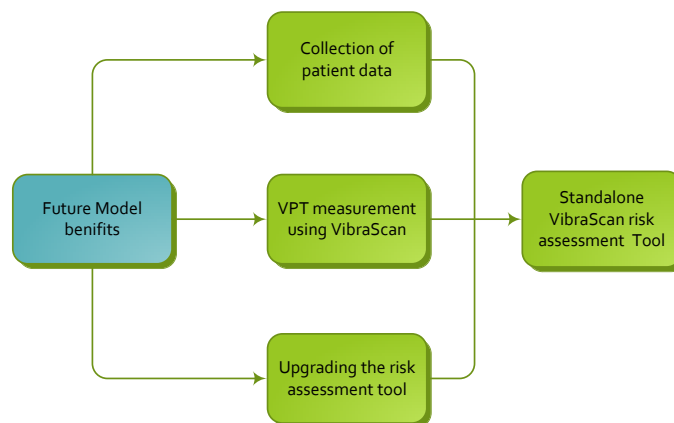
Figure 7.2: Overall benefits of the futuristic model

Using this latest model we can obtain mainly three benefits like a collection of the patient data, VPT measurement using VibraScan device and enriching the dataset of the risk assessment tool.

1. **Collection of patient data**: At the moment the tool was modeled using simulated data, however with this proposal, it will eventually replace all the existing simulated patient data with new patient data. A large amount of patient data can be collected with this method covering the whole range of VPT. There is a possibility of considering more attributes for research purpose during the collection of data. It is also possible to collect the data using internet where many VibraScan devices and risk assessment tool can be connected to the cloud for data collection.

2. **VPT measurement using VibraScan device:** This method gives an opportunity of using VibraScan for measuring VPT instead of Neurothesiometer. By using VibraScan device, it can be tested on patients as well.

3. **Upgrading risk assessment tool:** The risk assessment tool will be upgraded on a timely basis. Neural networks should show their potential of performing better when more data is fed into it. In this way, the risk assessment tool can be updated to improve its prediction over time.

When neural network model is trained with a large amount of the patient data which involves the VPT measurement using VibraScan, the updated version of the risk assessment tool should work as the standalone tool for predicting VPT without using the VibraScan device. Later on, the final version of the risk assessment tool software can be used as a mobile application where patients/subjects can easily measure their risk levels of diabetic neuropathy.

Hence, the state-of-the-art diabetic neuropathy assessment tool VibraScan has been developed in the current project. This is an advanced tool with its intuitive mode of operation and independently assessing the disease based on the clinical history of the patient. There is further scope where knowledge of VibraScan can be converted into a smart application in which patients can just access the user-friendly risk assessment tool to get an instant assessment of diabetic neuropathy in terms of their risk level.

References

Abbott, C. A., Malik, R. A., Ernest, R., Kulkarni, J. and Boulton, A. J., 2011a. Prevalence and Characteristics of Painful Diabetic Neuropathy in a Large Community-Based Diabetes Population in the UK. *Diabetes Care*, DC_111108.

Abbott, C. A., Malik, R. A., van Ross, E. R., Kulkarni, J. and Boulton, A. J., 2011b. Prevalence and characteristics of painful diabetic neuropathy in a large community-based diabetic population in the UK. *Diabetes Care*, 34 (10), 2220-2224.

Abraham, R. M. and Abraham, R. R., 1987. Absence of the sensory action potential of the medial plantar nerve: a sensitive indicator of diabetic neuropathy. *Diabetic medicine*, 4 (5), 469-474.

Adler, A. I., Boyko, E. J., Ahroni, J. H., Stensel, V., Forsberg, R. C. and Smith, D. G., 1997. Risk factors for diabetic peripheral sensory neuropathy: results of the Seattle Prospective Diabetic Foot Study. *Diabetes Care*, 20 (7), 1162-1167.

Alleman, C. J., Westerhout, K. Y., Hensen, M., Chambers, C., Stoker, M., Long, S. and van Nooten, F. E., 2015. Humanistic and economic burden of painful diabetic peripheral neuropathy in Europe: A review of the literature*,* 215.

Almeida, R. J., Kaymak, U. and Sousa, J. M., 2010. A new approach to dealing with missing values in data-driven fuzzy modeling, *Fuzzy Systems (FUZZ), 2010 IEEE International Conference on* (pp. 1-7): IEEE.

Anastasiadis, A. D., Magoulas, G. D. and Vrahatis, M. N., 2005. New globally convergent training scheme based on the resilient propagation algorithm. *Neurocomputing*, 64, 253-270.

Andersen, S. T., Witte, D. R., Andersen, H., Bjerg, L., Bruun, N. H., Jørgensen, M. E., Finnerup, N. B., Lauritzen, T., Jensen, T. S. and Tankisi, H., 2018. Risk-factor trajectories preceding diabetic polyneuropathy: ADDITION-Denmark. *Diabetes Care*, 41 (9), 1955-1962.

Apfel, S. C., Asbury, A. K., Bril, V., Bruns, T., Campbell, J. N., Chalk, C. H., Dyck, P. J., Dyck, P. J., Feldman, E. L. and Fields, H. L., 2001. Positive neuropathic sensory symptoms as endpoints in diabetic neuropathy trials. *Journal of the neurological sciences*, 189 (1-2), 3-5.

Association, A. D. and Neurology, A. A. o., 1988. Report and recommendations of the San Antonio conference on diabetic neuropathy. *Diabetes Care*, 11 (7), 592-597.

Ayoub, H., Griveau, S., Lair, V., Brunswick, P., Cassir, M. and Bedioui, F., 2010. Electrochemical characterization of nickel electrodes in phosphate and carbonate electrolytes in view of assessing a medical diagnostic device for the detection of early diabetes. *Electroanalysis*, 22 (21), 2483-2490.

Bansal, D., Gudala, K., Muthyala, H., Esam, H. P., Nayakallu, R. and Bhansali, A., 2014. Prevalence and risk factors of development of peripheral diabetic neuropathy in type 2 diabetes mellitus in a tertiary care setting. *Journal of diabetes investigation*, 5 (6), 714-721.

Bansal, V., Kalita, J. and Misra, U., 2006. Diabetic neuropathy. *Postgraduate medical journal*, 82 (964), 95-100.

Biothesiometer, B. b. e. c.-. 2017a. Biothesiometer. *http://arcbro.sale.ecer.co.uk/pz6c58711-biothesiometer.html*.

Biothesiometer, D. F. C. I. P. L.-D., 2017b. Digital Biothesiometer. *http://www.diabeticfootcareindia.com/digital-biothesiometer-vibrometer.php*.

Birke, J. and Sims, D., 1986. Plantar sensory threshold in the ulcerative foot. *Leprosy review*, 57 (3), 261-267.

Bland, J. M. and Altman, D., 1986. Statistical methods for assessing agreement between two methods of clinical measurement. *The lancet*, 327 (8476), 307-310.

Bloom, S., Till, S., Sönksen, P. and Smith, S., 1984. Use of a biothesiometer to measure individual vibration thresholds and their variation in 519 non-diabetic subjects. *Br Med J (Clin Res Ed)*, 288 (6433), 1793-1795.

Booya, F., Bandarian, F., Larijani, B., Pajouhi, M., Nooraei, M. and Lotfi, J., 2005. Potential risk factors for diabetic neuropathy: a case control study. *BMC neurology*, 5 (1), 24.

Botez, S. A., Liu, G., Logigian, E. and Herrmann, D. N., 2009. Is the bedside timed vibration test reliable?*,* 221.

Boulton, A. J., 2008. The diabetic foot: grand overview, epidemiology and pathogenesis. *Diabetes/metabolism research and reviews*, 24 (S1), S3-S6.

Boulton, A. J., Malik, R. A., Arezzo, J. C. and Sosenko, J. M., 2004. Diabetic somatic neuropathies. *Diabetes Care*, 27 (6), 1458-1486.

Boulton, A. J., Vinik, A. I., Arezzo, J. C., Bril, V., Feldman, E. L., Freeman, R., Malik, R. A., Maser, R. E., Sosenko, J. M. and Ziegler, D., 2005a. Diabetic neuropathies. *Diabetes Care*, 28 (4), 956-962.

Boulton, A. J., Vinik, A. I., Arezzo, J. C., Bril, V., Feldman, E. L., Freeman, R., Malik, R. A., Maser, R. E., Sosenko, J. M. and Ziegler, D., 2005b. Diabetic neuropathies: a statement by the American Diabetes Association. *Diabetes Care*, 28 (4), 956-962.

Bowker, J. H. and Pfeifer, M. A., 2008. *Levin and O'Neal's the diabetic foot*. Elsevier Health Sciences.

Box, G. E. and Cox, D. R., 1964. An analysis of transformations. *Journal of the Royal Statistical Society. Series B (Methodological)*, 211-252.

Bril, V., England, J. and Franklin, G., 2011. American Association of Neuromuscular and Electrodiagnostic Medicine; American Academy of Physical Medicine and Rehabilitation. Evidence-based guideline: Treatment of painful diabetic neuropathy: report of the American Academy of Neurology, the American Association of Neuromuscular and Electrodiagnostic Medicine, and the American Academy of Physical Medicine and Rehabilitation. *Neurology*, 76 (20), 1758-1765.

Casellini, C. M., Parson, H. K., Richardson, M. S., Nevoret, M. L. and Vinik, A. I., 2013. Sudoscan, a noninvasive tool for detecting diabetic small fiber neuropathy and autonomic dysfunction. *Diabetes technology & therapeutics*, 15 (11), 948-953.

Chawla, A., Bhasin, G. and Chawla, R., 2013. Validation of neuropathy symptoms score (NSS) and neuropathy disability score (NDS) in the clinical diagnosis of peripheral neuropathy in middle aged people with diabetes. *The Internet Journal of Family Practice*, 12 (1).

Cheng, J., Wang, Z. and Pollastri, G., 2008. A neural network approach to ordinal regression, *Neural Networks, 2008. IJCNN 2008.(IEEE World Congress on Computational Intelligence). IEEE International Joint Conference on* (pp. 1279-1284): IEEE.

Cheppali, S., 2014. ARDUINO BOARDS-PIN MAPPING. *http://icircuit.net/arduino-boards-pin-mapping/141*.

Chu, W. and Ghahramani, Z., 2005. Gaussian processes for ordinal regression. *Journal of machine learning research*, 6 (Jul), 1019-1041.

Coppini, D., Wellmer, A., Weng, C., Young, P., Anand, P. and Sönksen, P., 2001. The natural history of diabetic peripheral neuropathy determined by a 12 year prospective study using vibration perception thresholds. *Journal of Clinical Neuroscience*, 8 (6), 520-524.

Corbin, D., Young, R., Morrison, D., Hoskins, P., McDicken, W., Housley, E. and Clarke, B., 1987. Blood flow in the foot, polyneuropathy and foot ulceration in diabetes mellitus. *Diabetologia*, 30 (7), 468-473.

Dave, J. M, Dubey, V. N, Lowes, V., Beavis, J. and Coppini, D., 2018. A 'smarter'way of diagnosing the at risk foot: Development of a novel tool based on vibratory measurements in subjects with diabetes.

Dave, J. M., Dubey, V. N., Coppini, D.V. and Beavis, J., 2018. VibraScan: A smart device to replace Neurothesiometer for measuring diabetic vibration perception threshold *BioMedEng18*, (ISBN 978-1-9996465-0-9), 200.

Davies, M., Brophy, S., Williams, R. and Taylor, A., 2006. The prevalence, severity, and impact of painful diabetic peripheral neuropathy in type 2 diabetes. *Diabetes Care*, 29 (7), 1518-1522.

Davis, C. Q. and Freeman, D. M., 1998. Using a light microscope to measure motions with nanometer accuracy. *Optical Engineering*, 37 (4), 1299-1305.

DiabetesUK, 2016. Facts and Stats. *https://www.diabetes.org.uk/Documents/Position%20statements/DiabetesUK_Facts_Stats_Oct16.pdf*.

Dros, J., Wewerinke, A., Bindels, P. J. and van Weert, H. C., 2009. Accuracy of monofilament testing to diagnose peripheral neuropathy: a systematic review. *The Annals of Family Medicine*, 7 (6), 555-558.

Dyck, P. J., 1988. Detection, characterization, and staging of polyneuropathy: assessed in diabetics. *Muscle & nerve*, 11 (1), 21-32.

Dyck, P. J., Davies, J. L., Litchy, W. J. and O'brien, P., 1997. Longitudinal assessment of diabetic polyneuropathy using a composite score in the Rochester Diabetic Neuropathy Study cohort. *Neurology*, 49 (1), 229-239.

Dyck, P. J. and Harper, C. M., 1998. Paresthesia, Pain and Weakness in the Hands of Diabetic Patients Is Attributable to Mononeuropathies or Radiculopathy, Not Polyneuropathy: The Rochester (RDNS) and Pancreas and Renal Transplant (MC-PRT) Studies. *Neurology*, 50 (4).

Dyck, P. J., Sherman, W. R., Hallcher, L. M., John Service, F., O'Brien, P. C., Grina, L. A., Palumbo, P. J. and Swanson, C. J., 1980a. Human diabetic endoneurial sorbitol, fructose, and myo-inositol related to sural nerve morphometry. *Annals of Neurology: Official Journal of the American Neurological Association and the Child Neurology Society*, 8 (6), 590-596.

Dyck, P. J., Sherman, W. R., Hallcher, L. M., Service, F. J., O'Brien, P. C., Grina, L. A., Palumbo, P. J. and Swanson, C. J., 1980b. Human diabetic endoneurial sorbitol, fructose, and myo-inositol related to sural nerve morphometry. *Annals Of Neurology*, 8 (6), 590-596.

Edmonds, M., Roberts, V. and Watkins, P., 1982. Blood flow in the diabetic neuropathic foot. *Diabetologia*, 22 (1), 9-15.

EH Schwarz, P., Brunswick, P. and Calvet, J.-H., 2011. EZSCAN™ a new technology to detect diabetes risk. *The British Journal of Diabetes & Vascular Disease*, 11 (4), 204-209.

Fausett, L., 1994. *Fundamentals of neural networks: architectures, algorithms, and applications*. Prentice-Hall, Inc.

Fei-Fei, L., Jan 2015. CS231n: 'Convolutional Neural Networks for Visual Recognition'. http://vision.stanford.edu/teaching/cs231n/syllabus.html.

Feldman, E. L., Stevens, M., Thomas, P., Brown, M., Canal, N. and Greene, D., 1994. A practical two-step quantitative clinical and electrophysiological assessment for the diagnosis and staging of diabetic neuropathy. *Diabetes Care*, 17 (11), 1281-1289.

Feng, Y., Schlösser, F. J. and Sumpio, B. E., 2009. The Semmes Weinstein monofilament examination as a screening tool for diabetic peripheral neuropathy. *Journal of Vascular Surgery*, 50 (3), 675-682. e671.

Foot, I. W. G. o. t. D., 2015. Prevention and management of foot problems in diabetes: a Summary Guidance for daily practice 2015, based on the IWGDF Guidance documents. *Prevention and management of foot problems in diabetes: a Summary Guidance for daily practice 2015, based on the IWGDF Guidance documents*.

Franklin, G. M., Shetterly, S. M., Cohen, J. A., Baxter, J. and Hamman, R. F., 1994. Risk factors for distal symmetric neuropathy in NIDDM: the San Luis Valley Diabetes Study. *Diabetes Care*, 17 (10), 1172-1177.

Galer, B. S., Gianas, A. and Jensen, M. P., 2000. Painful diabetic polyneuropathy: epidemiology, pain description, and quality of life. *Diabetes Research and Clinical Practice*, 47 (2), 123-128.

Garrow, A. P. and Boulton, A. J., 2006. Vibration perception threshold—a valuable assessment of neural dysfunction in people with diabetes. *Diabetes/metabolism research and reviews*, 22 (5), 411-419.

Goldberg, J. and Lindblom, U., 1979. Standardised method of determining vibratory perception thresholds for diagnosis and screening in neurological investigation. *Journal of Neurology, Neurosurgery & Psychiatry*, 42 (9), 793-803.

Goldfeld, K. S., 2018. Simulating study data. *https://cran.r-project.org/web/packages/simstudy/vignettes/simstudy.html*.

Gutierrez, P. A., Perez-Ortiz, M., Sanchez-Monedero, J., Fernandez-Navarro, F. and Hervas-Martinez, C., 2016. Ordinal regression methods: survey and experimental study. *IEEE Transactions on Knowledge and Data Engineering*, 28 (1), 127-146.

Gutiérrez, P. A., Tiňo, P. and Hervás-Martínez, C., 2014. Ordinal regression neural networks based on concentric hyperspheres. *Neural networks*, 59, 51-60.

Hager, W. W. and Zhang, H., 2006. A survey of nonlinear conjugate gradient methods. *Pacific journal of Optimization*, 2 (1), 35-58.

Hamasaki, H. and Hamasaki, Y., 2017. *Diabetic Neuropathy Evaluated by a Novel Device: Sural Nerve Conduction Is Associated with Glycemic Control and Ankle–Brachial Pressure Index in Japanese Patients with Diabetes*. Vol. 8.

Harris, M., Eastman, R. and Cowie, C., 1993. Symptoms of sensory neuropathy in adults with NIDDM in the US population. *Diabetes Care*, 16 (11), 1446-1452.

Hartemann, A., Attal, N., Bouhassira, D., Dumont, I., Gin, H., Jeanne, S., Said, G., Richard, J.-L. and Diabetology, , 2011. Painful diabetic neuropathy: diagnosis and management. *Diabetes & metabolism*, 37 (5), 377-388.

He, X. and Xu, S., 2010. *Process neural networks: Theory and applications*. Springer Science & Business Media.

Hernandez, J., Carrasco-Ochoa, J. A. and Martínez-Trinidad, J. F., 2013. An empirical study of oversampling and undersampling for instance selection methods on imbalance datasets. *Progress in Pattern Recognition, Image Analysis, Computer Vision, and Applications.* Springer, 262-269.

Ho, S., Xie, M., Tang, L., Xu, K. and Goh, T., 2001. Neural network modeling with confidence bounds: a case study on the solder paste deposition process. *IEEE Transactions on Electronics Packaging Manufacturing*, 24 (4), 323-332.

Igel, C. and Hüsken, M., 2003. Empirical evaluation of the improved Rprop learning algorithms. *Neurocomputing*, 50, 105-123.

Illigens, B. M. and Gibbons, C. H., 2009. Sweat testing to evaluate autonomic function. *Clinical Autonomic Research*, 19 (2), 79.

Ince, P., Abbas, Z. G., Lutale, J. K., Basit, A., Ali, S. M., Chohan, F., Morbach, S., Möllenberg, J., Game, F. L. and Jeffcoate, W. J., 2008. Use of the SINBAD classification system and score in comparing outcome of foot ulcer management on three continents. *Diabetes Care*, 31 (5), 964-967.

Isaacson, W., 2003. *Benjamin Franklin: An American Life*. Simon and Schuster.

Jabre, J. F., 1981. Surface recording of the H-reflex of the flexor carpi radialis. *Muscle & nerve*, 4 (5), 435-438.

Jaiswal, M., Divers, J., Dabelea, D., Isom, S., Bell, R. A., Martin, C. L., Pettitt, D. J., Saydah, S., Pihoker, C. and Standiford, D. A., 2017. Prevalence of and risk factors for diabetic

peripheral neuropathy in youth with type 1 and type 2 diabetes: SEARCH for Diabetes in Youth Study. *Diabetes Care*, dc170179.

Jambart, S., Ammache, Z., Haddad, F., Younes, A., Hassoun, A., Abdalla, K., Selwan, C. A., Sunna, N., Wajsbrot, D. and Youseif, E., 2011. Prevalence of painful diabetic peripheral neuropathy among patients with diabetes mellitus in the Middle East region. *Journal of International Medical Research*, 39 (2), 366-377.

Jang, W. M., Eun, S. J., Lee, C. E. and Kim, Y., 2011. Effect of repeated public releases on cesarean section rates. *J Prev Med Public Health*, 44 (1), 2-8.

Jayaprakash, P., Bhansali, A., Bhansali, S., Dutta, P., Anantharaman, R., Shanmugasundar, G. and Ravikiran, M., 2011. Validation of bedside methods in evaluation of diabetic peripheral neuropathy. *The Indian journal of medical research*, 133 (6), 645.

Jones, L. K., 2012. Nerve conduction studies: basic concepts and patterns of abnormalities. *Neurologic clinics*, 30 (2), 405-427.

Kannel, W. and McGee, D., 1979. Diabetes and glucose tolerance as risk factors for cardiovascular disease: the Framingham study. *Diabetes Care*, 2 (2), 120-126.

Karl Guttormsen, P. C., 2017. Diabetic neuropathy: Beyond the basics. *http://www.thejournalofdiabetesnursing.co.uk/media/content/_master/4872/files/pdf/jdn21-1-17-22.pdf*, 17-22.

Kasznicki, J., 2014. Advances in the diagnosis and management of diabetic distal symmetric polyneuropathy. *Archives of medical science: AMS*, 10 (2), 345.

Kincaid, J. C., Brashear, A. and Markand, O. N., 1993. The influence of the reference electrode on CMAP configuration. *Muscle & nerve*, 16 (4), 392-396.

Kumar, D., Alvaro, M. S., Julka, I. S. and Marshall, H. J., 1998. Diabetic peripheral neuropathy: effectiveness of electrotherapy and amitriptyline for symptomatic relief. *Diabetes Care*, 21 (8), 1322-1325.

Lauria, G., Cornblath, D., Johansson, O., McArthur, J. C., Mellgren, S., Nolano, M., Rosenberg, N. and Sommer, C., 2005. EFNS guidelines on the use of skin biopsy in the diagnosis of peripheral neuropathy. *European journal of neurology*, 12 (10), 747-758.

Lauria, G. and Lombardi, R., 2007. Skin biopsy: a new tool for diagnosing peripheral neuropathy. *Bmj*, 334 (7604), 1159-1162.

Lin, C.-C., Chen, C.-C., Chen, F.-N., Li, C.-I., Liu, C.-S., Lin, W.-Y., Yang, S.-Y., Lee, C.-C. and Li, T.-C., 2013. Risks of diabetic nephropathy with variation in hemoglobin A1c and fasting plasma glucose. *The American journal of medicine*, 126 (11), 1017. e1011-1017. e1010.

Londhe, S. and Deo, M., 2004. Artificial neural networks for wave propagation. *Journal of coastal research*, 1061-1069.

Løseth, S., Nebuchennykh, M., Stålberg, E. and Mellgren, S. I., 2007. Medial plantar nerve conduction studies in healthy controls and diabetics. *Clinical neurophysiology*, 118 (5), 1155-1161.

Lowenthal, L. M., Derek, T. and Hockaday, R., 1987. Vibration sensory thresholds depend on pressure of applied stimulus. *Diabetes Care*, 10 (1), 100-102.

Malik, R., 2008. Neuropad: early diagnostic test for diabetic peripheral neuropathy. *Prescriber*, 19 (22), 42-45.

Mathieson, M. J., 1996. Ordinal models for neural networks, *Proc. 3rd Int. Conf. Neural Netw. Capital Markets* (pp. 523-536).

Mathworks, 2018. Choose a Multilayer Neural Network Training Function.

Mayaudon, H., Miloche, P.-O. and Bauduceau, B., 2010. A new simple method for assessing sudomotor function: relevance in type 2 diabetes. *Diabetes & metabolism*, 36 (6), 450-454.

Mayfield, J. A., Reiber, G. E., Sanders, L. J., Janisse, D. and Pogach, L. M., 1998. Preventive foot care in people with diabetes. *Diabetes Care*, 21 (12), 2161.

Mayfield, J. A. and Sugarman, J. R., 2000. The use of the Semmes-Weinstein monofilament and other threshold tests for preventing foot ulceration and amputation in persons with diabetes. *Journal of Family Practice*, 49 (11), S17-S17.

Michelle Branigan, S. W., 2014. Diagnosing DPN. *http://www.podiatrym.com/cme/CME1114.pdf*, 103-108.

Mondelli, M., Aretini, A. and Baldasseroni, A., 2012. Distal symmetric polyneuropathy in diabetes. Differences between patients with and without neuropathic pain. *Experimental and clinical endocrinology & diabetes*, 120 (01), 45-50.

Moreira, R. O., Castro, A. P., Papelbaum, M., Appolinário, J. C., Ellinger, V., Coutinho, W. F. and Zagury, L., 2005. Translation into Portuguese and assessment of the reliability of a scale for the diagnosis of diabetic distal polyneuropathy. *Arquivos Brasileiros de Endocrinologia & Metabologia*, 49 (6), 944-950.

Morrish, N., Wang, S.-L., Stevens, L., Fuller, J. and Keen, H., 2001. Mortality and causes of death in the WHO Multinational Study of Vascular Disease in Diabetes. *Diabetologia*, 44, S14-S21.

Mountcastle, V. B., Talbot, W. H., Darian-Smith, I. and Kornhuber, H. H., 1967. Neural basis of the sense of flutter-vibration. *Science*, 155 (3762), 597-600.

Mukesh, B. N., Le, A., Dimitrov, P. N., Ahmed, S., Taylor, H. R. and McCarty, C. A., 2006. Development of cataract and associated risk factors: the Visual Impairment Project. *Archives of ophthalmology*, 124 (1), 79-85.

Mulnier, H., 2012. Macrovascular disease in diabetes. *J Diabetes Nurs*, 16, 307-314.

Murray, H. J., Young, M. J., Hollis, S. and Boulton, A. J., 1996. The association between callus formation, high pressures and neuropathy in diabetic foot ulceration. *Diabetic medicine*, 13 (11), 979-982.

Nagsayi, S., Somasekhar, C. and James, C. M., 2010. Diagnosis and management of diabetic amyotrophy. *pathogenesis*, 2, 3.

Neurothesiometer, A. U.-. 2017. Neurothesiometer. *http://www.algeos.com/neurothesiometer.html*.

Neurothesiometer, t.-. 2016. Horwell - Neurothesiometer Rechargable Battery. *http://trimbio.co.uk/r-to-s/reconditioned-equipment/reconditioned-podiatry-items/horwell-neurothesiometer-rechargable-battery.html*.

O'Brien, T. and Karem, J., 2014a. An initial evaluation of a proof-of-concept 128-Hz electronic tuning fork in the detection of peripheral neuropathy. *Journal of the American Podiatric Medical Association*, 104 (2), 134-140.

O'Brien, T. and Karem, J., 2014b. *An Initial Evaluation of a Proof-of-Concept 128-Hz Electronic Tuning Fork in the Detection of Peripheral Neuropathy*. Vol. 104.

O'Connell, A. A., 2006. *Logistic regression models for ordinal response variables*. Sage.

Ohnishi, A., Haba, S., Yamamoto, T., Murai, Y. and Ikeda, M., 1994. Comparative studies on the evaluation of vibratory perception thresholds using three different instruments, vibratron II, TM-31A and SMV-5--reliability, correlation with age and interrelationship. *Journal of UOEH*, 16 (1), 61-70.

Olmos, P. R., Cataland, S., O'Dorisio, T. M., Casey, C. A., Smead, W. L. and Simon, S. R., 1995. The Semmes–Weinstein monofilament as a potential predictor of foot ulceration in patients with noninsulin-dependent diabetes. *The American journal of the medical sciences*, 309 (2), 76-82.

Pan, C. L., Tseng, T. J., Lin, Y. H., Chiang, M. C., Lin, W. M. and Hsieh, S. T., 2003. Cutaneous innervation in Guillain–Barré syndrome: pathology and clinical correlations. *Brain*, 126 (2), 386-397.

Papanas, N., Boulton, A., Malik, R., Manes, C., Schnell, O., Spallone, V., Tentolouris, N., Tesfaye, S., Valensi, P. and Ziegler, D., 2013. A simple new non-invasive sweat indicator test for the diagnosis of diabetic neuropathy. *Diabetic medicine*, 30 (5), 525-534.

Papanas, N., Giassakis, G., Papatheodorou, K., Papazoglou, D., Monastiriotis, C., Christakidis, D., Piperidou, H. and Maltezos, E., 2007. Sensitivity and specificity of a new indicator test (Neuropad) for the diagnosis of peripheral neuropathy in type 2 diabetes patients: a comparison with clinical examination and nerve conduction study. *Journal of Diabetes and its Complications*, 21 (6), 353-358.

Papanas, N., Paschos, P., Papazoglou, D., Papatheodorou, K., Paletas, K., Maltezos, E. and Tsapas, A., 2011. Accuracy of the Neuropad test for the diagnosis of distal symmetric polyneuropathy in type 2 diabetes. *Diabetes Care*, 34 (6), 1378-1382.

Papanas, N. and Ziegler, D., 2011. New diagnostic tests for diabetic distal symmetric polyneuropathy. *Journal of Diabetes and its Complications*, 25 (1), 44-51.

Papanas, N. and Ziegler, D., 2013. Corneal confocal microscopy: a new technique for early detection of diabetic neuropathy. *Current diabetes reports*, 13 (4), 488-499.

Papanas, N. and Ziegler, D., 2015. Corneal confocal microscopy: recent progress in the evaluation of diabetic neuropathy. *Journal of diabetes investigation*, 6 (4), 381-389.

Pasnoor, M., Dimachkie, M. M. and Barohn, R. J., 2013. Diabetic neuropathy part 2: proximal and asymmetric phenotypes. *Neurologic clinics*, 31 (2), 447-462.

Pataky, Z., 2012. *Prevention of Diabetic Foot Ulcers: From Biomechanics to Therapeutic Patient Education.* University of Geneva.

Pataky, Z., Golay, A., Faravel, L., Da Silva, J., Makoundou, V., Peter-Riesch, B. and Assal, J., 2002. The impact of callosities on the magnitude and duration of plantar pressure in patients with diabetes mellitus. *Diabetes Metab*, 28 (5), 356-361.

Pérez-Ortiz, M., Gutiérrez, P., Tino, P., Casanova-Mateo, C. and Salcedo-Sanz, S., 2018. A mixture of experts model for predicting persistent weather patterns, *2018 International Joint Conference on Neural Networks (IJCNN)* (pp. 1-8): IEEE.

Perkins, B. A., Grewal, J., Ng, E., Ngo, M. and Bril, V., 2006. Validation of a novel point-of-care nerve conduction device for the detection of diabetic sensorimotor polyneuropathy. *Diabetes Care*, 29 (9), 2023-2027.

Pourhamidi, K., Dahlin, L. B., Englund, E. and Rolandsson, O., 2014. Evaluation of clinical tools and their diagnostic use in distal symmetric polyneuropathy. *Primary care diabetes*, 8 (1), 77-84.

Ratner, B., 2009. The correlation coefficient: Its values range between+ 1/− 1, or do they? *Journal of targeting, measurement and analysis for marketing*, 17 (2), 139-142.

Rochester, U. o., 2007. The Somatosensory System. *Brain and cognitive Sciences courses*, http://www2.bcs.rochester.edu/courses/crsinf/240/24.pdf.

Schaper, N., Van Netten, J., Apelqvist, J., Lipsky, B., Bakker, K. and Foot, I. W. G. o. t. D., 2016. Prevention and management of foot problems in diabetes: a Summary Guidance for Daily Practice 2015, based on the IWGDF Guidance Documents. *Diabetes Research and Clinical Practice*.

Selvarajah, D., Cash, T., Davies, J., Sankar, A., Rao, G., Grieg, M., Pallai, S., Gandhi, R., Wilkinson, I. D. and Tesfaye, S., 2015. SUDOSCAN: a simple, rapid, and objective method with potential for screening for diabetic peripheral neuropathy. *PloS one*, 10 (10), e0138224.

Sharma, B. and Venugopalan, K., 2014. Comparison of neural network training functions for hematoma classification in brain CT images. *IOSR Journal of Computer Engineering (IOSR-JCE)*, 16 (1), 31-35.

Shy, M. E. and Frohman, E. M., 2003. Quantitative sensory testing: Report of the Therapeutics and Technology Assessment Subcommittee of the American Academy of Neurology: Reply from the Authors, 1628.

Singh, P. P., Bindra, S., Singh, S., Aggarwal, R. and Singh, J., 2012. Effect of Nerve Mobilization on Vibration Perception Threshold in Diabetic Peripheral Neuropathy. *Indian Journal of Physiotherapy and Occupational Therapy*, 40, 195.

Smieja, M., Hunt, D. L., Edelman, D., Etchells, E., Cornuz, J. and Simel, D. L., 1999. Clinical examination for the detection of protective sensation in the feet of diabetic patients. *Journal of general internal medicine*, 14 (7), 418-424.

Sola, J. and Sevilla, J., 1997. Importance of input data normalization for the application of neural networks to complex industrial problems. *IEEE Transactions on Nuclear Science*, 44 (3), 1464-1468.

Song, Q., Zhang, J. and Chi, Q., 2010. Assistant detection of skewed data streams classification in cloud security, *Intelligent Computing and Intelligent Systems (ICIS), 2010 IEEE International Conference on* (Vol. 1, pp. 60-64): IEEE.

Spallone, V., Ziegler, D., Freeman, R., Bernardi, L., Frontoni, S., Pop-Busui, R., Stevens, M., Kempler, P., Hilsted, J. and Tesfaye, S., 2011. Cardiovascular autonomic neuropathy in diabetes: clinical impact, assessment, diagnosis, and management. *Diabetes/metabolism research and reviews*, 27 (7), 639-653.

Stewart, J. D., Nguyen, D. M. and Abrahamowicz, M., 1994. Quantitative sweat testing using acetylcholine for direct and axon reflex mediated stimulation with silicone mold recording; controls versus neuropathic diabetics. *Muscle & nerve*, 17 (12), 1370-1377.

Sumner, C., Sheth, S., Griffin, J., Cornblath, D. and Polydefkis, M., 2003. The spectrum of neuropathy in diabetes and impaired glucose tolerance. *Neurology*, 60 (1), 108-111.

Tanenberg, R. and D. Donofrio, P., 2008. Problemas neuropáticos de los miembros inferiores en los pacientes diabéticos. 33-74.

TB6612FNG, S.-. 2017. SparkFun Motor Driver - Dual TB6612FNG (1A). *https://www.sparkfun.com/products/9457*.

Tesfaye, S., Malik, R., Harris, N., Jakubowski, J., Mody, C., Rennie, I. and Ward, J., 1996a. Arterio-venous shunting and proliferating new vessels in acute painful neuropathy of rapid glycaemic control (insulin neuritis). *Diabetologia*, 39 (3), 329-335.

Tesfaye, S., Stevens, L., Stephenson, J., Fuller, J., Plater, M., Ionescu-Tirgoviste, C., Nuber, A., Pozza, G., Ward, J. and Group, E. I. C. S., 1996b. Prevalence of diabetic peripheral neuropathy and its relation to glycaemic control and potential risk factors: the EURODIAB IDDM Complications Study. *Diabetologia*, 39 (11), 1377-1384.

Thaisetthawatkul, P., Fernandes Filho, J. A. M. and Herrmann, D. N., 2013. Contribution of QSART to the diagnosis of small fiber neuropathy. *Muscle & nerve*, 48 (6), 883-888.

Vamos, E. P., Millett, C., Parsons, C., Aylin, P., Majeed, A. and Bottle, A., 2012. Nationwide study on trends in hospital admissions for major cardiovascular events and procedures among people with and without diabetes in England, 2004–2009. *Diabetes Care*, 35 (2), 265-272.

Van Deursen, R. W., Sanchez, M. M., Ulbrecht, J. S. and Cavanagh, P. R., 1998. The role of muscle spindles in ankle movement perception in human subjects with diabetic neuropathy. *Experimental brain research*, 120 (1), 1-8.

Van Deursen, R. W. M., Sanchez, M., Derr, J., Becker, M., Ulbrecht, J. and Cavanagh, P. R., 2001. Vibration perception threshold testing in patients with diabetic neuropathy: ceiling effects and reliability. *Diabetic medicine*, 18 (6), 469-475.

Verrillo, R. T. and Bolanowski, S. J., 2003. Effects of temperature on the subjective magnitude of vibration. *Somatosensory & motor research*, 20 (2), 133-137.

Vinik, A. I., Erbas, T. and Casellini, C. M., 2013. Diabetic cardiac autonomic neuropathy, inflammation and cardiovascular disease. *Journal of diabetes investigation*, 4 (1), 4-18.

Watts, G., Shaw, K. and Long, G., 1986. Warning on the use of the biothesiometer. *Diabetic medicine: a journal of the British Diabetic Association*, 3 (1), 91.

Weber, F., 1998. The diagnostic sensitivity of different F wave parameters. *Journal of Neurology, Neurosurgery & Psychiatry*, 65 (4), 535-540.

Williams, G., Gill, J. S., Aber, V. and Mather, H. M., 1988. Variability in vibration perception threshold among sites: a potential source of error in biothesiometry. *British medical journal (Clinical research ed.)*, 296 (6617), 233.

Xu, F., Zhao, L.-h., Su, J.-b., Chen, T., Wang, X.-q., Chen, J.-f., Wu, G., Jin, Y. and Wang, X.-h., 2014. The relationship between glycemic variability and diabetic peripheral neuropathy in type 2 diabetes with well-controlled HbA1c. *Diabetology & metabolic syndrome*, 6 (1), 139.

Yajnik, C. S., Kantikar, V. V., Pande, A. J. and Deslypere, J. P., 2012. Quick and simple evaluation of sudomotor function for screening of diabetic neuropathy. *ISRN endocrinology*, 2012.

Yao, X. and Liu, Y., 1999. Neural networks for breast cancer diagnosis, *Evolutionary Computation, 1999. CEC 99. Proceedings of the 1999 Congress on* (Vol. 3, pp. 1760-1767): IEEE.

Young, M. J., Breddy, J. L., Veves, A. and Boulton, A. J., 1994. The prediction of diabetic neuropathic foot ulceration using vibration perception thresholds: a prospective study. *Diabetes Care*, 17 (6), 557-560.

Zaid, I. I. A., Hussein, M. A., Mousa, G. S., Mohamed, A. R., Badr, N. M. and Hamid, A. A., 2018. Acetylcholine iontophoresis in diabetic patients with and without peripheral neuropathy: a potential therapeutic tool. *The Egyptian Journal of Internal Medicine*, 30 (3), 140.

Ziegler, D., 2009. Painful diabetic neuropathy: advantage of novel drugs over old drugs? *Diabetes Care*, 32 (suppl 2), S414-S419.

Ziegler, D., Papanas, N., Vinik, A. I. and Shaw, J. E., 2014a. Epidemiology of polyneuropathy in diabetes and prediabetes. *Handbook of clinical neurology.* Elsevier, 3-22.

Ziegler, D., Papanas, N., Zhivov, A., Allgeier, S., Winter, K., Ziegler, I., Brüggemann, J., Strom, A., Peschel, S. and Köhler, B., 2014b. Early detection of nerve fiber loss by corneal confocal microscopy and skin biopsy in recently diagnosed type 2 diabetes. *Diabetes*, 63 (7), 2454-2463.

Ziegler, D., Siekierka-Kleiser, E., Meyer, B. and Schweers, M., 2005. Validation of a novel screening device (NeuroQuick) for quantitative assessment of small nerve fiber dysfunction as an early feature of diabetic polyneuropathy. *Diabetes Care*, 28 (5), 1169-1174.

Ziff, M. and Stark, R. J., 2017. How to assess tendon reflexes of the lower limb in the elderly. *Journal of the neurological sciences*, 372, 196-200.

Appendix

Appendix A: Research Ethics Checklist approved by Bournemouth University

Research Ethics Checklist

Reference Id	12548
Status	Approved
Date Approved	15/03/2017

Researcher Details

Name	Jugal Dave
School	Faculty of Science & Technology
Status	Postgraduate Research (MRes, MPhil, PhD, DProf, DEng)
Course	Postgraduate Research
Have you received external funding to support this research project?	Yes
RED ID	8395
Funding Body	Poole Hospital NHS Foundation Trust
Please list any persons or institutions that you will be conducting joint research with, both internal to BU as well as external collaborators.	Poole Hospital NHS Foundation Trust

Project Details

Title	Medical Device development for comprehensive clinical assessment of Peripheral Neuropathy
Proposed Start Date of Data Collection	15/03/2017
Proposed End Date of Project	05/10/2018
Supervisor	Venky Dubey

Approvor	Raian Ali

Summary - no more than 500 words (including detail on background methodology, sample, outcomes, etc.)
Diabetic peripheral neuropathy is one of the devastating and serious complications of Diabetes Mellitus. Early detection of the disease can help to reduce the risk of the foot ulcer and limb amputation. There is a sign of reduction in the protective sensation and vibration sensation which leads to numbness, tingling, and burning symptoms. There are commercially available devices such as Neurothesiometer which vibrates at the specific frequency and variable intensity. However, an operator is required to use this device that will hold the vibrator probe and apply at the different sites on the plantar surface of the foot. The vibration is changed from lower intensity and gradually increased till the patient feels the vibration. Based on the patient's feedback and voltage reading the level of the neuropathy could be estimated. The drawback of this method is human operators who conduct the test which can affect the reproducibility, and the method is semi-quantitative as it reliant on the patient's feedback. We have developed a prototype device which consists of a simple inclined plane having vibrators at different areas. It consists of the force sensors which are used to monitor the pressure distributed at the required sites of the foot. The patient will sit on the chair and place their bare foot on the inclined plane in such a way that the big toe is placed on the vibrator. The vibration is provided at the big toe with the minimum intensity and fixed frequency. The intensity of the vibration is increased till the patient feels the vibration. Based on the voltage reading of the device severity of the complication can be classified.

External Ethics Review

Does your research require external review through the NHS National Research Ethics Service (NRES) or through another external Ethics Committee?	No

Research Literature

Is your research solely literature based?	No

Human Participants

Will your research project involve interaction with human participants as primary sources of data (e.g. interview, observation, original survey)?	Yes
Does your research specifically involve participants who are considered vulnerable (i.e. children, those with cognitive impairment, those in unequal relationships—such as your own students, prison inmates, etc.)?	No
Does the study involve participants age 16 or over who are unable to give informed consent (i.e. people with learning disabilities)? NOTE: All research that falls under the auspices of the Mental Capacity Act 2005 must be reviewed by NHS NRES.	No
Will the study require the co-operation of a gatekeeper for initial access to the groups or individuals to be recruited? (i.e. students at school, members of self-help group, residents of Nursing home?)	No

Will it be necessary for participants to take part in your study without their knowledge and consent at the time (i.e. covert observation of people in non-public places)?	No
Will the study involve discussion of sensitive topics (i.e. sexual activity, drug use, criminal activity)?	No

Are drugs, placebos or other substances (i.e. food substances, vitamins) to be administered to the study participants or will the study involve invasive, intrusive or potentially harmful procedures of any kind?	No

Will tissue samples (including blood) be obtained from participants? Note: If the answer to this question is 'yes' you will need to be aware of obligations under the Human Tissue Act 2004.	No

Could your research induce psychological stress or anxiety, cause harm or have negative consequences for the participant or researcher (beyond the risks encountered in normal life)?	No
Will your research involve prolonged or repetitive testing?	No
Will the research involve the collection of audio materials?	No
Will your research involve the collection of photographic or video materials?	No
Will financial or other inducements (other than reasonable expenses and compensation for time) be offered to participants?	No

Please give a summary of the ethical issues and any action that will be taken to address these. Explain how you will obtain informed consent (and from whom) and how you will inform the participant about the research project (i.e. participant information sheet).
See attached documents.

Final Review

Will you have access to personal data that allows you to identify individuals OR access to confidential corporate or company data (that is not covered by confidentiality terms within an agreement or by a separate confidentiality agreement)?	Yes

Please explain below why your research requires the collection of personal data. Describe how you will anonymize the personal data (if applicable). Describe how you will collect, manage and store the personal data (taking into consideration the Data Protection Act and the 8 Data Protection Principles). Explain how you will obtain informed consent (and from whom) and how you will inform the participant about the research project (i.e. participant information sheet).

Participants will be contacted via email address to take part in the experiment. All data(email address and names) will be kept confidential in the same way as the current experiment (password protected with limited access). Contact details (email address) and the names of the participants will be kept confidential at a BU password protected secure network with limited access for the researcher (Jugal Manoj Dave) and project supervisor (Prof. Venky Dubey). Participants will first be provided with the participant information sheet before taking part in the experiment. Participant agreement form will be collected from the participant once they confirm to take part in the experiment after reading participant information sheet. After the experiment, names and email addresses of all the participants will be made anonymised by assigning a participant number and later on all the participants names and email address will be deleted.

Will your research involve experimentation on any of the following: animals, animal tissue, genetically modified organisms?	No
Will your research take place outside the UK (including any and all stages of research: collection, storage, analysis, etc.)?	No
Could conflicts of interest arise between the source of funding and the potential outcomes of the research?	No

Please use the below text box to highlight any other ethical concerns or risks that may arise during your research that have not been covered in this form.

Researcher Statement

JOURNALISM / BROADCAST RESEARCHERS: I confirm that I have consulted and understand the Research Ethics Supplementary Guide: For Reference by Researchers Undertaking Journalism and Media Production Projects (available on the Research Ethics page)	Yes

Appendix B: Participant Information sheet

The title of the research project

 Medical Device development for comprehensive clinical assessment of Peripheral Neuropathy

Invitation

You are being invited to take part in this research project conducted by Jugal Manoj Dave, a postgraduate researcher, in the Department of Computing and Informatics, Faculty of Science & Technology, Bournemouth University, UK. Before you decide, it is important for you to understand why the research is being done and what it will involve. Please take time to read the following information carefully and discuss it with others if you wish. Ask us if there is anything that is not clear or if you would like more information. Take time to decide whether you wish to take part.

Who is organizing/funding the research?

This research is being funded by Bournemouth University and Poole Hospital NHS Foundation Trust.

What is the purpose of the project?

The Purpose of this project is to detect diabetic neuropathy at the early stage. Diabetic neuropathy is the disease in which there is a reduction in the touch sensation causing the numbness in the feet and hands.

As per World Health Organization (WHO), approximately 150 million people have diabetes mellitus worldwide, and that number may well double by the year 2025. Diabetic Neuropathy is common complications of diabetes. Studies suggest that up to 50% of people with diabetes are affected to some degree. To get into the effectiveness we have developed a device to detect neuropathy and conduct an experiment which will provide us the data from the normal people i.e. people having no history of neuropathy, and helps in diagnosing diabetic neuropathy at the early stage.

You may have several questions in your mind such as:

When this research is focused on diabetic patients. Why are we looking for normal subjects? How will this going to contribute to the research? What will be the potential benefits when considering normal subjects?

As the focus is on early detection of neuropathy one has to establish the potential risk of neuropathy occurrence on normal people. It is important to explain that the subjects to be examined are to be provided with mechanical vibration to the foot so as to get whether the subject examined is normal or a progressive neuropathy patient. Due to diabetic neuropathy, patients may not feel the mechanical vibration in their extremities. It is important that level of neuropathy is identified in early detection of the disease.

Based on data analysis of the subject examined the threshold level of sensing the mechanical vibration of the normal subject can be determined.

Why have I been chosen?

This is an open call that aims to reach those who fulfills the criteria below can contribute to the research by providing their valuable feedback.

Criteria:

1.   above 18 years old.

2.   Should be non-diabetic.

3.   Should not have any injury or ulcers on the sole of the foot.

4.   Should not have any problem in foot movement.

Do I have to take part?

It is up to you to decide whether to take part. If you do decide to take part, you will be given this information sheet to keep (and be asked to sign a participant agreement form). You can withdraw at any time, up to the point where the data are processed and become anonymous, so your identity cannot be determined, without it affecting any benefits that you are entitled to in any way. You do not have to give a reason. Deciding to take part or not will not affect your treatment/care /education or studies at BU.

What would taking part involve?

Before the experiment:

- You will be asked to remove the shoes and socks.
- Once you are relaxed and ready test will start which will take approximately 5 minutes.

During the experiment:

- You will be given information about the study.
- You will be attached with three surface electrodes in such a way that it will capture the muscle activity as shown in the Fig.1.
- These electrodes are totally non- invasive and just stick to the surface of the skin as shown in Fig.1
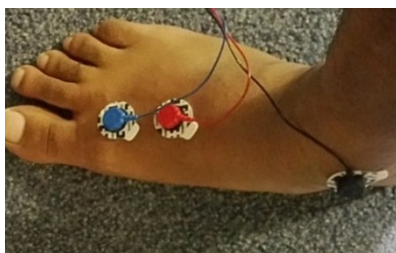
Figure 1: Electrodes attachment to capture muscle activity.

Figure 2: Inclined plane with vibrator for the placement of the foot.

- Then you will be asked to sit on the chair and to place your right foot on the inclined plate as shown in Fig 2 which consists of a vibrator and Force resistive sensor to monitor the pressure distributed at the planter surface of the foot.
- The device will provide mechanical vibration starting with a low intensity and increasing where the subject will be asked to respond 'Yes' or 'No' when the vibration sensation is felt. (Vibration intensity will be similar to that of mobile phone vibration).
- The Answer 'Yes' will be recorded against the vibration intensity level to determine the neuropathy level.
- The vibration intensity will only be increased gradually till the vibration is felt.

After the experiment:

- Surface electrodes will be removed and you will be free to pop up your socks and shoes.

What are the advantages and possible disadvantages or risks of taking part?

Whilst there are no immediate benefits for those people participating in the project. There could be long term benefit to diabetic patients once the efficiency of device is proven. There is very low risk in the experiment as the experiment is limited to low intensity mechanical vibration. Vibration provided by the system will be on the skin surface. It is not going to rupture the skin and is totally safe. There is no chance of electric shock or mechanical piercing. The vibration will be applied at the speed of 100 cycles per second with the maximum of 1 mm displacement. The whole setup is wireless to make it safe to operate. You can withdraw at any time if feeling uncomfortable.

Will my taking part in this study be kept confidential?

All the information that we collect about you during the research will be kept in accordance with the Data Protection Act 1998. You will not be able to be identified in any reports or publications. All data relating to this study will be kept for 5 years on a BU password protected secure network.

What type of information will be sought from me and why is the collection of this information relevant for achieving the research project's objectives?

The data collected are not going to be of a sensitive nature.

The test will help us getting the data of Vibration perception threshold (VPT) for the normal subjects and can lead to early detection of Diabetic Neuropathy in patients. Your participation is very important in analyzing the hypothesis for early detection of diabetic Neuropathy.

Who has reviewed the study?

This study has been reviewed and approved in line with Bournemouth University's Research Ethics Code of Practice.

Will I be recorded, and how will the recorded media be used?

Not applicable.

Contact for further information

If you have any queries about this research, please contact Prof. Venky Dubey by email on VDubey@bournmeouth.ac.uk or by phone on 01202 965986 or by post to:

Prof. Venky Dubey
Faculty of Science and Technology
Bournemouth University
BH12 5BB

Complaints

If you have any complaints about this project please contact Professor Keith Phalp, Executive Dean of the Faculty of Science and Technology at Bournemouth University at the following address:

Professor Keith Phalp

Poole House P426

Talbot Campus, Fern Barrow, Poole, BH12 5BB

E-mail: researchgovernance@bournemouth.ac.uk

Tel: 01202 965571

Thank you for taking the time to read this information sheet, and please do not hesitate to contact me if you have any queries

Appendix C: Participant Agreement Form

Full title of project: Medical Device development for comprehensive clinical assessment of Peripheral Neuropathy

Name, position and contact details of researcher: Jugal Manoj Dave, Postgraduate researcher, Department of Computing and Informatics, Faculty of Science & Technology, Bournemouth University. Email: jdave@bournmeouth.ac.uk

I have read and understood the participant information sheet for the above research project.	
I confirm that I have had the opportunity to ask questions.	
I understand that my participation is voluntary.	
I understand that I am free to withdraw up to the point where the data are processed and become anonymous, so my identity cannot be determined.	
During the tasks of the study, I am free to withdraw without giving a reason and without there being any negative consequences.	
Should I not wish to answer any particular question(s), complete a test I am free to decline.	
I give permission for members of the research team to have access to my anonymised responses. I understand that my name will not be linked with the research materials, and I will not be identified or identifiable in the outputs that result from the research.	
I agree to take part in the above research project.	

_____   _____
_____

Name or Initials of the Participant   Date   Signature

_____   _____
_____

Name or Initials of the Researcher   Date   Signature
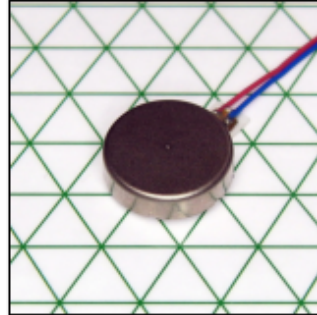
Appendix D: Datasheets

1. ERM motors:

312-101

12mm Vibration Motor - 3mm Type
Shown on 6mm Isometric Grid

PRECISION MICRODRIVES™

Product Data Sheet
Pico Vibe™
12mm Vibration Motor - 3mm Type

Model: 312-101

Ordering Information

The model number 312-101 fully defines the model, variant and additional features of the product. Please quote this number when ordering.
For stocked types, testing and evaluation samples can be ordered directly through our online store.

Datasheet Versions

It is our intention to provide our customers with the best information available to ensure the successful integration between our products and your application. Therefore, our publications will be updated and enhanced as improvements to the data and product updates are introduced.
To obtain the most up-to-date version of this datasheet, please visit our website at: www.precisionmicrodrives.com
The version number of this datasheet can be found on the bottom left hand corner of any page of the datasheet and is referenced with an ascending R-number (e.g. R002 is newer than R001). Please contact us if you require a copy of the engineering change notice between revisions.

If you have any questions, suggestions or comments regarding this publication or need technical assistance, please contact us via email at: enquiries@precisionmicrodrives.com or call us on +44 (0) 1932 252 482

Key Features

Body Diameter:	12 mm [+/- 0.1]
Body Length:	3.4 mm [+/- 0.1]
Rated Operating Voltage:	3 V
Rated Vibration Speed:	12,500 rpm [+/- 2,500]
Typical Rated Operating Current:	75 mA
Typical Normalised Amplitude:	2.6 G

Typical Vibration Motor Performance Characteristics
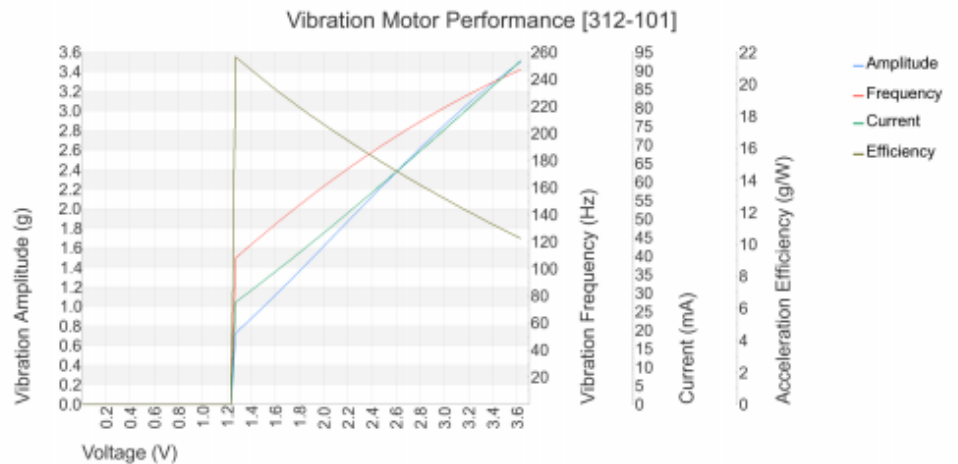
Vibration Motor Performance [312-101]

Physical Specification

PARAMETER	CONDITIONS	SPECIFICATION
Body Diameter	Max body diameter or max face dimension where non-circular	12 mm [+/- 0.1]
Body Length	Excl. shafts, leads and terminals	3.4 mm [+/- 0.1]
Unit Weight		1.7 g
Mounting	See drawing for details	Self Adhesive Sheet

Construction Specification

PARAMETER	CONDITIONS	SPECIFICATION
Motor Construction		Flat Coreless
Commutation		Precious Metal Brush
No. of Poles		6
Bearing Type		Sintered Bronze

Leads & Connectors Specification

PARAMETER	CONDITIONS	SPECIFICATION
Lead Length	Lead lengths defined as total length or between motor and connector	45 mm [+/- 2]
Lead Strip Length		2 mm [+/- 1]
Lead Wire Gauge		30 AWG
Lead Configuration		Straight

Operational Specification

PARAMETER	CONDITIONS	SPECIFICATION
Rated Operating Voltage		3 V
Rated Vibration Speed	At rated voltage using the inertial test load	12,500 rpm [+/- 2,500]
Max. Rated Operating Current	At rated voltage using the inertial test load	100 mA
Rated Inertial Test Load	Mass of standard test sled	100 g
Max. Start Voltage	With the inertial test load	2 V
Min. Vibration Amplitude	Peak-to-peak value at rated voltage using the inertial test load	1.55 G
Max. Operating Voltage		3.6 V
Max. Start Current	At rated voltage	170 mA
Min. Insulation Resistance	At 50V DC between motor terminal and case	1 MOhm

2. LRA motor

C10-100

PRECISION ™ MICRODRIVES

**Product Data Sheet
Precision Haptic™
10mm Linear Resonant Actuator - 4mm Type**
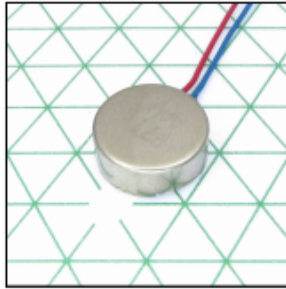
10mm Linear Resonant Actuator - 4mm
Type Shown on 6mm Isometric Grid

Model: C10-100

Ordering Information

The model number C10-100 fully defines the model, variant and additional features of the product. Please quote this number when ordering.
For stocked types, testing and evaluation samples can be ordered directly through our online store.

Datasheet Versions

It is our intention to provide our customers with the best information available to ensure the successful integration between our products and your application. Therefore, our publications will be updated and enhanced as improvements to the data and product updates are introduced.
To obtain the most up-to-date version of this datasheet, please visit our website at:
www.precisionmicrodrives.com
The version number of this datasheet can be found on the bottom left hand corner of any page of the datasheet and is referenced with an ascending R-number (e.g. R002 is newer than R001). Please contact us if you require a copy of the engineering change notice between revisions.

If you have any questions, suggestions or comments regarding this publication or need technical assistance, please contact us via email at:
enquiries@precisionmicrodrives.com or call us on +44 (0) 1932 252 482

Key Features

Body Diameter:	10 mm [+/- 0.1]
Body Length:	3.65 mm [+/- 0.1]
Rated Voltage (RMS):	2 V
Rated Vibration Frequency:	175 Hz
Typical Rated Operating Current:	69 mA
Typical Norm. Amplitude:	1.5 G

Typical Linear Resonant Actuator Performance Characteristics

Resonator Performance [C10-100]
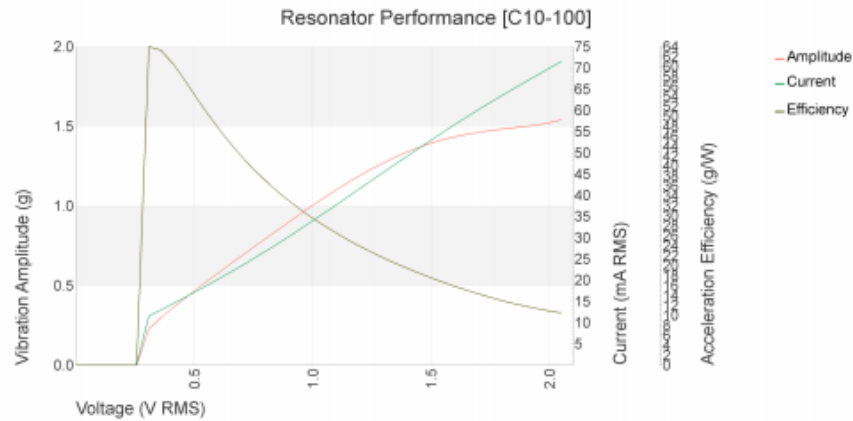
C10-100

Physical Specification

PARAMETER	CONDITIONS	SPECIFICATION
Body Diameter	Max body diameter or max face dimension where non-circular	10 mm [+/- 0.1]
Body Length	Excl. shafts, leads and terminals	3.65 mm [+/- 0.1]
Unit Weight		2 g

Leads & Connectors Specification

PARAMETER	CONDITIONS	SPECIFICATION
Lead Length	Lead lengths defined as total length or between motor and connector	100 mm [+/- 2]
Lead Strip Length		1.5 mm [+/- 0.5]
Lead Wire Gauge	UL3302	32 AWG
Lead Configuration		Straight

Operational Specification

PARAMETER	CONDITIONS	SPECIFICATION
Rated Voltage (RMS)	Sinusoidal waveform at Rated Vibration Frequency. Voltage specified as RMS	2 V
Auto-Resonance Driving	Performance with drivers using auto-resonance is greatly influenced by the application. 30% (typ.) voltage reduction in driving voltage and case-by-case validation is required.	
Rated Vibration Frequency		175 Hz
Max. Rated Operating Current	RMS Value. At rated voltage using the inertial test load	90 mA
Max. Start Voltage	Certified starting voltage. Sinusoidal waveform at Rated Vibration Frequency. Voltage specified as RMS	0.4 V
Rated Inertial Test Load	Mass of standard test sled	100 g
Max. Operating Voltage	Sinusoidal waveform at Rated Vibration Frequency. Voltage specified as RMS	2.05 V
Min. Vibration Amplitude	Peak-to-peak value at rated voltage using the inertial test load	1 G
Min. Insulation Resistance	At 50V DC between motor terminal and case	1 MOhm
Resonant Frequency		174 Hz [+/- 7]

3. C2 High displacement low frequency

C-2HDLF Tactor[†]
Product Data Sheet
ATAC Tactor

[†] US patent 7,798,982

Specifications

Physical Description:	1.2" (30.2 mm) diameter by 0.5" (13.0 mm) high
Weight:	30 grams
Exposed Material	Aluminum, polyurethane
Electrical Wiring	Flexible, insulated, twisted pair #26 AWG.
Body Contactor:	0.38" (9.7 mm) diameter by 0.33" (8.4 mm) high
Tactile Pulse Characteristics:	50-160 Hz, <2 ms rise time
Electrical Characteristics	8.5 ohms nominal, excluding wire length.
Transducer Linearity:	+/- 1 dB from sensory threshold to 0.02" (0.5 mm) peak displacement.
Recommended Drive:	Sine wave tone bursts 90-110Hz at 0.25A rms nominal with < 10% average duty cycle.
Recommended Controller	EAI Universal Controller

Product Description

The C-2HDLF (High Displacement) tactor is a high force actuator that has been designed to provide high displacement output at low frequencies. The C-2HDLF Tactor is intended for research applications exploring low frequency mechanoreceptor response and wearable haptics.

Applications

- Wearable tactile feedback
- Aviation
- Automotive
- Entertainment
- Biomedical

C-2HDLF Tactor

Operation

The C-2HDLF tactor is a moving magnet linear actuator that has been optimized for high force and high displacement. The C-2HDLF uses a low frequency mechanical resonance at approximately 125 Hz to provide stimulation in the 50 – 160 Hz range. With a nominal 8.5 Ω impedance, the C-2HDLF can be driven by conventional audio drivers, and is compatible with the Universal controller.

When an electrical signal is applied, the contactor oscillates perpendicular to the body, creating a strong localized sensation. By varying the electrical drive parameters, a wide variety of tactile sensations and haptic effects can be achieved.

Performance Data

C-2HDLF Frequency Sweep at 250 mA
Loaded Against a Skin Phantom

DIMENSIONS IN mm.
13.2
Ø31.7